A Model for Simulation of Fiber Suspension Flows

by

David Hammarström

May 2004
Technicl Reports from KTH Mechanics
Royal Institute of Technology
SE-10044 Stockholm, Sweden

Akademisk avhandling som med tillstånd av Kungliga Tekniska Högskolan i Stockholm framlägges till offentlig granskning för avläggandet av teknologie licentiatexamen fredagen 11 juni 2004, kl 10.00 i sal S40, Teknikringen 8, KTH, Stockholm

Universitetsservice US AB, Stockholm 2004

D.Hammarström 2004, **A Model for Simulation of Fiber Suspension Flows**
KTH Mechanics, Royal Institute of Technology
SE-10044 Stockholm, Sweden

1 Abstract

The fiber suspensions in the production line from wood to paper are subjected to many types of chemical and mechanical processes, in which the flow of the suspension is of vital importance. The flow of the suspension determines the degree of uniformity of the fibers through the processing, which in return affects the properties of the fiber suspension. In order to optimise the process, thorough knowledge of the suspension flow is necessary, both on the level of suspension, fiber networks and individual fibers. Knowledge of the fiber suspension behaviour combined with commercial CFD simulation provides an efficient design method for any unit operation in the papermaking process.

This work concentrates on macroscopic modeling of the behaviour of fiber suspensions from 0.5-5% dry content, pure fiber suspensions without fillers or additives. Any mechanisms causing the characteristic behaviour of the pulp suspension have not been included, they are only included through their influence on the suspension parameters. Excluded mechanisms are, for instance, the fiber-fiber coupling mechanisms that are the reason for the formation of fiber networks and parts of fiber network, flocs.

By combining a rheology model for the bulk suspension, a wall function that accounts for the slip layer and finally introducing turbulence, a model has been created that is able to simulate the flow of most fiber suspensions. The flow of the suspension is not constrained to any particular flow conditions; the models discussed in this work aim at describing the behaviour of the suspension for all flow rates and flow types. The models are developed under simple flow conditions, where all variables can be controlled, but the models are intended for usage within the industry-based flows in real pulp and papermaking applications.

Keywords: rheology, fiber, suspension, CFD, model, wall, slip, turbulence

2 Contents

3 Introduction

The flow of suspension in the fiber line can be divided in several levels; the suspension can be viewed at the suspension level, which is the focus in this work. It can also be investigated on the network or floc level, or at the fiber level. The difference between these aspects is that on the suspension scale the properties of individual flocs are not of interest, only their influence on the flow of the suspension is desired. On the network and floc level, the individual fibers are not of interest, only their contribution to the strength of the formed agglomerates is included. On the fiber level, the properties of the fibers and the fines is included. This send its images to the upper levels, but the mechanisms have to be modeled. By comparing the sizes the need for data abstraction is clear, the fibers in the picture 1 are roughly 3 mm long and 50 µm wide, the flocs are 3-30 mm in diameter, whereas the suspensions fills the container, up to several meters.

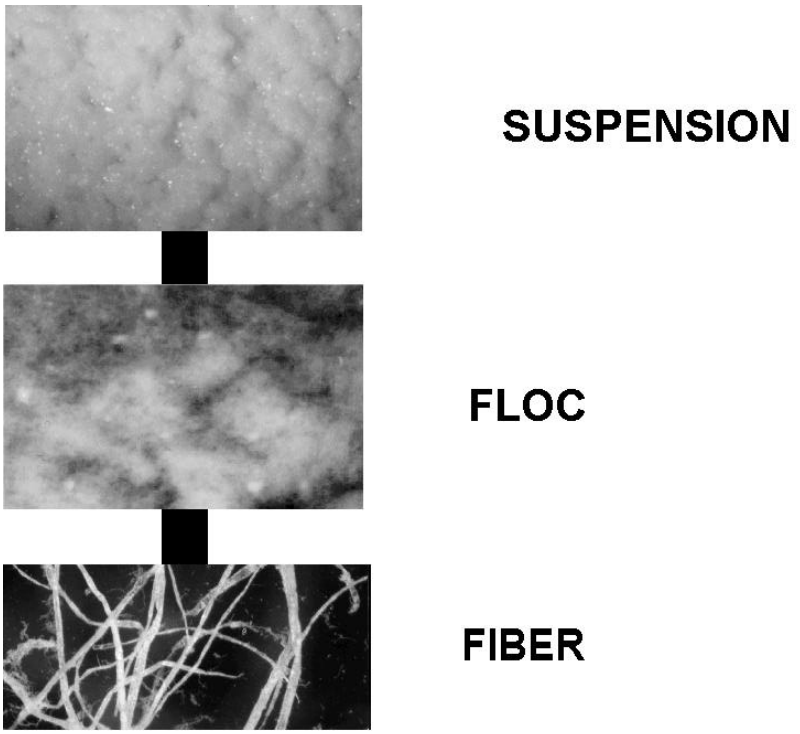

Picture 1 Principles of data abstraction in fiber suspension modeling. Pictures of chemical long-fiber pulp. Photos by courtesy of Ulf Björkman, STFI, Sweden

It is evident that the smallest parts, the fibers, are responsible for anything that occurs within the flow. But for engineering purposes it is not possible to include every fiber in any simulation model. It is possible to include the floc formation, or at least the probability of it, but this again requires modeling of other macro-scale events. In the design of computer programs a similar approach is called "top-down" design, whereas the opposite is termed the "bottom-up" design. Top-down implies that at first a working program structure in built, on which the individual details are added when they are completed, and thus the program is under constant development.

This work contains a "top-down" method of examining the properties of the fibers. All macro-scale phenomena can be recorded on the suspension level, from which new insights regarding the behaviour of flocs and suspended fibers may arise.

3.1 Fiber Suspensions

The properties of the pulp fibers depend on many properties, such as the wood species and the processing they have been subjected to. The softwoods such as pine and spruce usually have longer and more flexible fibers than the hardwoods have, e.g. birch and aspen. This sends its images on the properties of the suspension.

The processing the fibers have been subjected to is quite as important. Chemical pulping produces whole fibers, the suspension does not contain much fines that are produced from broken fibers. Mechanical pulping, on the other hand, tends to result in much more damaged fibers, the fiber length distribution is different than for a chemical pulp. Groundwood is another pulp type that contains large amounts of fines.

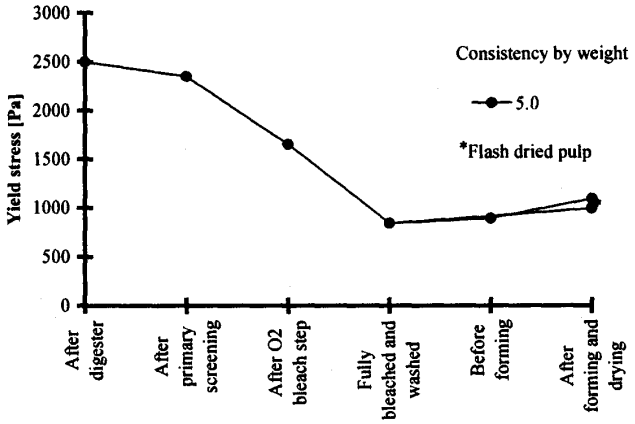

Picture 2 The influence of different processing on the yield stress of a pulp suspension, measured by Wikström [1]. Picture reproduced with permission from Wikström.

Bleaching removes lignine, which is the 'glue' that keep the fiber together in the tree. By removing the lignine, the fibers become more flexible. Other processing may also influence the properties of the fiber suspensions. Picture 2 shows how the yield stress of a fiber suspension is changed by the different unit processes in a pulp mill. This type of change of suspension properties cannot be predicted by any macro-scale model, but it can be included as model input data, if enough measurement data is available. It may seem to be a time-dependent feature of the fibers, but it is not, the properties of the fibers depend on the

processing they have been subject to, in this case nothing can be said about transient properties of the fibers and suspension.

The interaction between individual fibers cannot be implemented in this type on model, due to the large number of fibers. In the dry contents discussed in this work (c_{mass}>0.5%) the fibers are in continuous contact with each other. That the fibers are in more or less constant contact with each other, is one of the key assumptions on which this work is based.

The friction between individual fibers have been investigated, among others, by Andersson and Rasmusson [2], [3]. The stick-slip friction limit was investigated for both dry and wet fibers. The forces acting on the fibers were presented as the normal force component μN, but that also an additional adhesive force that is independent on the normal force. The additional adhesive force has not been implemented in any of the yield stress models presented. The normal forces increase with crowding factor, which means that the yield stress of a fiber suspension would be different for suspensions characterized by a large adhesive force than for suspensions with a larger friction coefficient μ. The adhesive force and friction forces relate to the state of the fiber, the degree of fibrillation and swelling, a swollen fiber may have gel-like properties on the surface.

One of the most prominent features of fibrous material is the tendency to form larger agglomerates, for wood fiber suspensions usually termed 'flocs'. The flocs are present at virtually all concentrations that are of relevance within the pulp and paper industry, only at much lower concentrations the fiber suspensions can be regarded as free from flocs. In the dry contents included in this work, the suspended fibers are in continuous contact with each other, hence the formation of fiber clusters is always present. The crowding number was first presented by Kerekes and Schell [4], recently a generalized version of the crowding number for a suspension with varying lengths of the fiber fraction has been presented by Huber et al [5]. A softwood pulp of c_{mass}=3% would have a crowding factor of approximately 400, where 60 is the limit where the fibers are to be in continuous contact.

Ross and Klingenberg [6] simulated the flow of suspended, flexible fibers, that were modeled as connected spheroids on a chain. One of the main interests, is the tendency to form mechanical entanglements, that are the cause for the formation of flocs and networks. A similar simulation by Fan et al [7] for rigid glass fibers is presented in picture 5, page 19. In the simulation method of Ross and Klingenberg, the flexibility of the fibers can be mimicked by the stresses in the joints between the spheroids. The simulation results showed that the flexibility of the fibers resulted in the formation of weak fiber networks. The networks were broken by shear.

Karema et al [8] determined the degree of flocculation and the mean floc size after a step change in a channel flow. The turbulent velocity fluctuations were measured with a pulsed ultrasound Doppler anemometer. The mean floc size was determined using digital imaging techniques.

Hyensjö et al [9] has done simulations using the 'Fiber Flocculation Concept' presented by Steen [10], comparing the results against the measurements performed by Karema et al [8]. The FFC has mainly been used for very dilute suspensions and does not contain any model for the pulp rheology, it uses the viscosity of water. The rheology and wall slip models presented in this work are capable of returning the velocity profile and the pressure loss of the pulp suspensions, but so far the models of this report are not detailed enough to be used together with the flocculation models.

3.2 Measurements

3.2.1 Flow Measurements

The anomalies in the flow of paper pulp stock was lively discussed in the mid 20^{th} century, where many authors debated the similarity and differences between their measurement series. Apparently none of the old measurement series are comparable to one another, and some have quite short calming lengths before the measuring points. One example is the Brecht and Heller [11] measurements, especially the larger pipes in this experimental set have barely 10 pipe diameters calming length between a 180° bend and the first measuring point, whereas an appropriate calming length would be at minimum 50 pipe diameters, sometimes over 80 diameters, Möller [12]. The short calming length in the Brecht and Heller series may be seen when comparing the measured head losses of two different pipes, 5.90 and 7.87 inch diameters.

In the University of Maine measurement series the head loss was measured for several different pulps in several pipe diameters. Later also the head loss over some typical pipe fittings were recorded. Picture 3 is a typical example of head loss data of the early work, with only a few measurement points for each flow regime. Many of the early curves do not even give the measured points, only the curve that has been fitted to these. For the model development, the fitted curve is as good as the measured points, but with too few measured points the reliability is low.

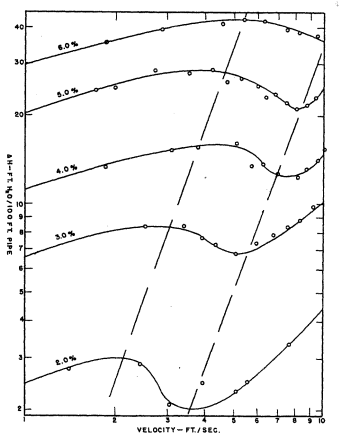

Fig. 2. Pressure drop—velocity relationships for bleached sulphite stock through 6.34-in. spiral-welded steel pipe

Vol. 37, No. 10 October 1954 · TAPPI

Picture 3 Durst and Jenness [13] measurements of bleached sulphite pulp, different consistencies in 6.34 inch pipe. Picture reprinted with permission from TAPPI, October 1954, vol 37, no 10 page 420.

Duffy [14], [15], [16] has performed excellent measurement series, many of which have been performed under identical conditions and with good accuracy, this type of measurement results are the best available reference data for developing of any flow models. By performing multiple measurements on identical suspensions except for one parameter which is varied, the influence of any of the fiber properties can be included in the flow models.

Recently, Ari Jäsberg at Jyväskylä University [61]-[62] performed head loss measurements in a 40 mm diameter pipe. The measurements contained data from a few different pulp types, at several fiber concentrations. The flow rate in the pipe cover a wide range, from very low flow rates to reasonably high flow rates, with several hundred measurement points between, giving the measurement a very high reliability. The flow models presented in this report are mainly presented based using this new and outstanding data.

3.2.2 Velocity Profile Measurements

The first attempt to determine the velocity profile in a the flow of pulp suspensions in a 5.9 inch pipe was published by Brecht and Heller [11]. They presented one graph, which unfortunately presented pulp measurements at a different dry content than had been used in the rest of their paper. The Brecht and Heller velocity profile was measured with a counter-current pitot tube. Due to the fibrous nature of the material, an ordinary pitot tube will be clogged immediately, instead a pitot tube with a counter current water flush is used. The velocity profiles look surprisingly realistic, considering the generalized Newtonian properties of the suspension and the wall slip layer that probably

has been formed in all cases, and the two highest velocities are probably already in the ´turbulent´ region.

A later attempt is presented by Mih and Parker [17], who have performed the measurements on bleached birch using also a counter current pitot tube. They also supply head loss measurement data with the velocity profiles. The Mih and Parker data will be discussed in section 9.3.

The use of ultrasound for measuring fiber motion is based on the echo sent by the fibers. The suspending medium does not interfere with the sound waves, but if the number of particles is large or the measured depth is large the noise may be too large for obtaining a reliable result.

Unlike laser light, the propagation of sound is not affected as much in fiber suspensions. The fibers cause a large distortion of the echo, but with enough transmitted power a signal may be detected above the noise level. Therefore, the method is mainly suited for moderate consistencies ($c_{mass} < 5\%$) and mainly in small pipe dimensions ($R<25$ mm)

Wiklund et al [18]-[19] have used a pulsed ultra sound analyser in combination with head loss measurement, which is an excellent thing. The measurements have been performed on a viscoelastic shampoo and on a fiber suspension. The flow loop is a 23 mm diameter pipe, total length a few meters.

The capacity of the UVP-PD method seems to be excellent, the thesis contains measured curves for suspensions up to 3% dry content, and in private communications the author informed that it is possible to go up to 5% consistency. The frequency of the signal needs to be lower when using high consistency, and the high consistency also results in a very high degree of noise. The frequency of the pulsed ultrasound signal was 4 MHz, with a minimum spatial resolution of 0.74 mm.

Fiber suspensions require long times before the flow is fully developed, required calming lengths of up to 50-80 diameters have been reported by Möller and Norman [12]. Most authors have settled for 50 diameters. The current device has the first pressure transducer immediately after a bend, and the second right before another bend and the UVP transducer in the middle, where the velocity profile is probably not fully developed. The data is used in order to demonstrate a computational method for determining the rheological properties of a pulp suspension on which there is not enough data to build the model in the way that is described in this work.

Nuclear magnetic resonance (NMR) is a non-invasive method, that uses the magnetic properties of the nuclei. A strong magnetic field is applied on the

flow domain, and using electromagnetic pulses, the nuclei can be exited. The nuclei then emits detectable signal when returning to the equilibrium state. The analysis of the NMR spectra is based on that the frequency at which the nucleus absorbs or emits energy is proportional to the strength of the magnetic field. When a gradient exists in the magnetic field, the protons will emit energy at different frequency depending on their location. Due to this, the method can be used for measuring local velocities in a flow where other measurement methods are not possible.

Picture 4 shows the resulting velocity profile as measured by Li et al [20]. The picture clearly shows that a very high velocity gradient exists near the pipe wall. The results will be used in section 9 of this work. In all, the report by Li show that NMR is a highly capable instrument for determining the flow profiles of the difficult pulp suspension flows.

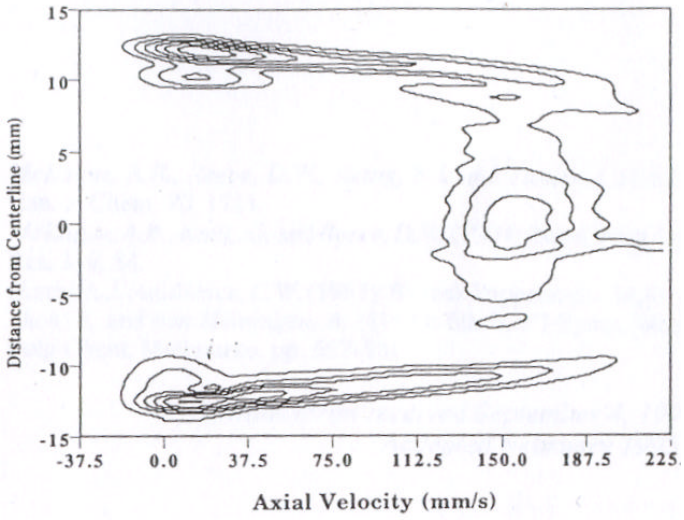

Picture 4 Velocity profile in a 26.2 mm pipe, as measured by Li and Ödberg [21]. Picture reproduced with the permission from the authors and the Nordic Pulp and Paper Research Journal, Li et al, picture 22, vol 2, 1995.

3.2.3 Rotating Shear Tester

Flow in rotary devices are a useful complement for the model development. The flow in a rotating shear tester operating at different velocities will return much information regarding the rheology of the pulp suspensions. Bennington et al [21] has performed the only such series which is applicable to this model, the Bennington device is shown in picture 67-68 on page 71. It is a shear tester with lugs on the walls to prevent slippage. The rotational speed and the corresponding torque was measured for a few consistencies.

The question regarding the flow in all rotating devices is whether the flow is homogeneous. If a concentration gradient is formed due to fiber migration due

to centrifugal or other forces, then the model predictions will be incorrect, as the models cannot account for fiber migration.

The rotary devices without baffles on the wall present a very challenging task for the models. Möller [12] use a device in which the flow can be regarded as two-dimensional. The device used by Durst and Jenness [13] can maybe not be considered a two-dimensional flow. The advantages of Couette flow over pipe flow for determining the suspension rheology is that the size of the apparatus is smaller, and also the required volume of suspension significantly smaller.

3.3 Flow Models

Flow modeling of fiber suspensions started as early as 1959 when Baines [23] presented the Navier-Stokes based solution for the height of the water annulus, the existence of which had been determined by Head and Durst [24]. Baines solved the annulus thickness for a dilute fiber suspension, using the viscosity of water. He did not present any solution against any measured pulp flows. Later Soszynski [25] used a similar method to solve the annulus thickness assuming that the "plug" velocity equals the mean pipe velocity for a few measured pulp flows. The calculations of Soszynski are compared to the predictions of the pulp model in section 8.

Myréen introduced the rheology modeling in his papers [26], [27]. In the first paper, the rheology model is shown to work for both the Couette flow and the pipe flow on the Durst [13] measurements. This was an important step, because he introduced a flow model that was not restricted to pipe flow, but could be applied in any other geometry. In his second paper the wall slip was introduced. Here the bulk pulp is calculated with the power-law rheology model and the water annulus with the properties of water. He presented the slip film thickness as a function of a slip ratio, but did not give a solution an the annulus thickness. This was later given by Hämäläinen [28], who made a similar approach and offered the analytical solution for one measured set of head losses, the results of which are presented in section 8 and compared to the results of the pulp model presented in this report.

Huhtanen [29] applies the generalized Newtonian models to the flow of paper pulp suspensions, his data is the same as used by Hämäläinen [28]. He showed that the commercial flow simulation programs, in this case POLYFLOW, are able to model the plug flow region, and also the wall slip phenomenon. He used the generalized Navier's law {equation 16}, which is implemented in POLYFLOW. The main part of the work, however, is a set of rotating disc measurements on a very dense pulp suspension.

The use of rheology based modeling for fiber suspension flows has been debated in the literature, mostly due to the multi-phase nature of the suspensions. All flow phenomena can not be described by the simplest flow models, but in fact the rheology models are very similar to the empirical head loss correlations presented by e.g. Duffy [30]. The significant difference is that the rheology models are applicable to any arbitrary geometry instead of pipe flow alone, which makes them superior compared to empirical correlations. The empirical head loss correlations are very useful for e.g. process simulation purposes, where the influence of piping is included only in form of pressure drop and time delay, but are useless for analysing complex three-dimensional flows in real papermaking applications.

The validity of the rheology and slip modeling was studied by Hammarström et al [31]. Earlier, the rheology model had been applied to the plug-flow regime, and the wall slip regime had been described by the slip model as presented by the earlier authors. Hammarström et al showed that the flow of pulp can be simulated with the same material and wall function for both the plug-flow and wall-slip regime. The material function is largely identical as used by previous authors, but the wall function is different. The most important observation in this model is that the user does not need to input whether he has ordinary laminar flow or wall slippage, this is a result of the simulations. The slippage calculated by the model originate from the flow conditions within the bulk suspension, and not from the wall, this difference is of fundamental importance.

Meyer and Wahrén [32] presented the shear modulus of a fiber network as a function of the fiber aspect ratio, the ratio of the physical dimensions of the fiber. They connected the fiber aspect ratio to the number of contact points per fiber and to the volumetric concentration of the fibers.

The yield stresses of the fiber networks have been investigated by Bennington et al [21] and Andersson et al [33]. The yield stress of the network were measured in a rotary shear testers, with baffles on both walls, presented in picture 67-68on page 71. Bennington presents a correlation for the yield stress for the dry content for a few pulp types. There are other parameters that influence the yield stress, but the concentration is the most important of all. Andersson et al [33] noticed that the addition of a small amount of long fibers into a short fiber suspension resulted in a large change of the yield stress towards the value of the long fiber suspension.

The correlations for the yield stress are (Bennington et al [21]):

$$SBK: \quad t_y = 4.12e5\ C_m^{2.31} = 3.82e5\ C_v^{2.72}$$

$$SGW: \quad t_y = 1.10e6\ C_m^{2.99} = 1.08e6\ C_v^{3.36}$$

$$TMP: \quad t_y = 1.38e6\ C_m^{3.56} = 2.63e6\ C_v^{3.56}$$

(SBK=Semi-bleached kraft, SGW=Stone ground wood, TMP=Thermo-mechanical pulp)

Wikström and Rasmusson [34] presents measurements and CFD simulation results for two types of rotary shear testers, both of these were simulated with a yield stress model. The simulations agree reasonably well with the measurements. The transitional flow modeling was applied to a industrial screening application. In his model turbulence was added to the rheology model.

The viscoelastic properties of fiber suspensions were investigated by Damani et al [35] for 2-13% suspensions, and Swerin et al [36] evaluated 3-8% pulp suspensions. They investigated the loss and storage modulus for different straining frequencies and amplitudes. The maximum straining amplitude corresponded quite well with the yield stresses, as measured by Bennington, but this is hardly surprising. Concentrated fiber suspensions may show very large extensional viscosities, without having any elastic effects. For practical purposes, the more or less stationary fiber suspensions may or may not have viscoelastic properties, for modeling of flowing fiber suspensions under high shear, any possible viscoelasticity can be disregarded.

3.4 Turbulence Modeling

Turbulence is present in most applications involving flow of pulp suspensions. Turbulence is assumed to be one of the most important mechanisms behind formation and destructions of fiber flocs.

As the material properties are very different from any single-phase fluids, the parameters of any of the existing turbulence models are probably not suited for the fiber suspensions. In fact, each fiber suspension probably needs its own addition to the turbulence models, for instance in the form of additional damping depending on the fiber length, concentration and degree of fibrillation of the fibers.

Bennington and Mmbaga [37] used mixing-sensitive chemicals to investigate the energy dissipation in fiber suspensions. The assumption was that energy is dissipated only in the fluid phase, any differences between this and the input energy value would be due to breaking of fiber-fiber bonds. It was shown that turbulence was dampened by the fibers.

Among the earlier efforts for describing turbulent flow of fibers suspensions, the work of Wikström [1] is the first commercial CFD based study of different methods for simulating both the laminar and turbulent state of the fiber suspensions. Hämäläinen [28] introduced mathematical modeling of dilute fiber suspensions in application-based flows with a simulation program for head box flows.

Lindroos et al [38] studied the effect of the fibers on turbulence created in a backward facing step, based on an additional dissipation term in the Reynolds stress model. The concentration in Lindroos work is much lower than in the work of this report, but a similar approach is assumed possible at higher concentrations as well. Kuhn and Sullivan [39] made a similar set of measurements and simulations of a flowing fiber suspension after a grid in a thin 2D channel. The simulations were transient large-eddy simulations, the turbulent intensity was equal to the measured values. Contrary to what is claimed in the literature, Kuhn and Sullivan state that the results indicate that the strains imposed by the mean motion, instead of the small-scale turbulence, is responsible to the breaking of flocs.

Of the earlier descriptions of fiber flows, Hemström et al [40] noted that the point of significant plug disruption could be calculated as a function of the suspension velocity and the concentration (%-mass) for the flow in a 100 mm pipe. Gullichsen and Härkönen [41] interpreted this as the point at which full turbulence occurs, but this type of determination of the onset of turbulence can be put in question. For any fluid flow, it is not the velocity, but the velocity fluctuations that is turbulence. Hemström puts in question whether a fully developed flow regime ever exists after a certain fiber concentration is exceeded. In the present work the concentration is well above this limit, at which a continuous networks is formed. A 'fully developed' flow means that the flow profile is not changing with distance in the flow direction, the flow is dissipating as much energy as is generated. For a boundary layer this can be explained by that the boundary layer is dissipating the same amount of energy as it receives from the main flow, the height of the boundary layer is constant. Gullichsen's argument that the hydrodynamic properties of turbulent fiber suspensions resemble those of Newtonian fluids remains. This is very close to the common practice to simulate dilute fiber suspensions with the fluid properties of water, as done by Hämäläinen [28] and Steen [10] and Lindroos et al [38].

Bennington et al [21] discusses whether the turbulent state is identical to the "fluidised" state of a fiber suspension, a term which has received some criticism. Fluidisation means that the fibers are free to move relative to each other, all network bonds within the fiber suspensions are broken. The results by Bennington will be used in section 9 to investigate the suitability of using the point of full fluidisation for developing flow models.

Wikström and Rasmusson [34] simulated an industrial screening application with a combination of a yield-stress rheology model and a turbulence model. The laminar-turbulent transition in his simulations were based on a threshold in the shear rate, above the limiting value the effective viscosity was assigned value of the turbulent viscosity, below the limit the effective viscosity was assigned the value returned by the Bingham model, in which the viscosity is infinite before a certain stress on the fiber suspension in exceeded.

In his results Wikström noted that the use of the viscosity of water is not quite correct, and that the pressure pulses are overestimated. This is due to the absence of any additional damping caused by the fibers. The trends were correct in Wikström's simulation results, but he concluded by announcing for a new treatment of the boundary layers of fiber suspensions, which is the topic of this report.

3.5 Particle Suspension Flow

Flowing suspensions may give a uneven flow field. This may manifest itself as a decreasing viscosity, which is caused by migration of the suspended particles. Different models for particle migration have been proposed, describing the particle diffusion as a function of the fluctuation motion of the particle. The motion of the particles suspended in the liquid has been simulated with Stokesian dynamics by Välimäki [42], where the motion of the particles in a coating paste was simulated. The Stokesian dynamics method solves the motion of N particles, with or without hydrodynamic interaction. The simulations relate to the measurements made by Kokko [43], where the non-Newtonian aspects of coating pastes were discussed. The paper coatings are complex, extremely dense aqueous suspensions with particle sizes 0.1-2.0 μm.

Johnson and Jackson [44] discuss constitutive relations for granular materials. The object of their research is the intermediate consistency where both frictional and collisional transport of stresses. The total stress tensor is divided into a frictional and a collisional component. The boundary conditions used included a slip velocity between the particle phase and the wall, that is obtained by equating the tangential force exerted by the particles on the wall to the corresponding stress within the particle phase close to the boundary. The force per area is the sum of collisional and frictional forces. They considered the material to be in a "critical state", in which the shear stress is proportional to the normal stress. The "critical state" theories often associated with soil mechanics uses a set of yield surfaces in the stress space, one yield surface for each density level.

In general the paper coating suspensions are used and characterized at very high shear rates, usually their flow properties are determined with a capillary

viscometer, sometimes with different capillary diameters in order to determine the viscosity for different shear rate regions. In these measurements the Bagley correction, or the Hagenbach-Couette method, is used to correct for the entry and exit flow of the capillaries.

Some dilatant effects are also visible in the coating process, for instance in the blade coating process after the compressed coating paste is released from the pressure exerted by the coating blade, the stored energy causes the volume to expand. If the water absorbed in the paper during the coating is not able to flow back, a change of suspension consistency has occurred.

The work of Kokko also discussed the meaning of water retention from the coating pastes. The formation of a lubricating water layer on the capillary walls would point at the water retention of the coating. This is connected to the particle migration, as studied by Välimäki [42] and Phillips et al [45] and Nott and Brady [46]. Phillips modeled the suspension as a Newtonian fluid with empirical relations for the particle concentration in Couette and Poiseuille flow with a few constants that describe the particle transport. Nott used Stokesian dynamics for calculating the velocity profile and local particle concentration.

Huhtanen [29] applied rheology modeling to the forward roll coating process. The flow of the coating colour was simulated using POLYFLOW. The material was modeled with the power-law model. The simulation results showed reasonable agreement to measurements published in the literature, both for a few cases of film-splitting flow.

3.6 Slurry and Emulsion Flow

Emulsions of various kind are also widely used in the process industry, many emulsion may resemble the fiber suspensions, especially regarding the complex rheology. The main difference in rheology lies in that the viscosity of an emulsion is on a lesser degree dependent on the volume fraction of the dispersed phase than is the case for suspensions and undeformed droplets. Deformable drops do not form large clusters, unlike the rigid particles in suspensions.

In low Re shear flow, the rheology of the suspension is determined by the volume fraction of the dispersed phase, the viscosity ratio between the dispersed and the continuous phase and the capillary number. The capillary number determines the importance of drop deformation, and is thus a form of dimensionless shear rate. Loewenberg and Hinch [47] simulated the flow of a suspension, using a periodic flow with 12 droplets. The droplets were initially capsule-shaped, but were allowed to deform during the calculations. The simulations in their paper showed that the drops deform more, and orient more

into the flow direction when the volume fraction of the dispersed phase is increased. This could possible be the case with flocculated fiber suspensions as well, the flocs are free to deform, and to orient themselves according the flow. The results also indicate that emulsion droplet break-up occurs at lower capillary numbers at higher dispersed phase volume fraction. The viscosity of the emulsion proved to be almost linear to the dispersed phase volume fraction, without the sharp peak found for suspensions of rigid particles. The deformation of the droplets inhibits the formation of large agglomerates.

Turian et al [48] discuss the flow of non-Newtonian slurries, here concentrated slurries of laterite and gypsum is considered. The paper discusses several generalized Newtonian models and their use with slurries, and presents means to predict the laminar-turbulent transition point. Of the non-Newtonian models especially the Sisko {equation 5} model proved to be very useful for many industrial fine-particulate slurry of high dry content. Of the models presented in their paper, the Bingham {equation 7}, Herschel-Bulkley {equation 8} and Casson {equation 9} models contained a yield stress parameter. Of the models tried for the slurries, the Bingham and Herschel-Bulkley models proved to be the least suited, partly due to the difficulty of determining the model parameters, and they proved to be very sensitive to the assumed parameters. The slurries were noticed to reach a limiting Newtonian behaviour at high shear rates, usually preceded by a power-law behaviour.

In the Sisko model, theinfinite shear viscosity is readily available. The model thus follows an almost Newtonian shear curve at high shear rates, and a power-law type curve at lower shear rates. This was true for the whole range of slurry type and concentrations measured. The Casson model also performed well, and is often used to describe the properties of biological matter, such as foodstuff and bodily fluids like blood. Kim et al [49] determined the slightly non-Newtonian properties of blood with the power-law {equation 6} model. In capillary flow of blood, the red blood cells tend to move towards the centre of the tube, as any other flow of suspended particles.

3.7 Glass Fiber Suspension Flow

Fiber suspensions have been given a lot of attention within the polymer processing industry, at least the reinforcement glass fibers. The aim of these studies has been to establish the rheology, fiber distribution and orientation of the glass fibers in both Newtonian and non-Newtonian fluids used for injection moulding.

According to Ramazani et al [50], the properties of the fiber suspensions used in the polymer industry do not only depend on the fiber characteristics, but also on the orientation of the fibers. Both the first normal stress difference and the

viscosity increase with the concentration at low shear rates. At high shear rates the viscosity and first normal stress difference become almost independent on fiber concentration and fiber characteristics. For both Newtonian and non-Newtonian fluids the suspended fibers increase the zero shear viscosity and the first normal stress difference. Fiber orientation depends on both the strain tensor and the rate-of-strain tensor.

In their article Fan et al [7] simulate 300 fibers in a unit cell, at different shear rates. The results indicate that the fibers that are randomly orientated at zero shear rate are reordered when subjected to a strain. A similar type of shear behaviour is assumed to be the explanation for the pseudoplastic properties of wood fiber suspensions, with the exception that wood fibers are flexible, which the glass fibers are not.

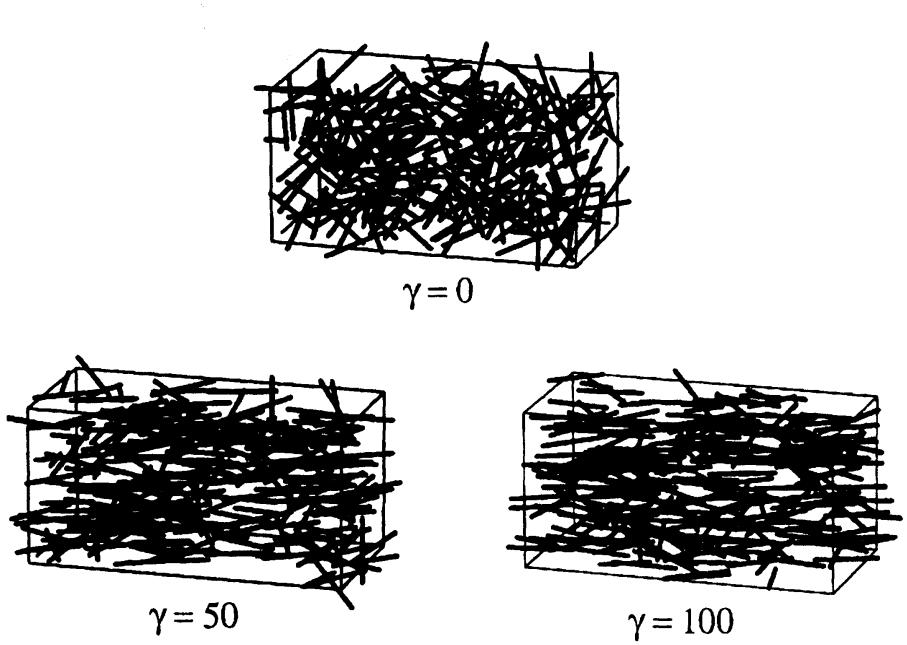

Picture 5 Picture of the fiber configuration at different strain in the direct simulation of Fan et al [7]. Picture reprinted with permission by ELSEVIER from the Journal of Non-Newtonian Fluid Mechanics, Fan et al, picture 1, p113-135, vol 74, 1998.

In his article on the rheology of fiber suspensions Petrie [51] makes use of a specific viscosity, which is the proportional increase in viscosity caused by the suspended fibers. Petrie refers to earlier research stating that there is no evidence of 'elasticity' due to the addition of fibers. The storage modulus is not affected by the suspended fibers. The glass fibers are lined up in the flow direction, as can also be seen in picture 5 from Fan et al [7], which reduces the friction losses in the suspension. Flow induced orientation is the reason for the Newtonian or non-Newtonian properties of a fiber suspension. A high extensional viscosity is not either evidence of elastic properties.

The term 'hyperconcentrated' suspension is introduced, where the fibers are all lined up and the suspending liquid can be regarded as a lubricant. This

resembles high concentration of a pulp suspension, again with the exception that the wood fibers are inhomogeneous, and have a different surface structure and form mechanical interlocking, which is not present for glass fiber suspensions.

3.8 Summary of Literature Review

As has been shown in this section, a lot of measurement data is available either to be used as reference for fitting material models, or to be used as validation for the simulations. There are only a few attempts at describing the flow phenomena through mathematical modeling, most of which are based on rheology. Measurements of fiber suspension flows with macro scale methods support the idea of using a macroscopic rheology approach for the bulk fiber suspensions. Of all the published measurement results, none contradict the hypothesis of using macro scale flow models, in fact, several measurements even suggest these to be correct. However, there are a few flow phenomena of fiber suspensions that the ordinary rheology model can not predict, which are the topic of the rest of this report.

4 Modeling

The flow of paper pulp suspensions is non-trivial, both regarding measurements and simulations. The suspension is often treated as a homogenous fluid, even though this is strictly not the case, many important and characteristic features are omitted. Many different fluid models have been presented for the flow modeling of wood fiber suspensions, they have all been based on macroscopic measurements, such as head loss measurements in Poiseuille flow or torque in Couette flow.

The flow regions of the pulp suspensions need illustrating, which is shown in picture 6. The first region, plug-flow is laminar and is assumed to have full contact with the pipe walls. Solid-solid friction is claimed to be the major contributor to the flow in this regime.

The regime where the head losses are decreasing despite an increasing flow rate is the wall slip regime. In this regime, a large part of the velocity gradient occurs within the very thin annulus at the walls.

The third regime has been referred to as the turbulent flow regime, but sometimes the first part of this has been termed the drag-reducing regime. The term drag-reduction comes from that the friction losses in the pipe are lower than the friction losses of water. In picture 6 the head loss curve of water would approximately follow the line between grey and dark grey. Finally, the head loss curve of the pulp suspension will merge with the head loss curve of water when the flow rate is high enough.

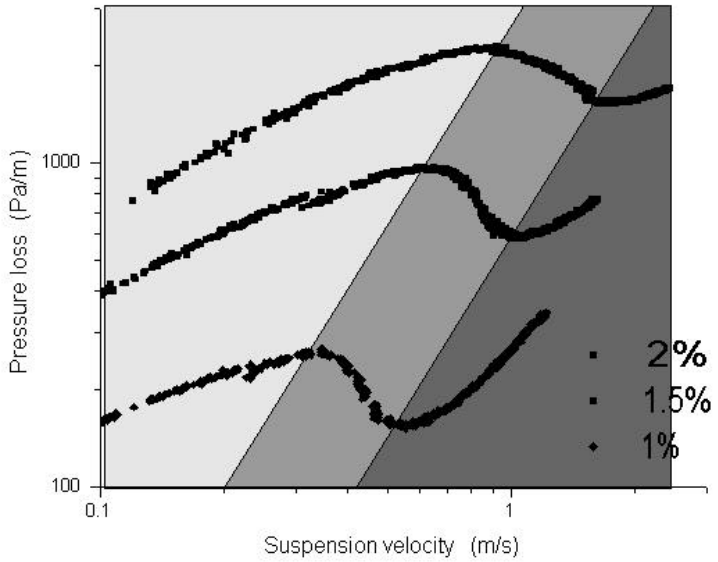

Picture 6 The flow regions of pulp suspensions shown for a birch pulp. Light grey: plug flow regime; grey: wall slip regime; dark grey: turbulent flow. The positions of the regions will be different for different suspensions and different concentrations.

4.1 Rheology Models

The choice of rheology model is not the main issue of the current report, therefore this discussion is left open until much more, and extremely detailed measurement results from velocity profiles of pulp suspensions is available. The quality of the different rheology models can be evaluated with no other inconvenience than long computational times by a method presented in section 9.

4.1.1 Newtonian

Simple, one-phase homogeneous fluids like water may be described by one constant value for the viscosity,

$$m(\dot{g}) = \text{constant} \qquad \{1\}$$

$$\dot{g}_{aw} = \frac{4Q}{p\,R^3} = \frac{8U}{D}$$

For laminar Newtonian flow in pipes, the mean shear rate is also presented in equation {1}. Complex multi-phase fluids such as fiber suspensions can probably never be properly described by one value. Determining the 'viscosity' of a pulp suspension under conditions as described in the TAPPI and SCAN standards may be useful for categorizing the pulp suspension, but is useless for flow simulation purposes.

4.1.2 Pseudoplastic Models

The generalized Newtonian models are laminar models, in which the viscosity is a function of the shear rate, which is also referred to as the strain rate or rate of deformation, or second invariant of the velocity gradient. The strain rate dependence may have any arbitrary function, but the strain itself is not included. Compare this to a Hookean spring and a dashpot in picture 7, which is termed the Maxwell model. The viscous resistance from the dashpot is included in the generalized Newtonian models, whereas the spring tension term in not included. A thorough presentation of the rheology models and their usage can be found in Morrison [52]

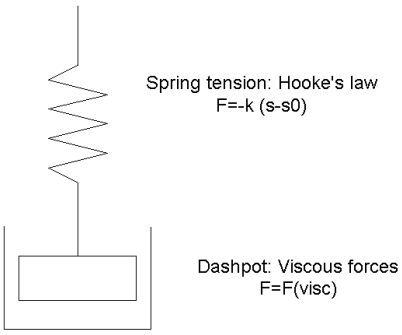

Picture 7 The Maxwell model

In order to fully describe the dependence between the viscosity and the shear rate at least four parameters are required. In case of an upper and a lower Newtonian plateau, as shown in picture 8, the limiting viscosity at low and infinite shear rates are included. The intermediate zone can be assigned any arbitrary function; usually a model of Cross {2} type is used.

$$m(\dot{g}) = \frac{m_0 - m_\infty}{1 + (k\dot{g})^m} + m_\infty \qquad \{2\}$$

Another perhaps more common alternative to the Cross model, is the Carreau model. The Carreau model {3} differs from the Cross model primarily in the curvature of the viscosity curve near the transition points between the Newtonian plateaus and the power region. This Carreau model is referred to as the Carreau-Yasuda model, if a=2 the model is also knows as the Bird-Carreau model.

$$m(\dot{g}) = \frac{m_0 - m_\infty}{\left[1 + (k\dot{g})^a\right]^{(n-1)/a}} + m_\infty \qquad \{3\}$$

The Cross model {2} can be simplified, in case only certain regions are of interest. The following special cases can be formed from the Cross law.

When the fluid is pseudoplastic and only the low and intermediate shear rates are of interest, the Ellis fluid model {4} can be used, in which a and $t_{1/2}$ are parameters of the model. $t_{1/2}$ defines the shear stress at which the apparent viscosity equals half of the zero shear viscosity, μ_0. a is a measure of the degree of shear thinning.

$$m(\dot{g}) = \frac{m_0}{1 + \left(\frac{t}{t_{1/2}}\right)^{a-1}} \qquad \{4\}$$

If the fluid possesses a significant viscosity at infinite shear rate, the Sisko model {5} can be used. k is the consistency coefficient, and n is the flow behaviour index determining the slope of the power region.

$$m(\dot{\gamma}) = k\dot{\gamma}^{n-1} + m_{\infty} \qquad \{5\}$$

If only the intermediate shear rates are of interest, the power law model {6} is used. This is the simplest and most common of all the generalized Newtonian models. The model is simple enough to allow analytical solutions to many flow problems, making it an ideal model. The shear rate at the wall in pipe flow for a power-law {10} fluid is also given in {6}, where the mean shear rate (= 8U/D) of the flow is corrected to account for the shear-thinning effects.

$$m(\dot{\gamma}) = l\dot{\gamma}^{n-1} \qquad \{6\}$$

$$\dot{\gamma}_{wall} = \frac{1}{4}\dot{\gamma}_{aw}\left(3 + \frac{1}{n}\right)$$

Due to the negative exponent of the shear-thinning fluids, the viscosity at low shear rates tends to infinity, which may cause computational difficulties. Therefore the power-law is usually assigned upper and lower limits for the viscosity, resulting in what is referred to as a truncated power law model. A truncated power law model is very similar to a Cross {2} or Carreau {3} model, except for the discontinuity points between the Newtonian plateaus and the power region.

Typical curves of the viscosity of the pseudoplastic fluid models are shown in picture 8. The curves have been plotted in order to visualize the differences between the models. As can be seen from the curves, only at low and high shear rates is there any significant difference between the models. It is of vital importance that the model is suited for the shear rates in each case.

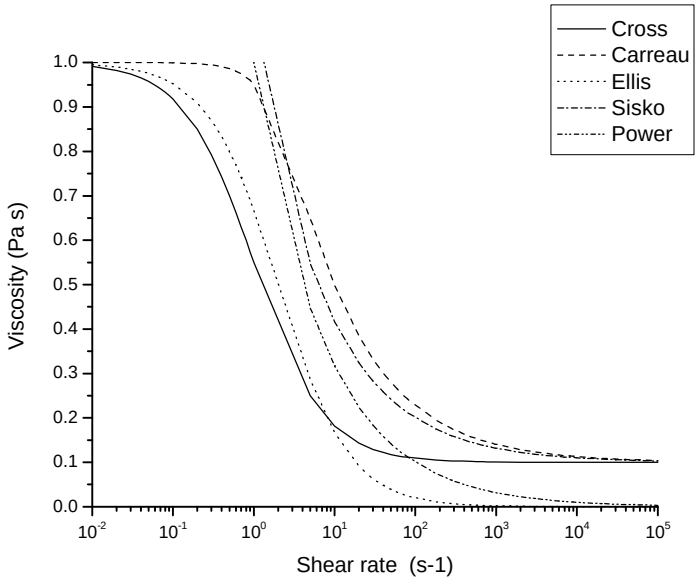

Picture 8 Viscosity- shear rate plot for the shear-thinning models. The model parameters are chosen in order to visualize similarity and difference between the models.

4.1.3 Viscoplastic models

Many complex fluids, and especially multicomponent fluids with either one or several different fluids and phases, are often by models containing a threshold in the shear stress - shear rate functions. If a constant stress is applied to a Newtonian fluid or the pseudoplastic fluids described in the previous paragraph, they will immediately deform. In the case of viscoplastic fluids this is not the case. If the applied stress is small enough, the fluid element will not deform, only exceeding a certain amount of stress, the yield stress, the fluid element will deform.

For a fluid displaying a linear ratio for shear stress and shear rate, but where the stress at zero shear rate does not become zero, the Bingham model {7} is used. The Bingham model is a special case of the power-law model, where the power exponent n is zero. The t_0 is the yield stress, the stress limit above which the fluid will deform. In this model the viscosity μ is a constant.

$$\begin{aligned} t &= t_y + m \cdot \dot{g} && , t \geq t_y \\ \dot{g} &= 0 && , t < t_y \end{aligned} \qquad \{7\}$$

If the viscosity μ is replaced with a power-law relation for the viscosity, the model is referred to as the Herschel-Bulkley model {8}. If n=1, the model is equal to the Bingham model. The fluid is pseudoplastic with yield stress if 0<n<1, and dilatant if n>1.

$$\begin{aligned} t &= t_y + k \cdot (\dot{g})^n && , t \geq t_0 \\ \dot{g} &= 0 && , t < t \end{aligned} \qquad \{8\}$$

The Casson model {9} differs in the curvature of the stresses plotted against shear rate, as shown by picture 9. The Casson model is little used, but has been claimed to be good for simulation of suspensions.

$$\begin{aligned} \sqrt{t} &= \sqrt{t_y} + \sqrt{m \cdot \dot{g}} && , t \geq t_y \\ \dot{g} &= 0 && , t < t_y \end{aligned} \qquad \{9\}$$

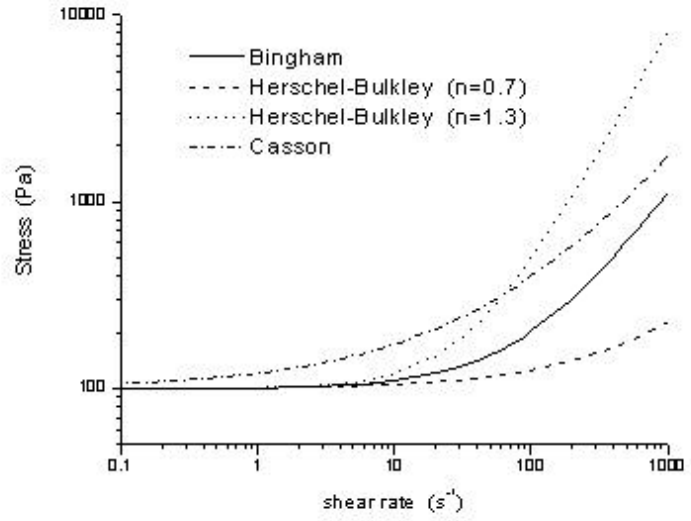

Picture 9 The viscoplastic models, the model parameters are vhosen in order to show the similarity and difference between the models.

The viscoplastic models, especially the Bingham and Herschel-Bulkley models have been used for flow modeling of fiber suspensions, and are probably slightly more widely used than the power-law model. There are some issues, though, which are related to the use of the viscoplastic models that need be considered. First, the existence of yield stresses has been questioned by, for instance, Barnes and Walters [53]. In their paper they present that the yield stress comes from extrapolating the shear behaviour data of the experiments. With low enough shear rate no clear yield stress can be seen. But they acknowledge that the yield stress hypothesis is very useful for modeling purposes.

Another issue that must be remembered, which is closely related to the partial success of especially the Bingham model, is the water slip annulus. If the yield stress is suitably chosen, the Bingham model will predict quite similar results as the model presented in this report, due to the modeling of the slip layer, which is the core of the report. The velocity profiles presented in section 9 of this report are very close to velocity profiles predicted by the power-law and

also very close to velocity profiles predicted by the Herschel-Bulkley model. The significant detail in this report is that the slip produces velocity profiles, both measured and simulated, that look very "flat", and easily lead to the questionable conclusion about the existence of yield stresses.

4.2 Turbulence Model

As the present work is based on large-scale measurements in pipes and the main issue in this project is the developed slip function, the turbulence model is chosen to be one of the simplest and most widely used models, the k-e model as presented in Wilcox [54].

The effects of turbulence is modeled by using an equation for the eddy viscosity,

$$n_T = C_m \frac{k^2}{e} \qquad \{10\}$$

which is the addition to the viscosity caused by turbulence to account for the Reynolds stresses. C_μ is a constant, k is the turbulent kinetic energy and e is the dissipation rate of the turbulent kinetic energy.

As the influence of viscosity cannot be disregarded in the turbulent region, a low Reynolds number approach might be considered. Wikström and Rasmusson [34] compared a high Reynolds number k-e model and a low Reynolds number k-? model. Both model predicted the shape of the pressure peak in the screening application quite well.

The high Reynolds number models use wall functions to set the stress velocity coupling at the walls, whereas the low Reynolds number models simulate the boundary layer to the viscous sublayer. Thus the mesh for using a low-Re model is required to be much denser near the walls.

Of the different low Reynolds number models that are available, and which are implemented in FLUENT [65], the Lam-Bremhorst modification of the k-e model is briefly discussed. The model is based on the addition of a viscous damping into the equations for the eddy viscosity. An addition is also made to the transport equation for the dissipation. The constants within the model are different.

In order to improve the Lam-Bremhorst low-Re k-e model to account for strongly non-Newtonian flows, Malin [55]-[57] made one modification to the viscous damping by introducing an empirical correlation for the fluid index n {6}. He showed that the model returns good results for pipe flow friction data over a large range of generalized Reynolds numbers and Hedström numbers for power-law {6}, Bingham {7} and Herschel-Bulkley {8} fluids.

The influence of the fluid index n is that the height of the viscous sublayer is decreased for smaller values of n. As the present work does not include measurements from within the fluid zone that are detailed enough to determine the water annulus thickness and velocity profiles in the pulp "plug" and within the water annulus, it is not sensible to compare turbulence models to one another before much more reference data is available.

For turbulent flow near a surface, the relation between velocity and shear stress varies with normal distance from the wall. The boundary layer is divided into the viscous sublayer, the buffer layer and the logarithmic layer, Wilcox [54]. The boundary layer is not solved at any stage of the computations within this work, but as the water annulus thickness is compared to the height of the boundary layer of fully turbulent flow, the equations are presented in brief.

For the laminar sublayer, in which viscous effects are dominant, the relation between the velocity and the boundary layer height is linear. As the viscosity of water is constant, the shear stress is

$$t_w = m\frac{\Delta u}{\Delta y} \qquad \{11\}$$

Further away from the wall the relation between the stress and velocity is no longer linear, but is modeled with wall functions, which have been developed based on measurements. Spalding [58] presented a model, which combines all regions of the boundary layer. This model {12} is usually valid up to y+> 100, up to the point where the outer layer increases more rapidly than the logarithmic layer.

$$y^+ = u^+ + e^{-kc}\left[e^{ku^+} - 1 - ku^+ - \frac{(ku^+)^2}{2} - \frac{(ku^+)^3}{6}\right] \qquad \{12\}$$

y+ is the dimensionless height of the boundary layer, for turbulent flow simulation there usually exist restrictions regarding grid resolution near the wall, usually given as the y+ value of the simulations. The y+ is calculated as

$$y^+ = \frac{u_t}{n}y \qquad \{13\}$$

where u_T is called the friction velocity,

$$u_t = \sqrt{\frac{t}{r}} \qquad \{14\}$$

The dimensionless velocity, u+, is the ratio of the velocity and the friction velocity.

$$u^+ = \frac{u}{u_t} \qquad \{15\}$$

4.3 Wall Slip

Many industrial fluids show a distinct slippage at the wall, this is a feature of most suspensions. As discussed in section 3, in flowing suspensions the particles tend to move away from the walls due to hydrodynamic forces. The mechanisms for the wall slip may differ, but some features are very similar. Joshi et al [59] presents a unified wall slip model for polymer solutions and melts, which is based on two mechanisms, weak interfacial slip based on network dynamics, and strong slip due to disentanglement and debonding of the polymer chains. The shape of the slip-stress curves presented seem quite similar to the typical pulp flow head loss curves, as in picture 3 on page 9. Joshi's model is capable of predicting influence of the pipe diameter on the flow curves, and also some hysteresis effects and the possibility of fluctuations in flow rate and pressure during extrusion.

The term wall slip does not mean that there would be zero friction at the wall, only that the velocity at the computational wall does not necessarily have to be zero. On the physical wall the velocity is zero, but as the annular slip film that is formed is infinitely thin compared to the other dimensions of the flow, this annular film is not included, it is modeled. Picture 10 shows the velocity profile for the two cases, implying the difference in shear stress as well.

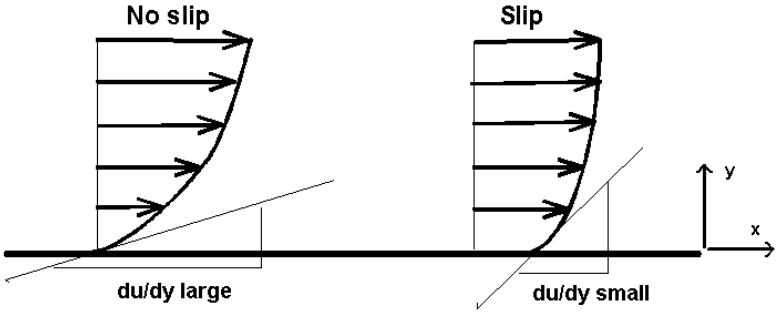

Picture 10 The difference between the normal no-slip case and wall slip. The shear stress is a function of the velocity gradient at the wall.

The slip models have been included in commercial flow CFD packages, in POLYFLOW [60] three different slip laws are available. The generalized Navier's law {16}, which is used later in this report, is the simplest version.

$$f_s = F_{slip}\left(u_{wall} - u_s\right)\left|u_s - u_{wall}\right|^{e_{slip}-1} \qquad \{16\}$$

Here u_{wall} is the velocity of the wall, which in most cases is zero. u_s is the slip velocity, which equals the velocity of the bulk fluid at the end of the annular slip film. F_{slip} and e_{slip} are constants that have to be determined for the material. f_s is the shear stress that is applied on the computational wall, this function may be given any arbitrary dependence on the slip velocity. There usually exists only one combination of mass and force balance that lead to a converged solution.

5 Pulp Model

For the fully developed pipe flow a stress balance can be made. The pressure drop (Δp) in a length of pipe (Δl) is proportional to the shear stress t at any distance from the pipe center according to

$$\frac{\Delta p}{\Delta l} = \frac{2}{r} t(r) \qquad \{17\}$$

for any r from the pipe center r=0 to the pipe wall r=R. For an axially symmetric pipe the axial direction component (z) of the Navier-Stokes equation is

$$-\frac{\partial s_{zz}}{\partial_z} - \frac{1}{r}\frac{\partial}{\partial r}(r s_{rz}) + ru \cdot \nabla u_z = r f_z$$

$$s_{zz} = -p + 2m\frac{\partial u_z}{\partial z} \qquad \{18\}$$

$$s_{rz} = m\left(\frac{\partial u_z}{\partial r} + \frac{\partial u_r}{\partial z}\right)$$

The volume force f_z is zero, as well as ∇u, σ_{zz} and $\partial u_r/\partial z$ in the σ_{rz} part. In a fully developed flow the z derivative vanishes. The equation becomes:

$$-\frac{1}{r}\frac{\partial}{\partial r}(r s_{rz}) + \frac{\partial p}{\partial l} = 0 \qquad \{19\}$$

The viscosity μ is given its shear rate dependence, now according to the power law {20}. Any of the other generalized Newtonian functions can be used instead, but the integration becomes more difficult due to the extra terms.

$$m = k\dot{g}^{n-1} \qquad \{20\}$$

Reordering the terms and integrating once with regards to dr results in

$$\frac{\partial p}{\partial l}\frac{r^2}{2} = r k\left(\frac{\partial u_z}{\partial r}\right)^n + C \qquad \{21\}$$

Here the integration constant C is zero, due to du/dy(0)=0. The term ∂p/∂z equals Δp/Δl for a fully developed pipe flow, see equation above. Integrating once more results in the expression for the velocity profile as a function of the position.

$$u(r) = -\left(\frac{\Delta p}{\Delta l\, 2k}\right)^{\frac{1}{n}} \frac{n}{n+1} r^{\frac{n+1}{n}} + D \qquad \{22\}$$

u(R) then should return the slip velocity, or equal zero in the case of a no slip condition.

$$u(r) = \left(\frac{\Delta p}{\Delta l\, 2k}\right)^{\frac{1}{n}} \frac{n}{n+1}\left(R^{\frac{n+1}{n}} - r^{\frac{n+1}{n}}\right) \qquad \{23\}$$

The velocity profile must also result in a chosen mean velocity u_{avg}.

$$u_{avg} = \left(\frac{\Delta p}{\Delta l\, 2k}\right)^{\frac{1}{n}} \frac{n}{3n+1} R^{\frac{n+1}{n}} \qquad \{24\}$$

If a linear wall slip function is introduced, in which F is a constant,

$$t = -F\, u_{slip} \qquad \{25\}$$

inserting u(r) and the wall shear stress, this equation becomes

$$\frac{\Delta p}{\Delta l\, 2} r + F\left(-\left(\frac{\Delta p}{\Delta l\, 2k}\right)^{\frac{1}{n}} \frac{n}{3n+1} r^{\frac{n+1}{n}} + D\right) = 0 \qquad \{26\}$$

Inserting D into equation {26} the velocity profile becomes

$$u = \left(\frac{\Delta p}{\Delta l\, 2k}\right)^{\frac{1}{n}} \frac{n}{3n+1}\left(R^{\frac{n+1}{n}} - r^{\frac{n+1}{n}}\right) + \frac{\Delta p}{\Delta l\, 2F} R \qquad \{27\}$$

This velocity profile must result in a chosen mean velocity u_{avg}, integrating the parts, and cleaning up results in

$$u_{avg} = \left(\frac{\Delta p}{\Delta l\, 2k}\right)^{\frac{1}{n}} \frac{n}{3n+1} R^{\frac{n+1}{n}} + \frac{\Delta p}{\Delta l\, 2F} \qquad \{28\}$$

where the first term on the right side is the solution of the no-slip case for a power-law fluid. The second part is the slip correction term, u_{slip}, it "adds" to the velocity to result in the correct bulk flow rate.

5.1 Non-Newtonian Flow and Turbulence

The combined use of a continuous rheology model and a continuous turbulence model is based on the assumption that in the beginning of the flow curve, the added friction by turbulence is negligible, but becomes significant at higher flow rates. Picture 11 describes the differences between the laminar and turbulent modeling approach. To the knowledge of the author, this is the first picture where this type of distinction between laminar and "turbulent" flow of pulp suspensions in pipes is presented.

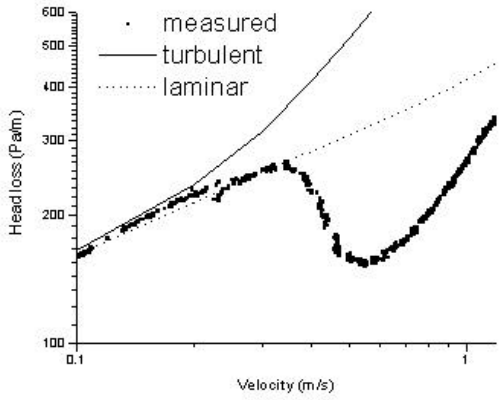

Picture 11 Comparing laminar and turbulent flow simulations to the measured values for 1.5% bleached birch. Both curves have been simulated using identical model constants, using standard (no slip) wall functions.

The picture presents the head loss measurement results of a birch pulp, and the results of the rheology model. The laminar simulation contains only the power-law model for viscosity, the turbulent simulation contains both the power-law viscosity model and a ke-turbulence model. The turbulent simulation contains both the molecular viscosity and the eddy viscosity. The molecular viscosity is a function of the shear rate, instead of constant, as usually in turbulent flow modeling.

$$\mu_{effective} = \mu_{laminar} + \mu_{turbulent} \qquad \{29\}$$

It is important that both of these are available in the flow simulation program, as the turbulent flow does not allow an analytical solution, as the laminar flow does. As the laminar viscosity is decreasing with increasing shear rate, and the eddy viscosity is increasing, there will be some location where the decrease of the laminar viscosity equals the increase in eddy viscosity. At this flow rate, the head loss curve predicted by the simulations will change type, from the logarithmic growth of the laminar curve to an exponential growth of the turbulent curve. This assumption regarding the flow of suspensions has never been presented before, and is one of the corner stones for the rest of the report.

This change of curve type is important for the development of the flow models. From picture 11 it can be noticed that the laminar curve will Cross the experimental curve at 2-3 m/s mean velocity in the pipe, a velocity which is not particularly high. The laminar flow model can be used for the regions where the predicted head losses are higher than the experimental data, this can be corrected by different types of slip functions, as described earlier. But at higher flow rates than the point where the laminar and experimental curves Cross, it is not possible to produce any kind of function that can return the correct friction. It is not possible to exceed the stresses that are resulted by the flow and rheology.

The turbulent flow curve, on the other hand, is growing exponentially, and seems to be a natural choice for the model. At low flow rates the laminar viscosity dominates, causing the head loss predictions to follow the 'plug flow' part of the measured curve, where the rheology model constants were determined. At infinite shear rate, the rheology model returns a very small viscosity, causing the head loss predictions to follow the head loss curve of water flow.

5.2 Wall Slip for Turbulent Flow

Extending the slip model to apply for the turbulent flow based on the rheology modeling presented earlier requires solving the cases. The rheology model and the turbulence model are both activated, and the simulations are performed with standard wall functions, that is, without slip at the walls. No analytical solution is possible for the turbulent case, therefore the slip modeling must rely on a previous simulation series.

Picture 12 shows the measured head losses and the simulated values, without the wall slip. The arrows in the graph show the influence of the wall slippage, and the relative part of the slip velocity compared to the mean velocity is presented. That the wall slip velocity amounts to 75% of the mean velocity shows that the flow will very much look like solid plug. Even if the velocity profile is determined, the profile will look quite "flat" unless the instrument has a very high spatial resolution near the walls.

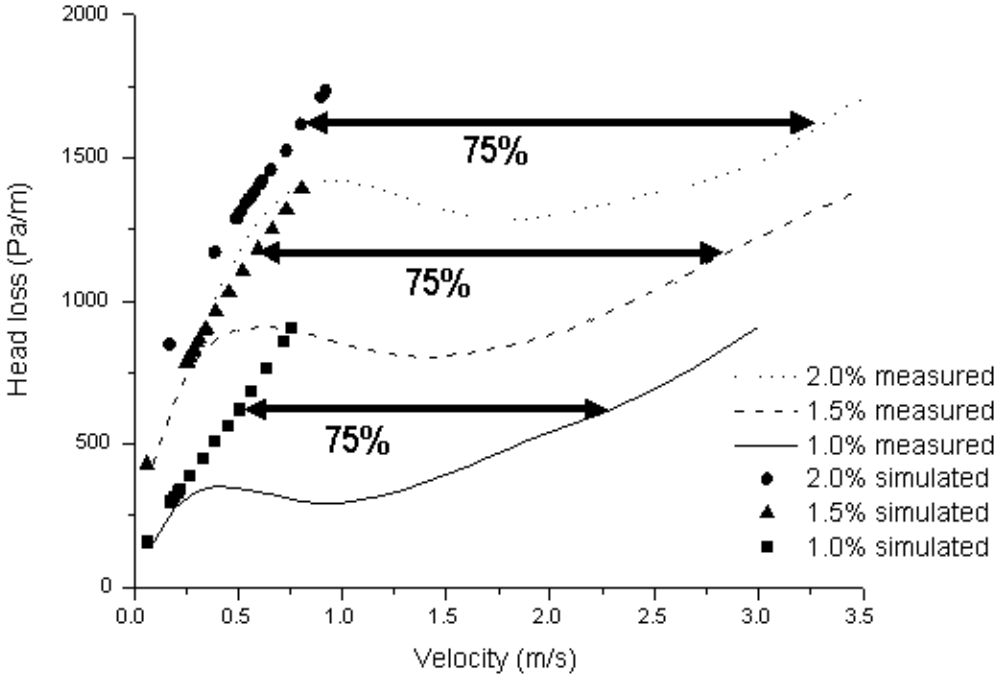

Picture 12 Spline interpolated curves representing the measured head loss values of pine pulp and simulations. The numbers indicate the approximate amount of wall slip, expressed as the ratio between the wall slip velocity and the bulk velocity. That the numbers are equal is a coincidence in the choice of reference points.

The wall boundary condition for the turbulent pulp flow is implemented in a similar way as the laminar slip model. For the low flow rates, the turbulent viscosity does not have any significant influence.

5.3 Comparing the Different Simulation Options

At very low flow rates the pulp can be simulated as laminar. At intermediate flow rates the wall slip is the most important phenomenon. At higher flow rates all laminar models fail. The wall slip model applied to the laminar flow shows a decent agreement to the measured values until the laminar and measured curve start merging. It is not possible to use laminar models with or without wall slip after the curves Cross. The different simulation options are compared in picture 13, and the result curves are presented separately in pictures 14-17.

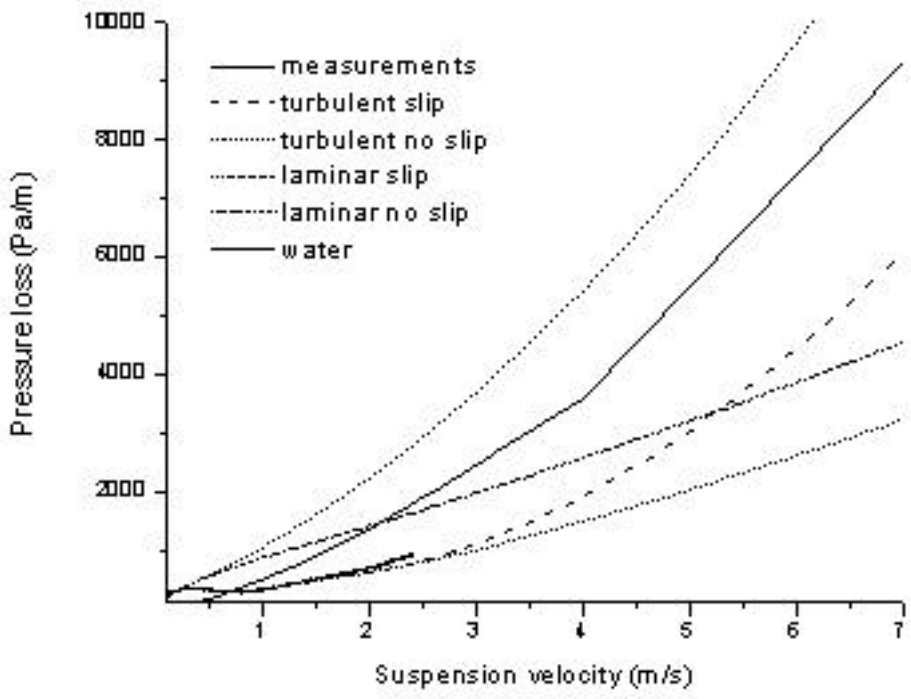

Picture 13 Different simulation options compared for 1% birch pulp in a 40mm pipe. The simulated curves are presented separately in the following pictures.

Picture 13 is the most important piece of results in the entire report, this picture summarizes all simulation alternatives and the outcome of the same. Based on picture 13 it is possible to say which of the simulation alternatives are real choices when building models for simulating any pulp flows, regardless of pulp type, fiber properties or fiber concentration. It is worth noticing that the methods used for fitting the different curves are not import, it is the shape of the curves that are to be compared.

In picture 14, the laminar simulation is isolated. Here only the rheology model has been activated. At very low flow rates the agreement with the measurements is good, the wall slipping region is not captured, which has already been discussed in section 3.3. As presented in section 3.2 and 3.3, the head losses of flowing fiber suspension will merge with the head loss curve of water at very high flow rates. The reason that the laminar flow models can be discarded, is that at higher flow rates, in picture 14 approximately at 5 m/s, the simulated curve Crosses the extrapolation of the measurement curve.

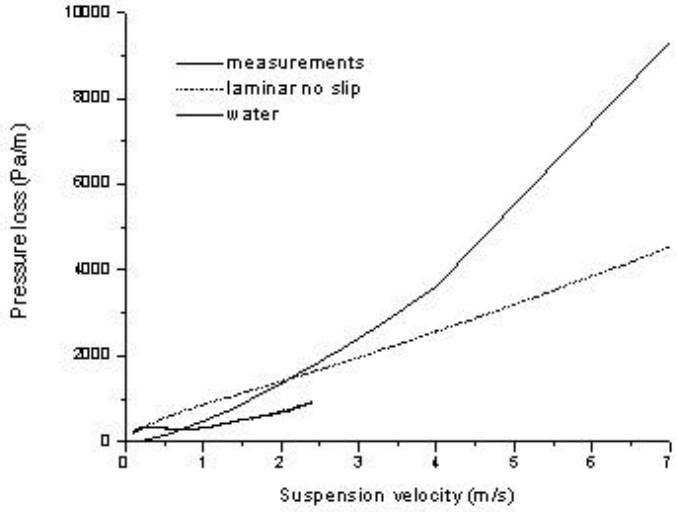

Picture 14 Laminar power-law flow.

In picture 15, the laminar rheology model has been equipped with a slip-stress model at the pipe wall. This corrects the head loss predictions in the wall slip region, and the agreement is reasonable all through the measured range. This is due to the limited range over which the velocity profile within the bulk suspension is spread. As the head losses of the suspension are bound to increase exponentially as the flow is measured at higher flow rates, the result of the laminar slip model becomes non-physical. It is not possible to exceed the stresses generated within the fluid with any kind of wall functions.

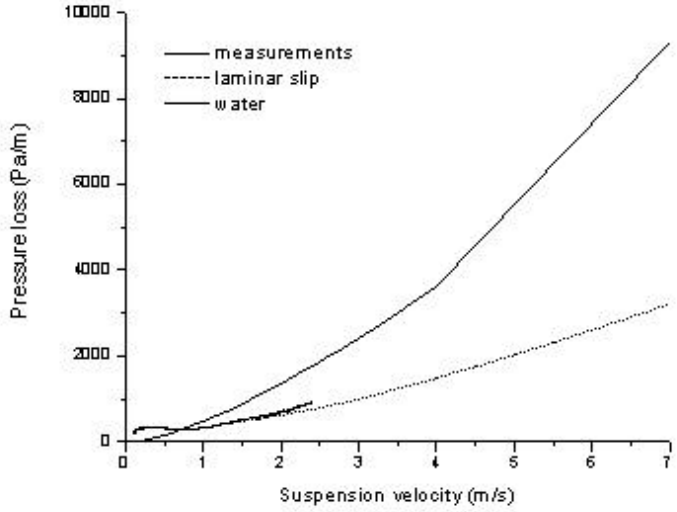

Picture 15 Laminar power-law flow with the slip model at the pipe wall.

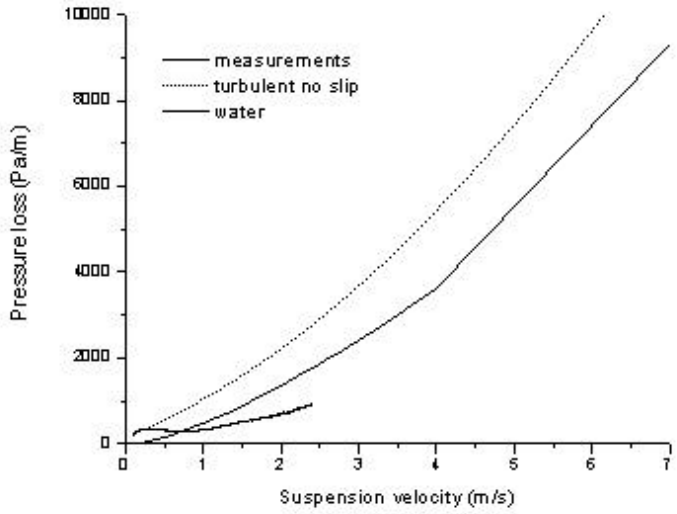

Picture 16 Turbulent power-law flow.

Picture 16 presents the logical combination for the exponentially increasing head losses, combining a turbulence model and a rheology model. Both models are active all the time, resulting in a reasonably good agreement in the beginning of the flow curve. As the flow rate is increased, the head losses are grossly over-predicted, but this is only as can be expected as the laminar model also returns too large head loss.

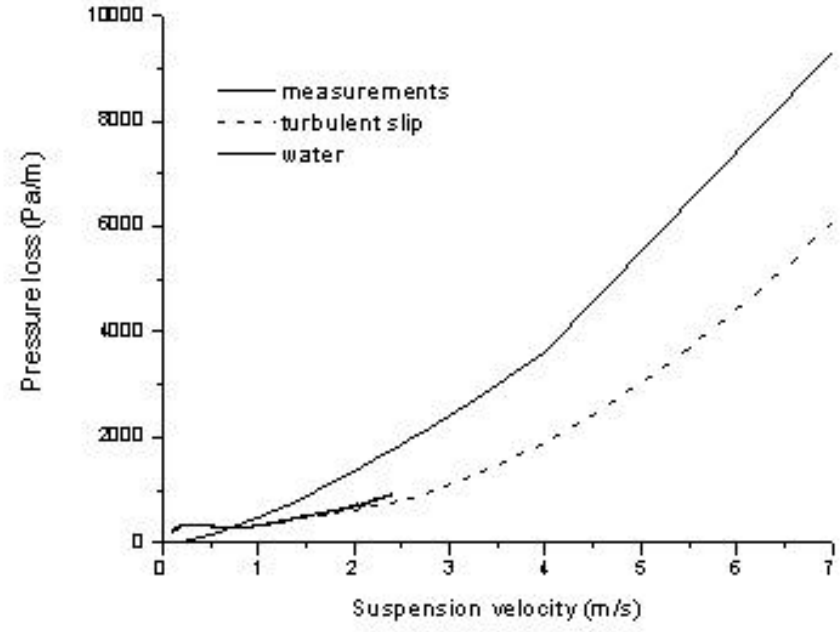

Picture 17 Turbulent power-law flow, with the slip model at the pipe wall, which all together make the pulp model.

The turbulent no-slip simulations result in far too high head losses already at moderate flow rates, but will never Cross the measured curve. The slip correction for the turbulent flow follows the measured curve, and can easily be

made to follow it through all flow rates. Picture 13 is probably the most important picture in this report, the picture summarizes all simulations models, and shows the new way to simulate all pulp flows with one function. This is of fundamental importance.

5.4 A Few Definitions for the Report

For the rest of the report the following expressions are used:

- rheology model: Refers to the power-law model.
- turbulence model: Refers to some version of the ke-turbulence model
- slip model: Refers to the slip-stress function specified at the wall, either laminar or turbulent. These are identical for the first part of the curve.
- wall function: Refers to the slip model
- standard wall function: Refers to the wall functions used at wall boundaries when simulating ordinary turbulent flows
- pulp model: Refers to the model developed in this report. This incorporates a rheology model, a turbulence model and a wall function, none of which can be removed or arbitrarily substituted.

6 Motivation of Approach

The work is based on a few assumptions:
1 - The suspension behaves asymptotically as a power-law fluid for small average velocities in a pipe.
2 - The deviation from the power-law fluid (no slip) at non-zero velocities may be explained by a positive slip velocity, added to the whole velocity profile of the power law fluid, originating from a thin fluid layer formed at the wall.
3 - For a given pulp and at a given concentration there exists a generally valid, geometry independent relationship between the wall shear stress and the slip velocity.
4 - A supporting hypothesis to the previous is that for a given pulp the shear stress versus velocity curve has a similar shape at various consistencies.

Motivation for the hypothesis point by point:
1. a) Indications from pressure drop experiments at low velocities; the parameters n and k can be fitted to data at small velocities independent of pipe radius.
   b) There are measurements on velocity profiles (presented in section 9.3) that also indicate a power law fluid shape, or at least do not defy it.
2. The power law fluid with no slip, as fitted to data at small average velocities, is always above the experimental curve (if turbulence model is included this is true also for the turbulent region). The fluid layer has been observed experimentally by several authors, as described in the introduction.
3. Almost all measurement series with more than one measured pipe diameter agree with this, in those few that do not, the cause of error has been show to be the measurements, usually the cause is a very short calming length, presented in sections 3.2 and 9.1.

6.1 Number of Fibers in a Few Applications

One demonstration in favour of the rheology models, is to estimate the number of fibers present in a specified volume. Using the fiber properties presented by Kerekes and Schell [4] for Douglas fir and aspen

Table 1: Fiber properties

	fiber length	fiber diam	density
Douglas fir	2.7 mm	40 µm	0.545
Aspen	0.83mm	18 µm	0.433

The volume of the individual fiber is roughly equal to

$$Volume = length * (\frac{diam}{2})^2 * p$$

The volumes of the two wood fibers are $V_{fir}=3.4*10^{-12}m^3$ and $V_{aspen}=0.21*10^{-12}$ m^3. For a 1% Douglas fir suspension, the crowding number is 151, and for a 1% suspension of aspen, the crowding number is 34. The crowding number gives an estimate on the tendency of the fiber suspension to form flocs.

Table 2 Number of fibers simultaneously present in applications

	approx volume (m^3)	approx conc (%)		number of fibers, Douglas fir	number of fibers, aspen
head box	1	1		5.41 e+9	1.09 e+11
Mixing tank	150	3		2.43 e+12	4.92 e+13

The number of fibers present in an application is proportional to the consistency and the volume, which is presented in table 2. This simple calculation shows that with the current computer capacity, it is not possible to include the individual fibers in the simulation of real papermaking equipment. Compare to picture 5, page 19, in this simulation only 300 fibers of identical and constant shape have been included in a linear flow field. Table 2 clearly shows that for quite some time, Lagrangian particle-tracking simulation methods will not be possible for industry cases, even though they may be successful in describing phenomena such as floc break-up under isolated, idealized conditions.

6.2 Determining Rheology

In order to determine the correct model for the pulp suspensions, rheograms of birch and pine suspensions are presented in pictures 18-19. Rheograms are an item of the past, the data that was once obtained by comparing curve slopes from the rheograms can now be obtained through numerical fit. The rheograms are presented in order to illustrate the rheological properties, and given as further proof of the chosen modeling approach. The rheograms are plotted based on the measurements of Jäsberg, presented in Hammarström et al [61]-[62] and in the appendix. The rheograms have the apparent viscosity {30} on the ordinata, and the mean shear rate of Newtonian fluids on the abscissa. To be noticed, for simplicity the mean shear rate for a Newtonian fluid, according to equation {10}, was used.

$$m_{apparent} = \frac{t_{wall}}{\dot{g}_{mean}} \qquad \{30\}$$

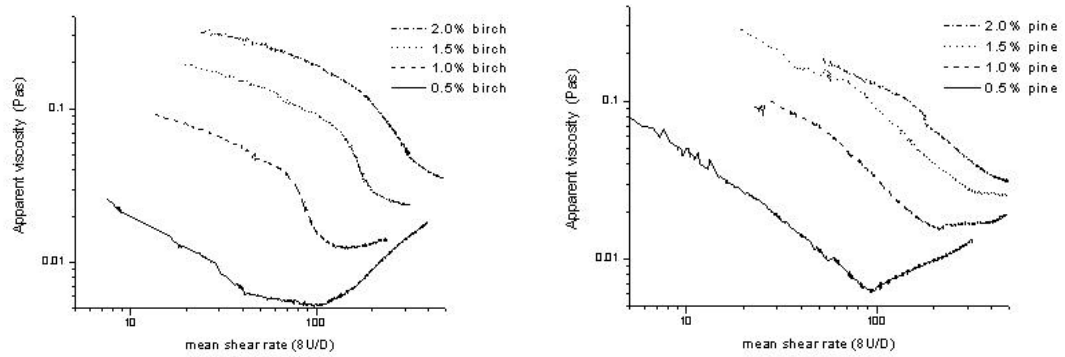

Picture 18-19 Rheograms of birch (left) and pine (right). Pulp data presented in Jäsberg et al [61]-[62].

Following the discussion in the preceding paragraphs, the first relatively straight slope in the rheograms suggest that the suspensions can be modeled using pseudoplastic models. The rapidly decreasing apparent viscosity, best seen for 1% birch pulp in picture 18, is explained by the slip layer. The apparent viscosity approaches a steady value for the higher consistencies. This is due to the choice of measuring range. A shear-thinning model that stabilizes on a constant viscosity for high shear rates suggest that the Sisko model would be the ideal choice for the modeling.

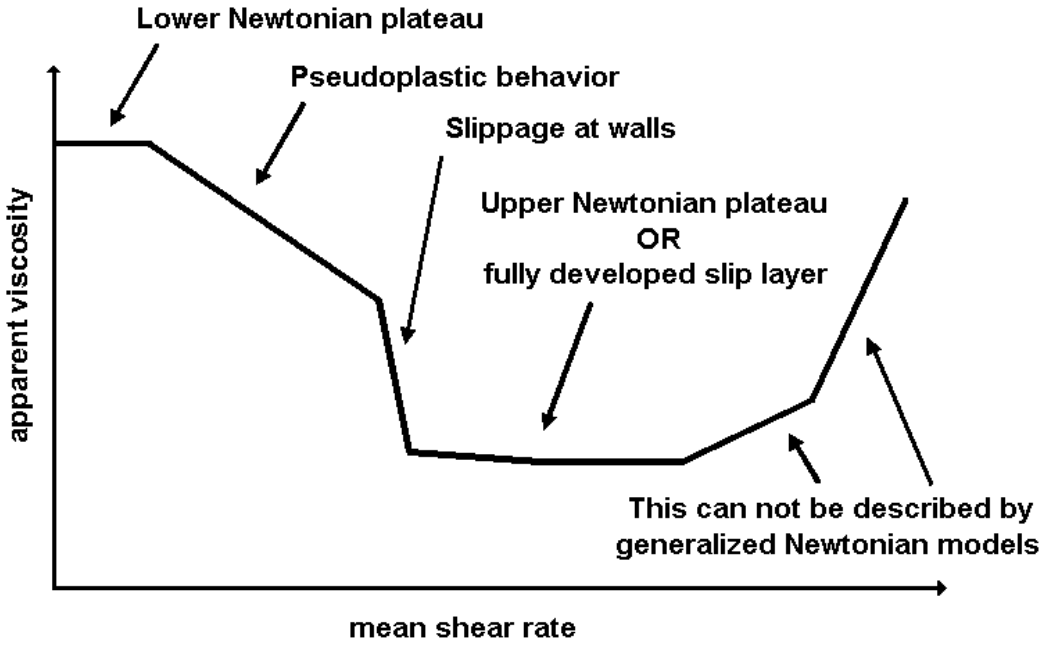

Picture 20 Illustration showing the different regions in a rheogram.

In order to point out the individual parts in the rheogram, a similar shape is drawn in picture 20. The rapidly decreasing part in the rheogram in picture 20 suggests that either the material is undergoing structural breakdown or reordering, or else a slip layer is formed. This interpretation of rheograms has to the knowledge of the author never been presented in any reference books on

rheology, it is part of the new flow features that have been presented within the project. The upper Newtonian plateau can be observed for many substances, but for a suspension which has been shown to possess a slip layer, it can also be interpreted as that the slip layer is fully developed, and behaves as a Newtonian lubrication layer between the bulk fluid and the wall.

But increasing the flow rate, until the increasing part of the curves is reached, best seen for 0.5% pulp of either suspension in pictures 18-19, can not be explained by any generalized Newtonian rheology model. An upper Newtonian plateau is possible, where the viscosity approaches a constant value, but an increasing value of the apparent viscosity is not possible for the pseudoplastic flow models. Instead, this increasing curve resembles turbulent flow, which has been shown to exist with suspensions.

In order to further illustrate the significance of the combination of a pseudoplastic model and the non-zero wall velocity, the laminar velocity profiles for pipe flow with different values of the power exponent n are plotted in picture 21. The profiles are significantly 'flatter' with increasing values of n. Typical values for pulp suspensions 1-3% consistency is n=0.3-0.6.

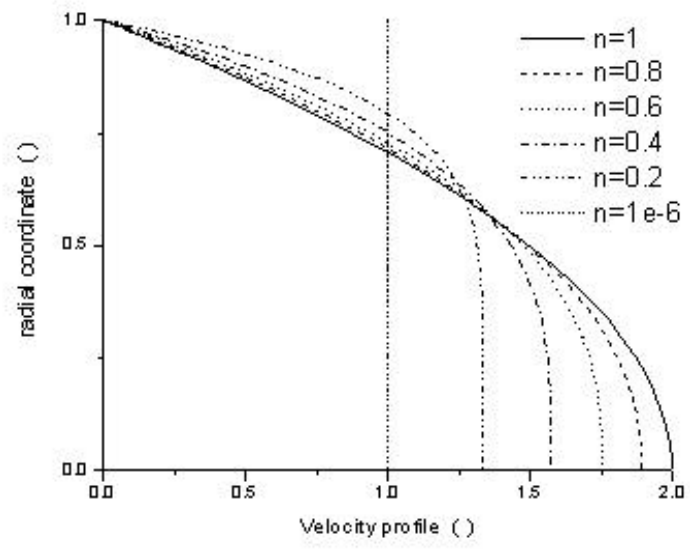

Picture 21 The velocity profile in a pipe for different values of n.

Picture 22 shows the corresponding velocity profiles for constant n, and varying shear stress at the pipe wall. The maximum shear stress at the pipe wall is of course identical to the shear stress required by the no-slip solution, and a zero shear stress returns a constant velocity profile. The maximum wall shear stress can not be exceeded, nor can the velocity at the wall exceed the velocity in the centre of the pipe, which equals the case of a zero stress at the wall. In this report the intermediate values of shear stress are of interest. Between the two limiting values, there are any number of possible shear stress values, for all of which there exists a unique velocity profile. For the case of the wall slippage

resulting from a water annulus, the slip velocity-shear stress ratio can be determined. It is important to remember that the shear stress within the bulk fluid and the shearing annulus must be equal, and must satisfy the conservation of mass.

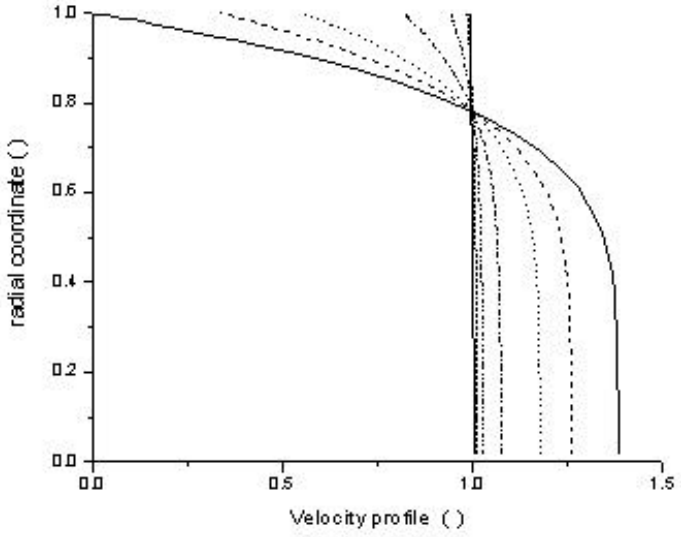

Picture 22 The velocity profile in a pipe for different wall shear stresses applied on the pipe wall.

6.3 Turbulence Modeling

Flow of paper pulp suspensions show qualities that are usually attributed to turbulence. Turbulent flow of pulp suspensions is, however, a non-trivial issue to which there has so far been done very little research that can be used for flow simulation purposes. Even the "onset of turbulence" has not been determined properly. The traditional way of determining whether a flow is laminar or turbulent is the Reynolds number. There are a few problems involved in using the Reynolds number for suspension flow, a few of which are shown by picture 23.

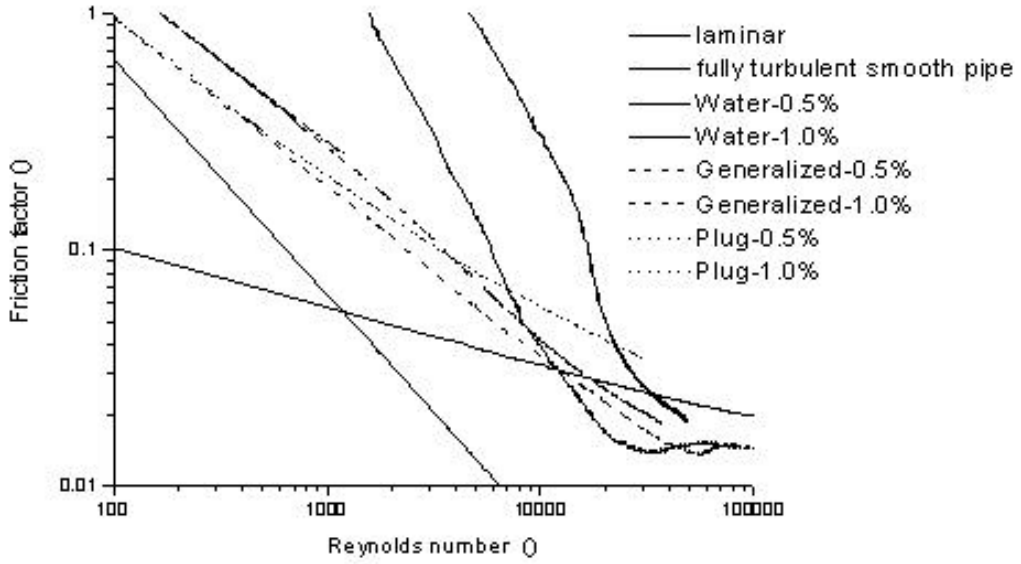

Picture 23 Friction factor diagram for 0.5 % and 1.0 % birch pulp, with different formulations for the Reynolds number. The purpose of the picture is to show that the Reynolds number is not a sensible number for pulp flows. "Laminar" and "turbulent" must be determined in other ways.

In the picture, the friction factors are plotted against a few Reynolds numbers. These are the Re based on water flow, the generalized Re for a power-law fluid, the Re based on water annulus height and generalized Re based on the velocity in the pulp core, the mean velocity reduced with the slip velocity.

$$f_{\text{laminar}} = \frac{64}{\text{Re}}$$

$$f_{\text{fully turbulent}} = 0.01 \cdot \left(\frac{10^6}{\text{Re}} + 18.7 \left(\frac{1000 \cdot k}{D} \right)^{1.094} \right)^{0.25} \qquad \{31\}$$

$$\text{Re} = \frac{U D r}{m}$$

$$\text{Re}_{generalized} = \frac{U^n D^{2-n} r}{m_{apparent}}$$

The water Re can immediately be discarded, and the water annulus Re is here a plot of itself over itself, as the annulus height is calculated using the water properties. Measurement results of the annulus height would change this. The friction factor of the fully turbulent pipe flow in a smooth pipe (wall roughness k=0.01mm) curve is included in order to show how the friction factor of the flowing pulp suspensions goes well below this curve, due to the wall slippage. The generalized Re for both the total flow and pulp core shows identical results for the first part of the curve, according to previous assumptions about a non-slipping laminar flow region. The difference between the curves at higher flow rates are a result of the slip layer, the friction factor is significantly decreased if

the slip layer is not considered. As the Reynolds number does not give any immediate help for categorizing pulp flows, the number will not be referred to in this report. If any reference to the Reynolds number needs to be made, this should preferably be the generalized Reynolds number based on the pulp core, excluding the wall slip.

Picture 24 again illustrates the importance of using the correct flow models when determining the rheology parameters. The laminar simulation is the power-law solution of a laminar flow in a pipe. The turbulent non-Newtonian curve is an identical simulation, with the exception that a turbulence model has been activated. Turbulent water is a simulation of water flow in the same pipe.

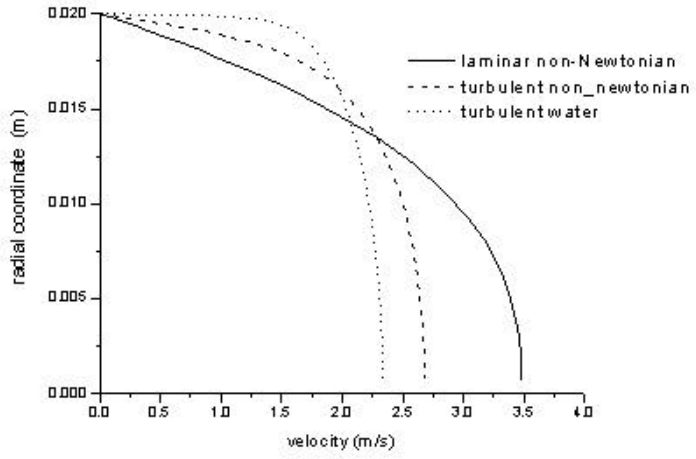

Picture 24 Illustration of the velocity profiles for a few cases.

The message of the picture is that the rheology parameters need be determined under correct conditions, combining head loss data and flow rate data. All three curves in picture 24 are similar enough that some rheology function can be fitted to all of them, of which only one is correct. The rheology parameters must be determined under conditions where turbulence has little or no influence on the result, see for instance picture 12 in section 5.

In picture 25 the wall slippage is introduced for the turbulent flow as well, the picture shows simulation results of pine pulp, c_{mass}=1.0%. As can be seen, the profiles very similar, hence care must be taken so that the fluid parameters are determined in the correct region. For a comparison against measured velocity profiles, a few measured velocity points from within the flow is not enough, the total flow rate must also be accurately determined.

As the current rheology model and slip-stress function are as simple as possible, it is likely that the slip velocity is rather over-estimated than under-estimated. As this is built into the model, the influence is only local.

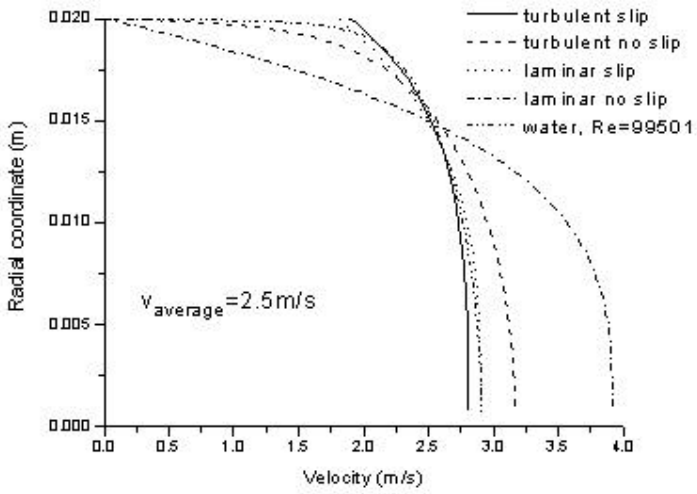

Picture 25 The same simulation performed with different models. The idea of the simulation is to show the similarity of all result curves.

Picture 25 also shows the feature of pulp suspensions at high shear rate, the are very similar in appearance to the velocity profiles of turbulent water. Despite the apparent similarity, the profiles are very different, as will be shown in the next section.

6.4 "Waterlike" Flow

The flow of fiber suspension at higher flow rates is said to be "water-like", the fiber suspension is "fluidised". Even though the pipe flow head loss curve of fiber suspensions merge with the head loss curve of water, it still does not mean that the fiber suspension follows the flow properties of water. Picture 26 illustrates the difference, which also is one of the observations made within the project. In the picture, the dotted line is the velocity profile of water, which is a well-known substance and hence easy to refer to and compare against. The solid line is the velocity profile of the pulp suspension, where the slip layer is represented with the dashed line. The circle highlights the meeting point of the water annulus and the pulp core.

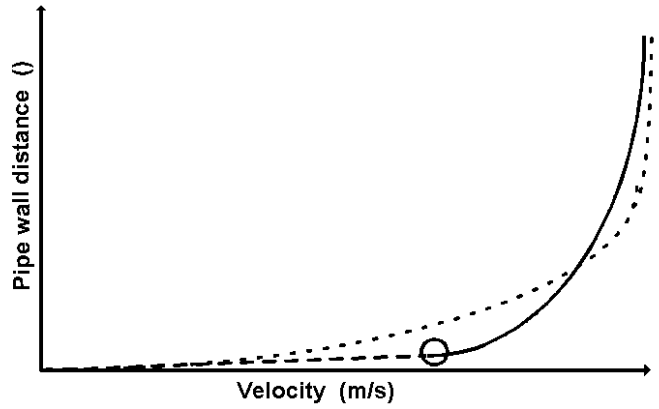

Picture 26 Illustration of the significance of the wall slip, a substance with "far-from-water" properties may look very "water-like" in case there is a significant slip on the walls. The dotted curve illustrates the velocity profile of water, the solid curve the suspension, and the dashed part is the slip annulus. The point where the slip annulus and the bulk flow meet is highlighted with a circle.

The picture is intended to highlight that even tough the two curves look very similar, and may be very difficult to distinguish in measurements, they are still totally different. It is the existence of the slip layer that brings the behaviour, that resembles the behaviour of water, to a substance which is far from water-like.

7 Setting Model Parameters

Pulp flow is an extremely complex flow, with at least two phases present, neither of which can be modeled in detail, for several reasons. It is vain to develop complex constitutive equations for the pulp suspensions, the constitutive equations may be very difficult to use, and as difficult to adapt to new pulp types or flow conditions. For practical purposes, the fluid models need be relatively simple to use, and easy to adapt to new pulp types. As has been shown in section 2, there are numerous way to model the pulp suspension, of which only a few can really be excluded. This is hardly surprising, since all rheology models basically are special cases of one another. Multiphase flow models, on the other hand, will crash into the condition that there are too many unknowns.

The models are not either connected to some particular flow type, even though they are developed using pipe flow as material. There does not exist such things as 'flow model for pipe flow' nor 'flow model for headbox flow', the models are fully capable of simulating all industry-based flows.

As this work is not about any particular device design, nor is numerics the issue, but the development of a fluid model, there is a considerable amount of "parameter fitting" involved. Fitting of parameters, model constants, or be they called whatever, is always present in fluid modeling. As the properties of the fluids have to described by more or less simple relations, which must be correlated against measurements, then all 'model constants' are more or less curve fits. Take for instance the parameters c and ? from equation {12} on page 28, these two numbers are just as much "curve fitted" as any other that are presented and used within this work.

Different parameters for different fluids, this is a natural thing within, i.e. chemical engineering and process technology, where multiple process streams may be mixed and reacting, again producing new substances, which also need new parameters. Within chemical engineering there are two main sources for material properties, Schmidt [63], "Properties of water and steam in SI units" and Barin and Knacke [64], "Thermochemical properties of inorganic substances". Schmidt's book contains the physical properties of water under different conditions, expressed as functions of different conditions, where every single property function is "curve fitted". Especially the Barin and Knacke contains nothing but material parameters, and is one of the corner stones in chemical reaction engineering.

This current work attempts at describing the flow phenomena of some typical pulp suspensions, and presenting generally valid parameters for these, but as the modeling does not yet contain all the flow phenomena, it cannot yet be called the "Barin and Knacke of Pulp Suspensions".

It is important to notice that the contribution of this thesis, both on the modeling and scientific forum, is not some set of equations, but a method. The user has full freedom of either directly using the model as presented in this report, or make his own version of it. It is neither a scientific nor relevant issue in what way the relation between the slip velocity at the wall and the corresponding shear stress is written, this is best set by the user needs and experiences from previous flow modeling of pulp flows.

7.1 Model Parameters

The parameters of the pulp are set by making a least squares fit of the equations as calculated in section 5, and the measured data. The first part of the head loss curve is the laminar flow curve, where the power-law parameters describing the viscosity of the fluid are determined, which is shown in picture 27. There may or may not exist some minute degree of slip on the walls in the upper part of this region, but for simplicity the wall slip is defined as zero at flow rates lower than that of the local maximum.

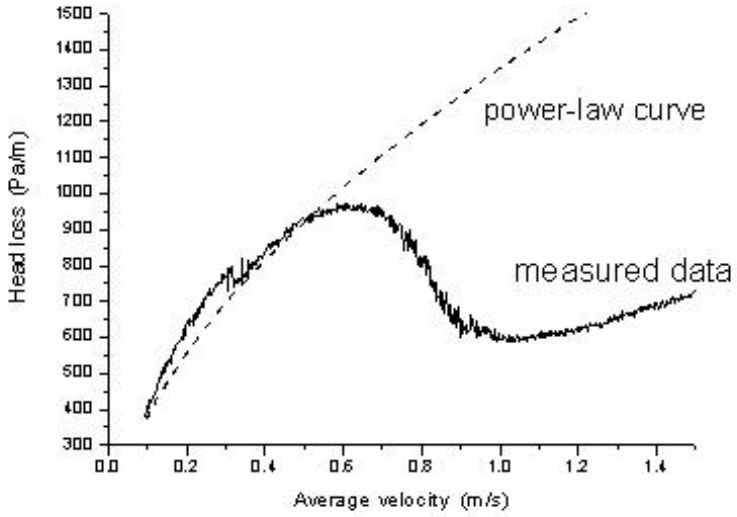

Picture 27 Setting the rheology parameters of the pulp.

The wall slip is determining the behaviour of the pulp flow in the second region, shown in picture 29. Even though the wall slip is assumed zero on the first part of the head loss curve, the part that was used to determine the viscosity parameters of the pulp, the wall slip function can still be used to describe the wall friction in this region.

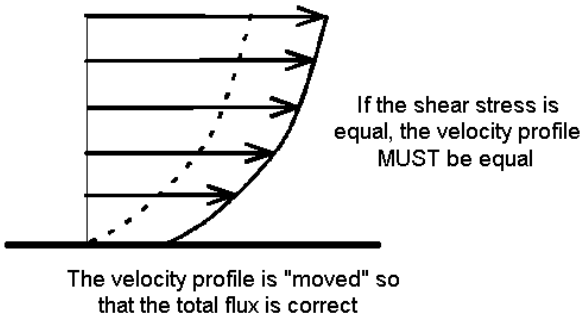

Picture 28 The dotted line is the velocity profile in the plug flow regime, and the solid line is the corresponding velocity profile in the wall slip regime, where the slip has been added so that the correct flux is gained. Notice the same shape of the velocity profiles.

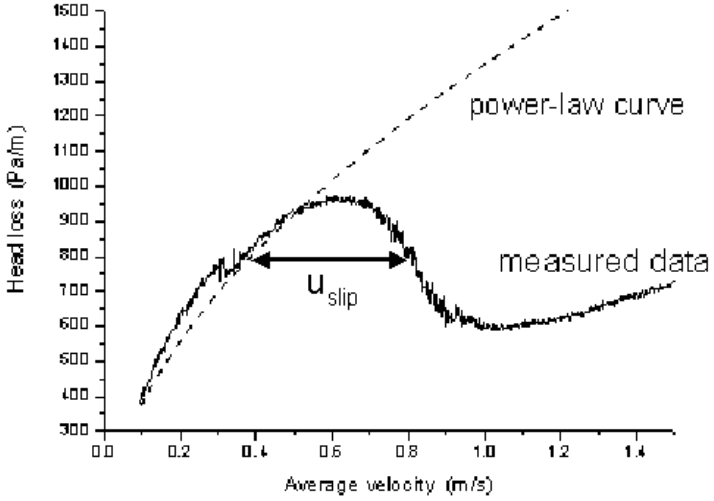

Picture 29 The wall slip function is defined on the "down" slope of the head loss curve

In the first part of the curve, the friction parameter F, equation {25}, is assigned a very large value. This forces the slip velocity towards zero, which allows us to use the same wall slip function in both regions of flow rate.

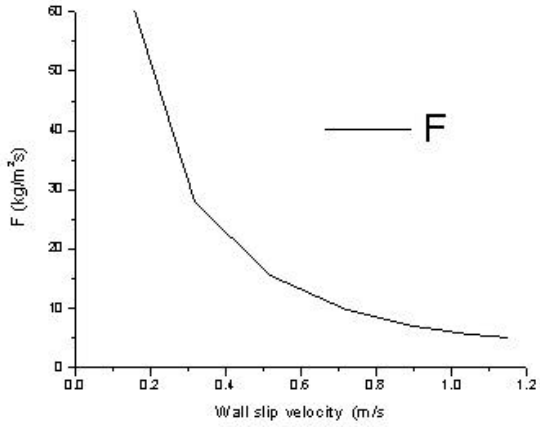

Picture 30 The value of F plotted against the slip velocity. In the first region of the head loss curve the slip velocity approaches zero, and F is very large.

The wall slip function does not need to be a linear function of the slip velocity, in the section 7.2 the suitability of a few types of functions are tested against measured head loss data.

For instance, if the wall slip is assumed to have an exponential relation as in equation {32},

$$t = -F\left(u_{slip}\right)^{e} \qquad \{32\}$$

the average velocity becomes

$$u_{avg} = \left(\frac{\Delta p}{\Delta l\, 2k}\right)^{\frac{1}{n}} \frac{n}{3n+1} R^{\frac{3n+1}{n}} + \left(\frac{\Delta p}{\Delta l\, 2F}\right)^{e} \qquad \{33\}$$

More complex relations can be used, as shown in pictures 33-35, but these require more parameters and are not likely to be solved analytically. A larger number of parameters do not present any problems for the numerical parameter fit, but the function type requiring the least number of parameters resulting in an adequate fit to the measured data is regarded as the most appropriate function.

The function should be valid to very small values of flow rate, but depending on the implementation of the function, it may be required to restrain the validity of the function to a certain stress at the wall, and use the fluid stress below this limit. This limitation does not cause any disturbances in the flow, but may inhibit un-physical results at very low stress levels.

7.2 Setting the Pulp Model Parameters from Measurements

The rheology model has presented so far, exclusively limit the flow to constant consistency on the pulp suspension, which of course is not always the case in real pulp flows. The concentration gradients are later shown to submit to the rheology model, but more research is needed in order to accurately predict the mixing phenomenon of multiple streams of pulp at different concentrations.

Turbulence needs to be further investigated, the turbulence modeling presented in this report is on phenomenological level, there does not exist enough data that validates the turbulence models of any kind, less along data that sets standards for the correct boundary conditions at turbulent pulp flow inlets.

The pulp properties are also included in both of the above mentioned investigations. The pulp properties need to be measured as follows: Identical flows of identical suspensions are compared, identical except for different value of the fiber property to be examined. Duffy [14] has performed exactly

the type of investigations necessary for this purpose. For instance, a suspensions at 1% dry content is measured with fiber lengths at 25%, 50% 75% and 100% of the original mean fiber length at all flow rates, the influence of the fiber length can safely be included as a parameter in the flow models.

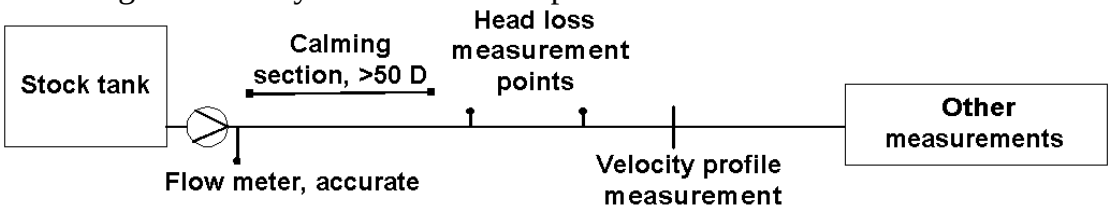

Picture 31 Illustration of the necessary measurement line for determining the model parameters.

The pulp research must be conducted under identical conditions, as for instance shown by picture 31. In the picture, the first item after the pump is a flow meter, which should be as accurate as possible. Any error in the flow measurements result in large errors in the prediction of velocity profiles and turbulent quantities, based on which all flow models for pulp are based.

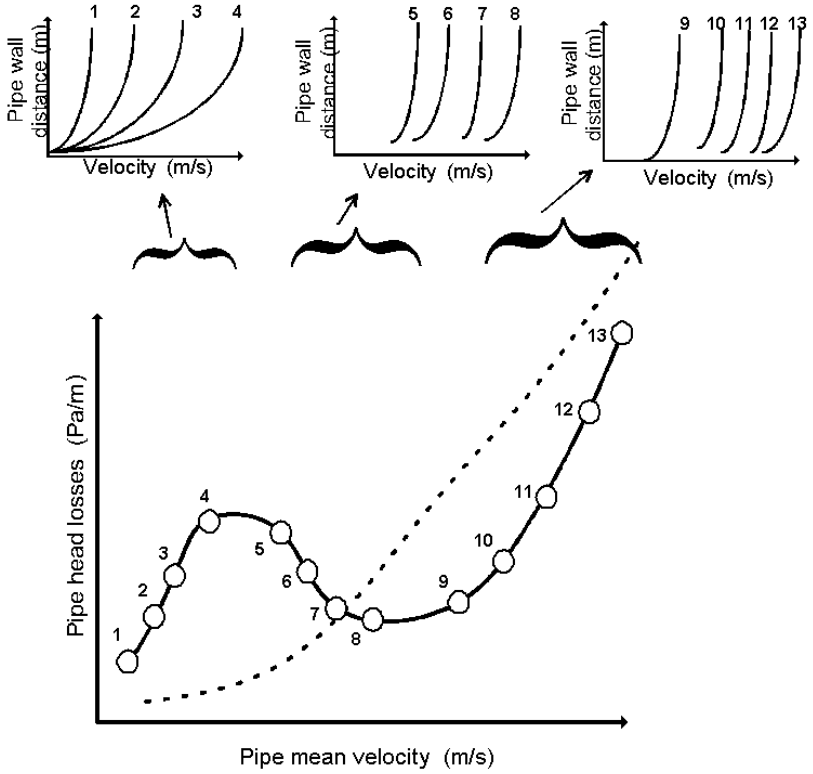

Picture 32 Sketch illustrating how the pipe head loss measurements should me made. The dotted curve is the water head losses, which should also be measured in order to verify the measurements. The circles represent measurement points, of which there should be enough in every region. The really low flow rates are of equal importance as the really high flow rates. If possible, the velocity profile should be measured from at least a few flow rates in each region.

Picture 32 shows how a typical head loss curve may look like, and the velocity profiles from the three different 'regions' are shown on top. Velocity profile measurements as shown in the small graphs in picture 32, can be used for model development just as well as the head loss measurements. By combining

the velocity profile measurements and head loss measurements, all the flow features of the suspension are captured. The rheology model, equation {6}, parameter 'n' describes the shape of the velocity profile, and also the shape of the head loss curve. The rheology parameter 'k' gives the stress level within the bulk fluid, based on the velocity gradients within the bulk suspension. Assuming that no structural breakdown is occurring within the suspension, everything else is resulting from the wall function, which can easily be adopted to suit the measurement data. This technique is illustrated at four different concentrations of a commercial fiber suspension in section 9.3.3.

After the pipe flow measurements have been performed, there exists enough rheological data that can be applied to the other measurement results. The simulations and measurements will probably not agree immediately, this is due to the other properties of the suspension which have not been included in the model at present, of which the most important is turbulence. Here the generation of turbulence within i.e. a backward facing step could be used to determine the significance of turbulence. The velocity profile may be measured, and the reattachment point can probably be determined fairly easy.

7.3 Comparison of Different Functions for the Wall Slip

Using the data of Durst and Jenness [13] to verify the suitability of the wall slip approach over a broad range of dry contents, and to determine the type of the slip-stress relation on the pipe walls.

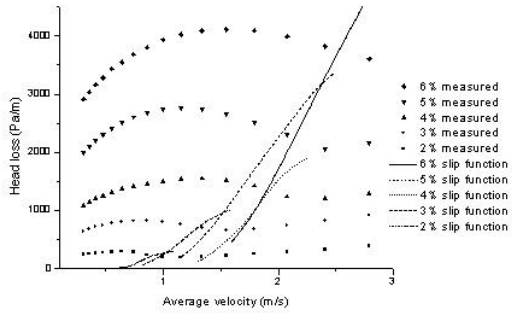

Picture 33 Linear

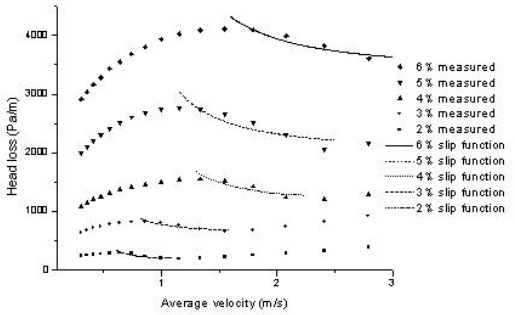

Picture 34 Exponential

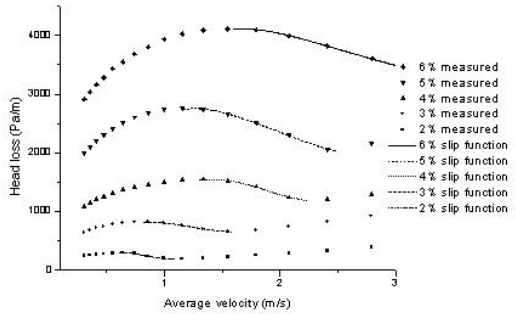

Picture 35 Exponential + linear

Table 3 Parameters for the slip stress functions for the 5% curves in picture 27-29. In all pictures the power-law parameters are the same.

	F_1	e_1	F_2
picture 27	61.25	1	-
picture 28	97.81	-0.1123	-
picture 29	123.96	0.0461	-21.2366

The points marking the measured data range were interpolated from the actual measured data as presented in picture 3. For each curve the power-law viscosity parameters and the wall slip parameters were determined by a least squares fitting to the measured data. The pulp is bleached sulphite, of which the viscosity parameters are kept constant during the slip-stress parameter fitting.

$$t = F_1 u^{e_1} + F_2 u \qquad \{34\}$$

The wall slip function was built as a series of exponential terms as in equation {34}. By assigning a zero value to some of the terms, the behaviour of the function was tried. Table 3 gives the values of the terms for each of the graphs. From the graphs it is evident that the function type represented by picture 35, the exponential + linear slip-stress relation is the best suited. This has the correct slope, with a minimum amount of parameters to be fitted, and the higher functions do not give any significant improvement over this.

7.4 Mesh Considerations for Using the Pulp Model

The use of the wall slip function puts its own demands on the mesh quality, as for any other simulation case. The mesh requirements when using the wall slip function was tested with the 1.5 % birch pulp data as measured by Jäsberg [61]. The same pipe and the same pulp was simulated with identical boundary conditions, the mesh size being the only parameter that was modified. The results of the simulations are presented in picture 36.

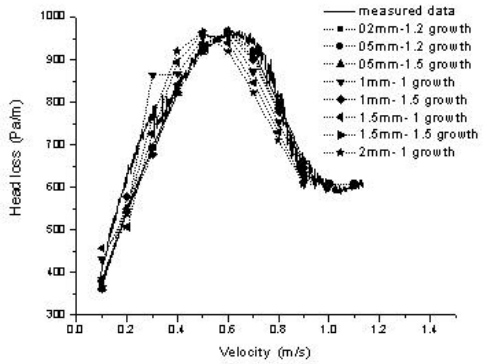

Picture 36 The head loss predicted with different cell sizes of the computational mesh.

The first number in the legend of the picture indicates the height of the first cell adjacent to the wall, for example, the first cell in one case was 0.2 mm high, and the following cells had a height that was increasing with a growth rate of 1.2. This is motivated by the power-law viscosity model, the strongly shear-thinning fluid experiences high shear rates near the walls, with large cell near the walls the viscosity and the stress in the fluid are not captured correctly, which also applies when using the wall slip function. As the velocity at the wall is not zero it could be expected that the influence of the mesh density would be larger than normal.

As can be seen from picture 36, the cases with a cell height of less than 0.5 mm returned a satisfactory fit with the measured data, whereas the cases with larger cells predicted a slightly different head loss curve. The difference is not large, but worth noticing. A good estimate on the height of the first cell, is that it should be comparable to the height of the water layer.

7.5 Solving the Cases

When using the wall slip function, the following observations were made for the Fluent solver. All simulations were made with the FLUENT version 6 in two dimensions with axial symmetry. FLUENT is a commercial CFD software that is widely used and has been subjected to appropriate testing, and therefore does need any further verification. The comments of this chapter only apply for the use of the wall slip function, which is implemented as a user defined function in Fluent, [65]

Even for the simple domain of a pipe flow, the second order upwind discretization scheme should be used. What was noticed to be important is that the under-relaxation coefficient for the momentum equation should be reduced, in many cases the standard coefficient does not lead to a converged solution, but by reducing this coefficient convergence is reached.

In the low flow rates of the no-slip flow region the convergence is not very nice. This can be corrected by adding a conditional statement in the function that turns off the wall slip function at certain conditions. The very low flow rates are not the most important flow for which this function will be used. Flow rates down to one tenth of a millimeter per second velocity in a 40 mm pipe were simulated, the corresponding wall shear rates can be calculated using the formula in chapter 5. For this level of flow rates the wall slip function definitely needs limiting, but this has not been done, as this is an issue regarding the implementation of the function and not an issue about the validity of the method.

The computation times are quite long even for the simple cases. This is due to the wall function, for a no-slip power-law fluid it takes quite long to reach a fully developed velocity profile, by using a non-zero velocity at the wall this becomes even longer. The speed of convergence might be speeded up by using some linearization for the wall slip function, but this has not been regarded as an important step within the project.

A word of warning, the developed functions are by no means intended to be "plug and play" functions. The functions are intended for expert users of CFD softwares. Modification of the functions to apply for the pulp that is to be simulated requires at least familiarity with user-defined functions in the software that is used. Knowledge of pulp behaviour is also necessary for determining that the simulated results are physically relevant.

8 Numerical Results

The model development so far has concentrated on verifying that pulp suspensions can be modeled using generalized Newtonian rheology models. So far little or no attention has been given to the properties of the suspended fibers.

At present, there is not enough measured data available to make a full survey of the influence of the fiber properties, but there is enough to take an estimate on the influence. This is done by plotting the rheology parameters for different values of the fiber properties, for cases where they have been clearly reported. Duffy et al [14] provides an excellent look into the influence of the fiber properties.

The most important, by far, is the concentration of the suspended fibers. The influence of the concentration could be deduced already earlier in this report, but in pictures 37-38, the resulting k and n parameters of some of the simulated cases in this report.
The curves are encouraging enough to say that the k parameter seems to depend exponentially on the fiber concentration. The n parameters does not seem to depend so much on the concentration, but instead on the minor properties of the fibers, such as degree of bleaching and fiber length.

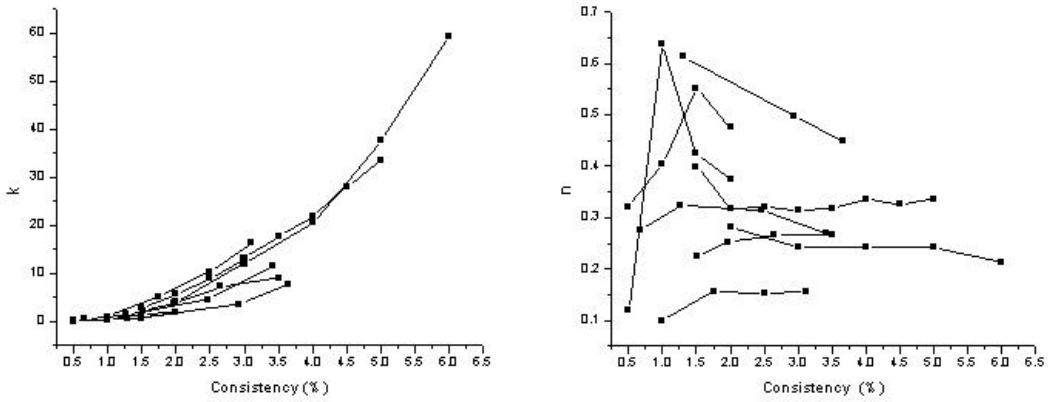

Picture 37-38 The rheology parameters from most simulation cases in this report. The graphs show the parameters of many different pulps, the legend is omitted with the purpose to show that there might be some trend in the parameters.

Taking a closer look on one of the cases, the measurements by Brecht and Heller [11] for a unbleached sulphite pulp, 822 SR in a 5.9 inch pipe. Picture 39 shows the simulation results, with the models for the rheology model activated, without the wall function. Picture 40 shows the corresponding values of the rheology parameter k plotted against pulp consistency. The graph quite clearly indicates that it is possible to build a function that is capable of simulating any arbitrary pulp concentration, and even permitting varying pulp concentration, instead of various, as has been used so far.

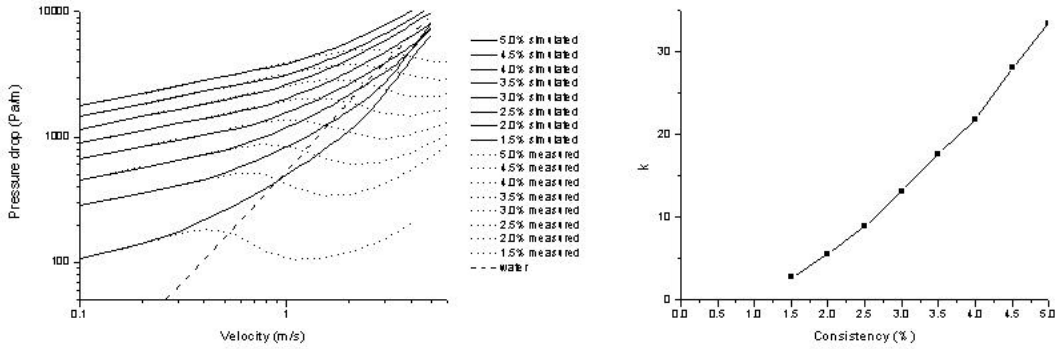

Picture 39-40 The Brecht and Heller [11] data for unbleached sulphite pulp, and the corresponding value of the rheology parameter 'k'.

Freeness is probably the most important fiber parameter that influences the pulp flow. Freeness is a measure on the degree of beating of the fibers, which is measured as the filtration of the fiber network. Smooth, complete fibers offer lower resistance to dewatering than broken fibers with fibrillated surface does.

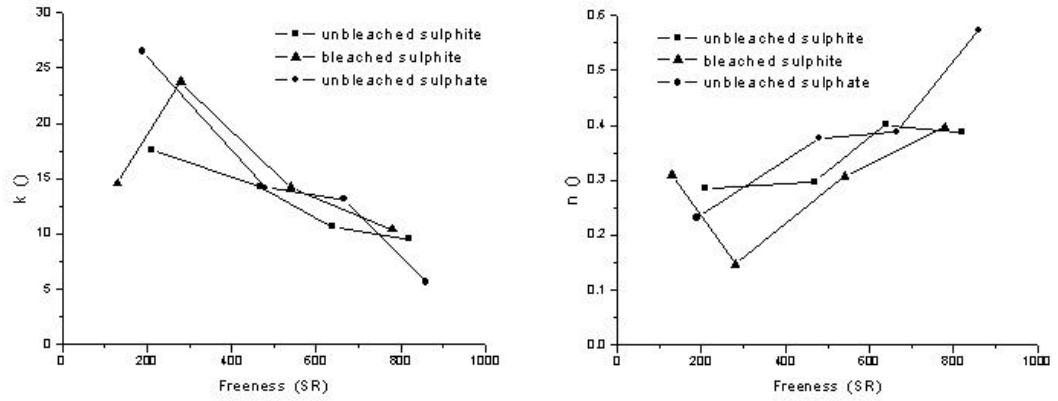

Picture 41-42 The influence of freeness on the pulp parameters. Measurement data compiled from Brecht and Heller [11]

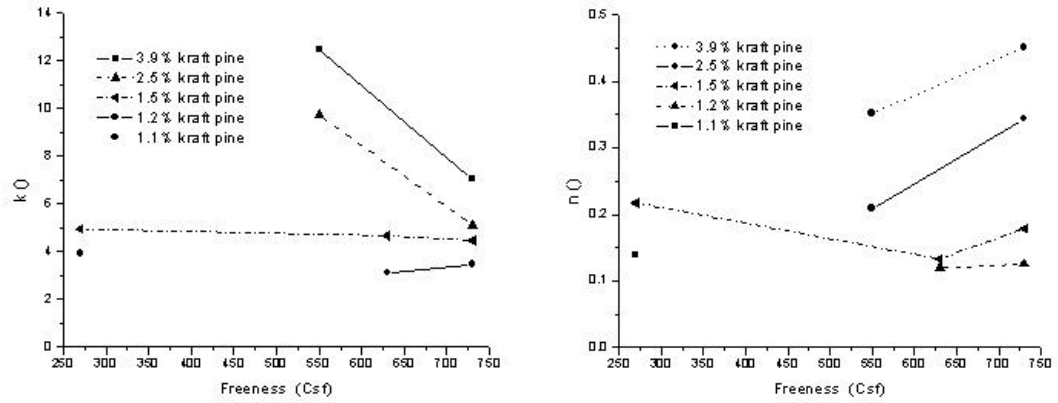

Picture 43-44 The influence of freeness on the parameters from measurements by Duffy et al [14]

As has been shown in the previous sections, a rheology model based simulation method is the most suited for pulp flows in any geometry. Therefore, a set of universal parameters for pulp suspensions can be constructed according to:

$$k = k\left(c_{mass}, l_{fiber}, d_{fiber}, k, T_{suspension}, m_{suspension}, ...\right)$$
$$n = n\left(c_{mass}, l_{fiber}, d_{fiber}, k, T_{suspension}, m_{suspension}, ...\right) \qquad \{35\}$$

where c_{mass} is the mass fraction of the fibers in the suspension, l_{fiber} and d_{fiber} are the fiber dimensions, either average length and width or later maybe even a distribution of both. ? is the "kappa value", the degree of bleaching, $T_{suspension}$ and $\mu_{suspension}$ are the temperature and viscosity of the suspending medium, where $\mu_{suspension}$ is usually a function of the temperature.

The type of these equations will not be presented, but especially from pictures 37 and 40 it is shown that at least the k parameter versus fiber mass fraction follows a quite simple and uniform trend. The value of n has a larger degree of scattering, but this value is more connected to the other parameters, such as fiber dimensions and fiber properties. The influence of the fiber properties on the flow of the suspension has been studied by, for instance, Duffy [14], [16].

8.1 Modeling a Flow With Multiple Solutions

Looking at the head loss curves presented in the previous section, it can be seen that most chemical pulps have a clear decrease in head loss plotted against the flow rate. Some mechanical pulps have the same phenomenon, but not as distinct. The decreasing head losses imply that some head loss values can be the result of three different flow rates. As the flow is forced, the solution is unique in the sense that the mass and stress balance can only result in one combination of shear stress and velocity at the pipe wall. If the problem is turned, and the pressure drop in the pipe is used as the boundary condition at the pipe inlet, then the problem does no longer have an unique solution, there are three different solutions, as shown by picture 39. This may have some importance, in case a certain pressure difference is kept over a length of pipe, what is the flow?

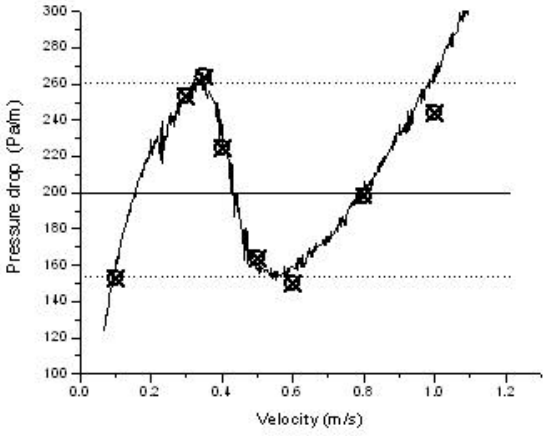

Picture 45 The head loss curve for a pulp. The dots give the initial solutions to the simulations. The solid, horizontal line crosses the measurement curve in three locations, that is, three different flow rates return the same head loss.

Picture 45 shows the head loss curve of a 1% bleached birch pulp suspension, the dotted lines indicate the level of the local maximum and minimum, between which the three solutions can exist. The solid line is the pressure boundary condition used in the simulations. The simulation was carried out in order to test if the pulp model has any preference among the three possible solutions. The simulation was started from a fully converged solution with a velocity boundary condition, these initial solutions are given by the dots in picture 45. The pressure drop in the pipe was given as the static pressure, the dynamic pressure was not included.

The simulations gave an interesting and slightly surprising result, all 8 cases converged to the solution with the lowest flow rate, average velocity 0.17m/s.

8.2 Estimated Power Required for Pumping

Even though the flow of paper pulp shows a significant drop in the head loss curve, this may not be seen as clearly in the power consumption of the pumps. The head loss curves presented in the previous sections are static head loss only, the dynamic pressure has not been included.

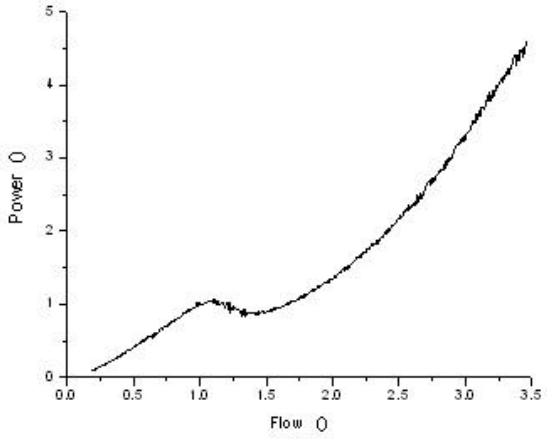

Picture 46 The normalized pumping power plotted against the normalized flow rate.

Picture 46 shows the birch data of Jäsberg [61], the flow rate has been normalized with respect to the local maximum, and the abscissa presents the pump power normalized with respect to the local maximum. The pump power has been calculated as the pressure drop multiplied with the volume flow. Even though the head loss curve shows a significant reduction due to the slip, this will not be as clearly visible in the power required.

8.3 Simulating a Mixing Flow

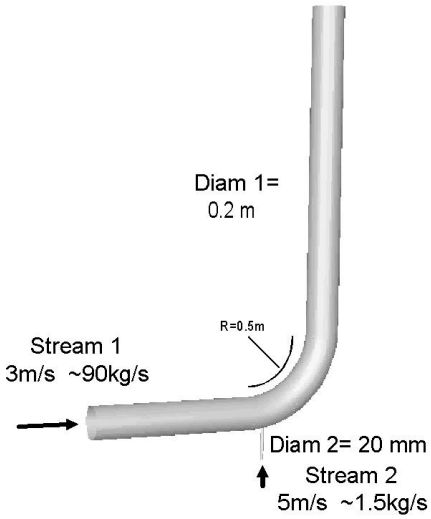

Picture 47 A mixing elbow for illustrating the influence of the pulp model. This type of mixing elbows are frequent as CFD tutorial cases.

For illustration purposes, a pipe bend with a side stream was simulated. The larger pipe is 200 mm diameter, the smaller is 20 mm. The layout is shown by picture 47. All values are "pulled from the hat". The mesh is rather coarse, but adequate for this purpose.

The simulations were carried out with three different material properties:
1- water - water
2- birch 2% - water
3- birch 2% - imaginary substance with 100 times water viscosity

Unlike earlier, here the pulp models have been extended to apply for a varying concentration, the pulp models are now using the local concentration, which does not need to be identical to the mean concentration. The mixing models are readily available in FLUENT, with transport of all species. The pulp model has been created from the parameters presented in Hammarström et al [61]-[62]. It is important to notice, that now the pulp models have been modified to apply for VARYING concentration instead of VARIOUS, as has been presented in the papers.

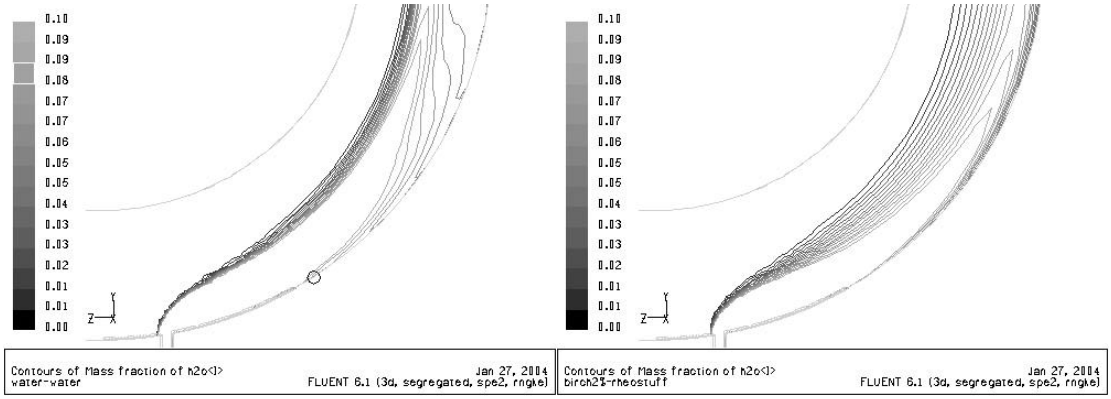

Picture 48-49 Mixing elbow centre plane, the pictures show the mass fraction of the side stream, the axis has been limited for clarity. The concentration profiles are completely different between the two cases.

A Cross-cut plane shows the concentration of the secondary feed in cases 1 (left) and 3 (right), there is a considerable difference in concentration profile. The difference in concentration profiles show how the substances are mixed. Already a very short distance from the secondary inlet, the mixing is totally different. This is of importance, for instance, when the addition of chemicals or dilution water is simulated. In case both species are then simulated with the properties of water, then the results are probably incorrect, whereas a combination of the pulp models presented in this report and the proper rheology model for the other species has a better chance of predicting the degree of mixing correctly. A poor mixing in an industrial case like this, might lead to a skew concentration of formation aids, which will then be seen in the quality of the final product, the paper.

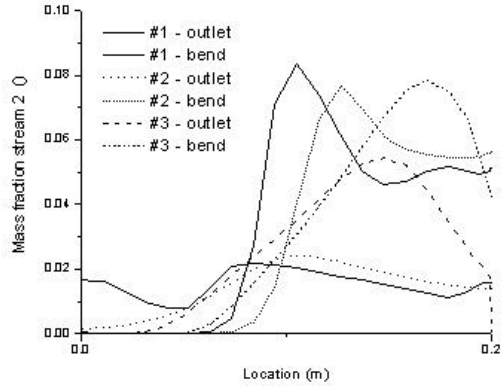

Picture 50 The concentration profile of stream 2.

The results graph should be interpreted so that the x-axis starts from the pipe wall, in the direction of the bend. The outlet is located 2 m above the bend. Please compare the lines for #1 outlet and #3 outlet, the difference is large. #1 is almost fully mixed, whereas #3 has almost formed a "plug" of the added substance near the wall. The influence of the wall slip function on the mixing behaviour of pulps is further illustrated with a following example, in which two equal streams of different pulp concentrations are mixed.

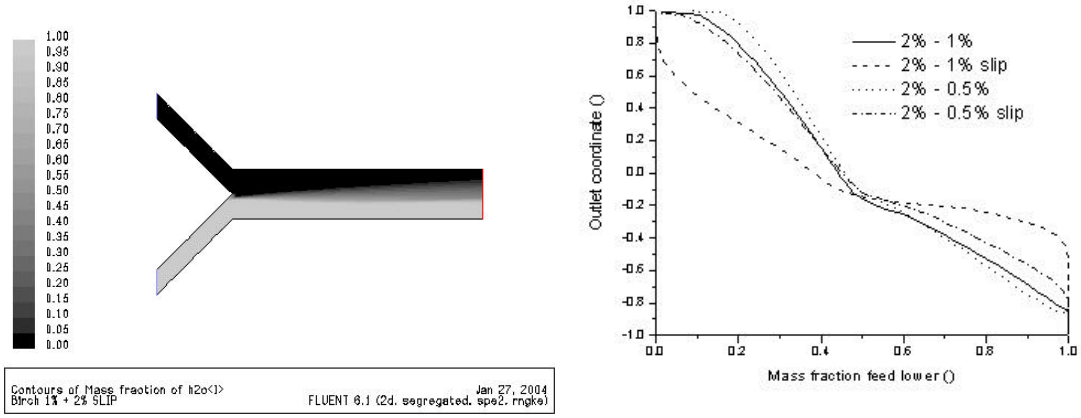

Picture 51-52 Mixing pulp of different consistency, the left picture shows a contour plot of the mass fraction of the lower stream, the right picture is a line graph from the outlet.

The left picture shows a contour plot of the concentration of the lower stream, and the right picture shows the profile at the outlet. The streams are birch pulp, the lower stream is 2% and the upper is either 1% or 0.5%, according to Hammarström et al [61]-[62]. The cases are identical, except for the activation of the wall slip, which is probably the most important feature of the suspensions.

The results of the simulations are that in the case of mixing pulp streams of 1% and 2%, the mixing will be very poor. In the case of 0.5% and 2% pulps, the same difference can be observed, but it is not so pronounced, this could probably be explained with the larger concentration gradient.

Unfortunately, no measurement results exist for either of the demonstrated cases, or this type of applications. But the cases still show the tremendous possibilities of simulating complex multiphase flows with relatively simple rheology models.

8.4 The Height of the Water Layer

Using the data calculated for the pulp suspensions, the height of the water annulus was estimated. Estimates of the water annulus height have been performed earlier by, for instance, Myréen [27], Soszynski [25] and Hämäläinen [28]. In these works the annulus height is calculated using the flow of the core pulp "plug" and calculating the annulus flow from the difference. Hämäläinen uses the full analytical solution on the head loss data measured by Hemström et al [40], which gives a very close fit with the values calculated from the wall slip function. Soszynski, on the other hand, presents a rough estimate about the annulus height based on the head loss measurements of Condolios, from Soszynski [25], which is based on the assumption that the plug velocity equals the bulk velocity. This does not give quite the same results as the wall slip function returns. Myréen does not give any specific annulus thickness for the pipe flow, which is measured by Durst & Jenness [13], but gives the annulus height as a function of a slip coefficient *s*.

By comparing the simulated results to the calculation by Hämäläinen [28] and Soszynski [25] in pictures 55-56, it can be said that the annulus height estimated by the current pulp model is in excellent agreement with other literature sources. That the results presented by Soszynski are larger than the simulated, that is only to be expected from the simplification made by Soszynski. It may be worth noticing, that using the power-law model for the rheology probably under-estimates the shear-rate at the wall rather than the opposite.

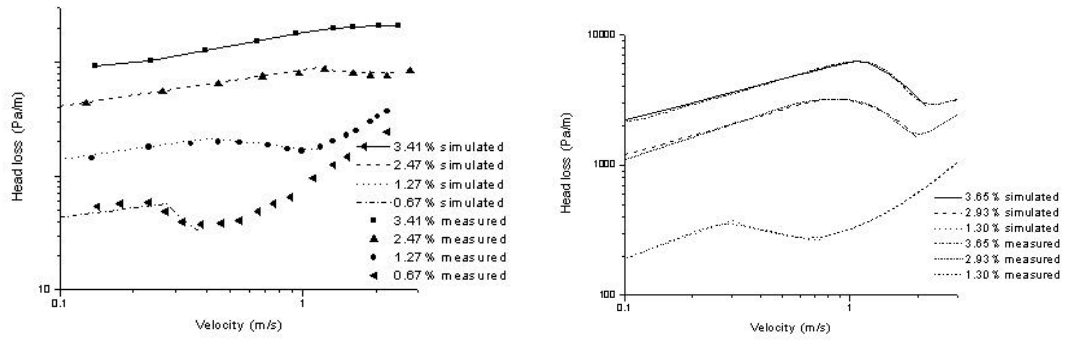

Picture 53 -54 Head losses as measured by Hemström et al [40] and simulated with the pulp model, left. Head losses as measured by Condolios [25] and simulated with the pulp model, right.

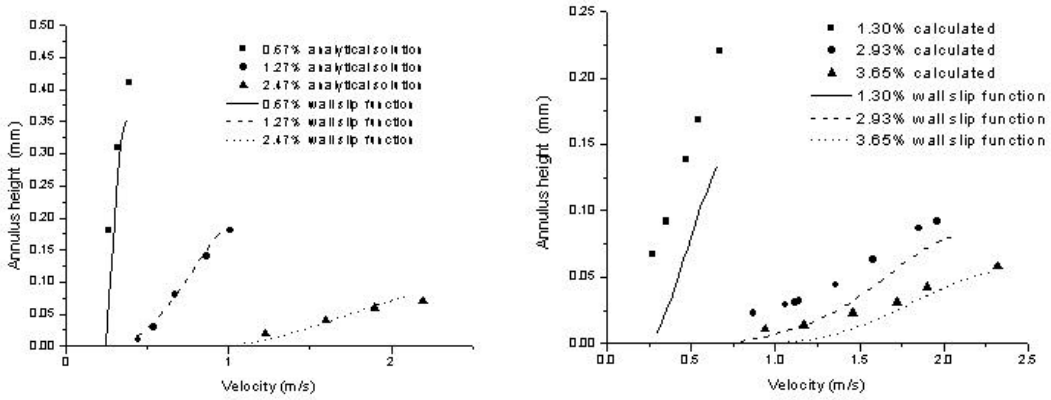

Picture 55-56 The annulus thickness as calculated analytically by Hämäläinen [28] and using the pulp model, left. The annulus thickness as approximated by Soszynski [25] and using the pulp model, right.

The annulus height of the current wall slip functions is estimated, not in the form of a total flow rate, which is already taken care of in determining the slip-stress ratio, but using the functions regulating the boundary layers of turbulent flow.

This approach seems to be justified, as the assumed slip velocity increases with a decreasing shear stress at the wall. The only possible explanation is that the height of the water annulus is growing more rapidly. But when a certain height of the water layer is reached, turbulence is introduced. Turbulence would probably disperse the pulp core, thus reducing the height of the water annulus. Turbulence is strongly dampened by the fibers.

The simplest way to estimate the annulus height is to assume a constant velocity gradient, as the height of the annulus is very small,

$$t = m\frac{u}{h} \qquad \{36\}$$

where t is the wall shear stress, which is assumed to be constant as proposed by Soszynski [25]. μ is the molecular viscosity of water, u is the slip velocity estimated according to the calculations in the previous section and h is the annulus height.

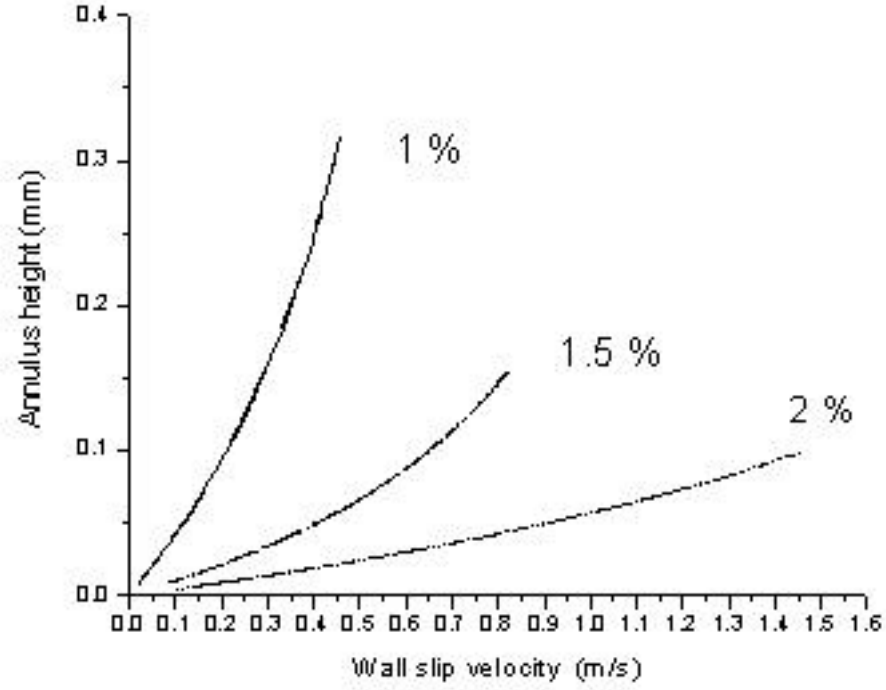

Picture 57 The annulus height of birch calculated with the wall slip function, laminar flow.

The ratio of the slip velocity against the mean velocity is a good thing to plot, from picture 58 can be observed that at high flow rates the slip velocity is increasing almost linearly with the mean velocity, but at a lower rate.

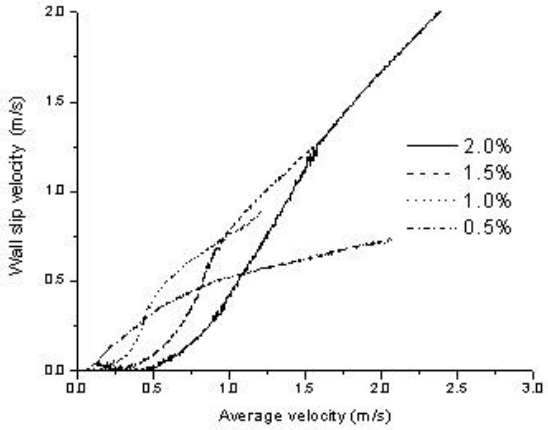

Picture 58 The wall slip velocity plotted against the mean velocity, all flow curves

But in order to determine more than just state the height of the water layer, the height of the water layer is compared to the height of the parts of the boundary layer, according to Spalding's law of the wall, as presented in equation {12} on page 28.

The resulting height of the water annulus is shown in picture 59. From the picture, it can be seen that the local minimum on the head loss curve presents

the highest value, as expected. But it also shows that the height of the water annulus is confined to the height of the logarithmic layer of a turbulent boundary layer. This is a very interesting feature, as it gives further indication that a balance is formed between the core fiber "plug" and the more or less laminar water annulus.

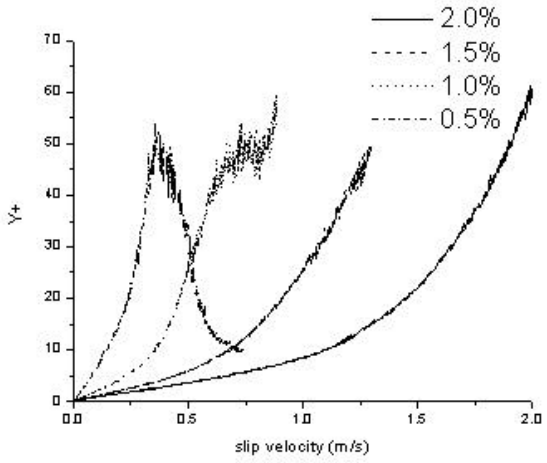

Picture 59 The dimensionless height of the water annulus, calculated with the wall slip function, all flow curves

9 Validation of Pulp Flow Model

Showing that the modeling is really geometry independent, consists of a few steps. First, the validity of the modeling approach is shown by performing the simulations for a few different pipe diameters. This is actually a verification that the pulp suspension can be modeled in the proposed way, not that the simulation program or rheology model are correctly implemented.

Second, the modeling is applied to rotating flows. The rotary flows are totally different, and most likely show some features which will not be captured by the models at the current state. The most likely phenomenon is fiber migration and secondary flows, which have been described by Björkman [66]. He investigated the Taylor vortices formed in the Couette flow of pulp at the same concentrations as used in this work.

As a third step, the velocity profile predicted by the simulations is compared against measured velocity profiles. The velocity profiles is the key evidence, which leaves little room for debate. The current pulp models will probably not capture all features of the velocity profiles, but this is a matter of measurement accuracy and model refining, until now no attention has been given to the turbulent properties of the suspension, and the rheology models have not been compared. Comparing rheology models and turbulent quantities will require a large amount of profile measurement data from straight pipes and channels with step changes in channel height.

9.1 Geometry Independence

The fundamental piece of evidence for the validity of the models is that they can be applied for any arbitrary pipe diameter, with agreeable accuracy. There exists only a few measurement series in which this can really verified. The pipe diameter independence was shown by Hammarström et al [31], comparing simulations to measurements made by Möller [12]. The measurements by Möller contained 3 different pulps that had been measured in 3-4 pipe diameters each, at several different dry contents and numerous flow rates. The number of flow rates for each consistency in the experiments is a bare minimum, but sufficient for this purpose. In pictures 60-66 two different pulps illustrate the independence of pipe diameter. This is a crucial piece of evidence, but this does not still offer any advantage over any of the existing empirical correlations. The advantage is the fact that the empirical correlations are restricted to pipe flow, whereas the models developed in this project can be applied to any arbitrary geometry.

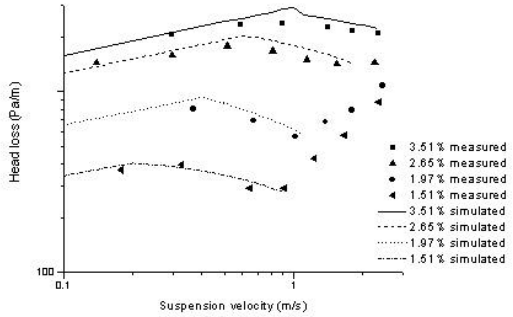

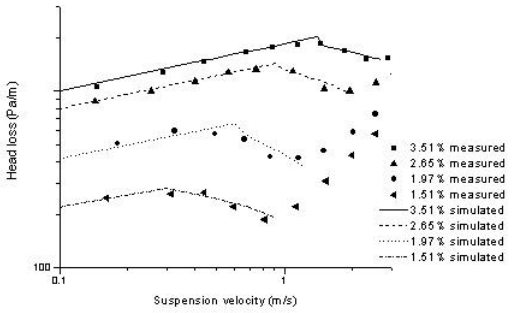

Picture 60-61 2 and 3 inch pipes, pulp Hudson birch (Möller [12] and Hammarström [31])

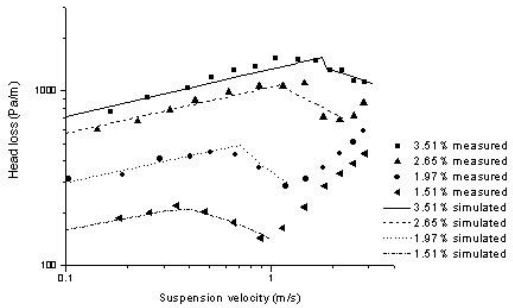

Picture 62 4 inch pipe, pulp Hudson birch (Möller [12] and Hammarström [31])

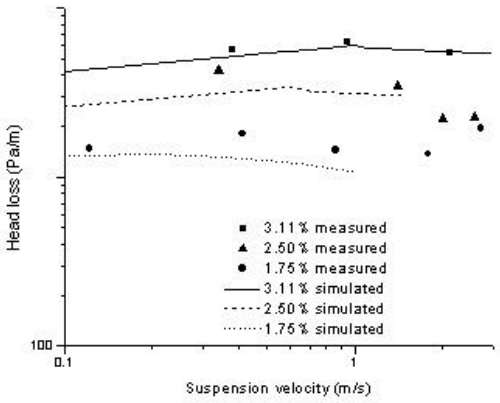

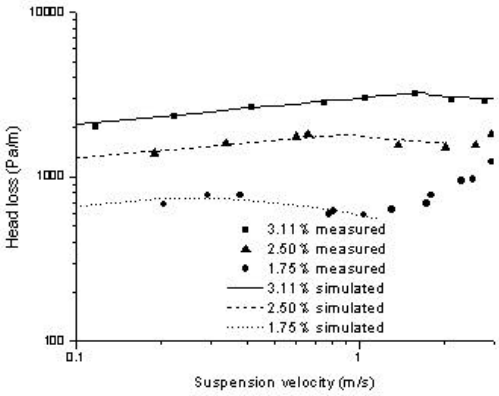

Picture 63-64 1 and 2 inch pipes, NZFP kraft pine (Möller [12] and Hammarström [62])

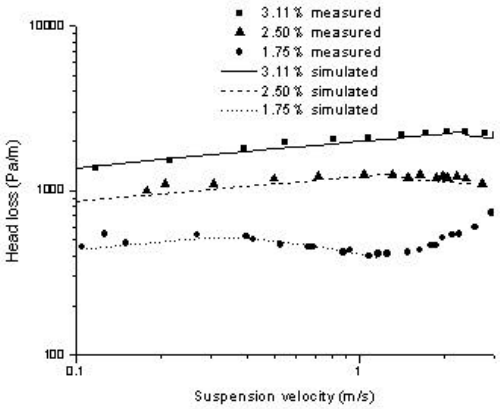

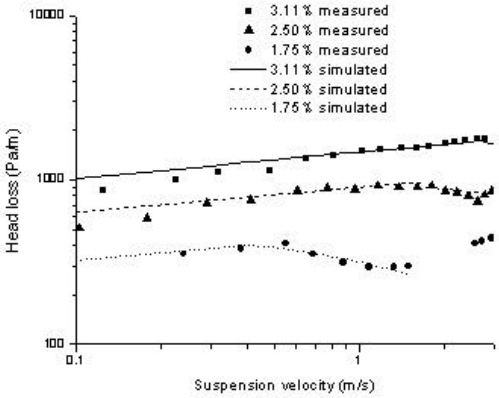

Picture 65-66 3 and 4 inch pipes, NZFP kraft pine (Möller [62] and Hammarström [62])

9.2 Rotating flows

9.2.1 No Slip

By using the equation {50} or {51} and comparing against measured data, the rheology of the fiber suspension can be determined. Bennington et al [68] measured the torque in a rotary shear tester at different rotational speeds, many of which were very high. The fiber suspension used by Bennington does not have any pipe flow measurements or any other data, which could be used for the model development.

But Bennington's data is useful for demonstrating another feature of the flow of suspensions. The use of laminar flow modeling in the beginning of the measured torques may give a view of the rheological parameters of the suspension, while then simulating the flow at higher flow rates will show how well the suspension in a rotary shear tester can be simulated by two-dimensional simulations. Possible secondary flow, which have been observed, can not be included in the simulation.

The general idea behind the simulations is that at low rotational speeds the flow field is uniform enough, so that the pulp rheology can be determined. The rotary devices were treated as two cylinders with slip-free walls formed by the plane described by the end of the baffles, which in picture 67-68 are described by the dashed lines and h is the free height in each device. The physical dimensions of the devices are given by Bennington et al [68].

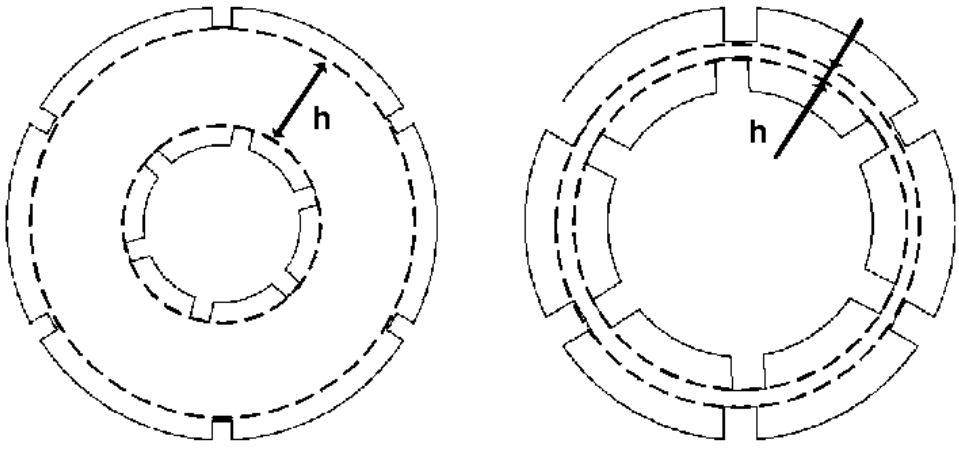

Picture 67-68 Rotary shear testers of Bennington et al [68]. The device with the wide gap has been used to set the rheology parameters, and the device to the right to compare the results.

The rheology models were set according to equation {37}, limiting the rotational velocity to the point where the suspension was said to be fully 'fluidised'. The model parameters were only defined for the device with the large gap between the baffles on the rotor and wall. The idea is that the parameters are set under certain conditions, and they are then applied under

other conditions. The sub index i refers to the inner diameter and the sub index o refers to the outer diameter.

$$w_i = \left(\frac{M}{h2pk}\right)^{\frac{1}{n}} \frac{n}{2}\left(1-\left(\frac{r_o}{r_i}\right)^{\frac{2}{n}}\right) r_i^{\frac{2}{n}} \qquad \{37\}$$

Table 3 Rheology parameters of a semi-bleached kraft pulp.

	k	N
2 %	9.53	0.871
4 %	86.99	0.464
6 %	303.19	0.382

The cases were simulated at a few rotational velocities, as transient simulations with the computational grid rotating for each time step. The RNG-ke model was used for the turbulence. The simulations were continued until the torque (M) had stabilized, this requires hundreds or thousands of time steps, in all of which a converged solution must be obtained before incrementing the solution. The amount of simulations is vast, and should not be attempted lightly. The computational power required for these simulations is of the order of one CPU-YEAR!

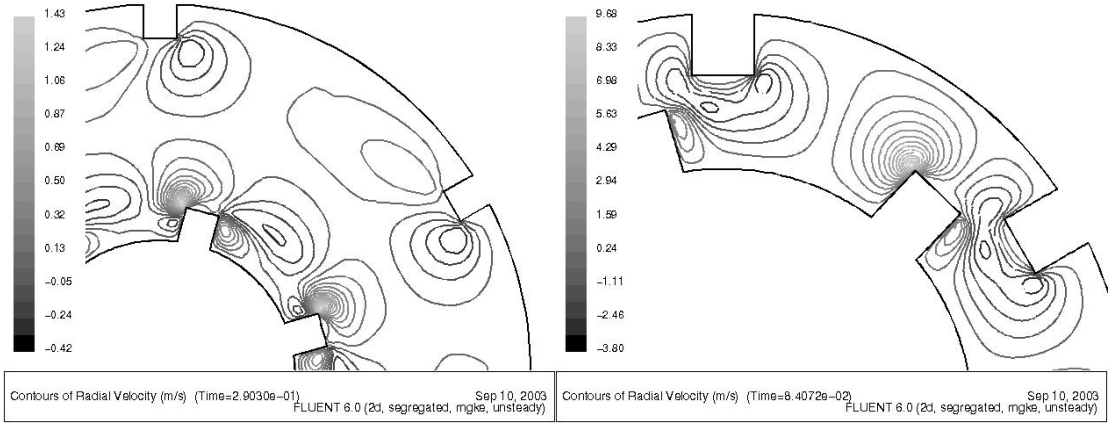

Picture 69-70 The radial velocity components at arbitrary time-step at 400 rad/s.

Picture 69-70 contains the radial velocity component at some arbitrary time step, both pictures from 2% consistency. The pictures show that the flow is not uniform at high rotational velocities, 400 rad/s. By comparing the measured torque to the simulated values, a estimate of the simulation model is gained. Picture 71 shows that the simulated values are in reasonable agreement at low rotational speeds for low rotational speeds, but there is a significant deviation at high rotational speeds. For the device with a narrow gap between the baffles, picture 72, the agreement is better. But the velocity field predicted by the simulations, picture 70, implicate that this device is not measuring the rheology of the pulp suspension, something else at best.

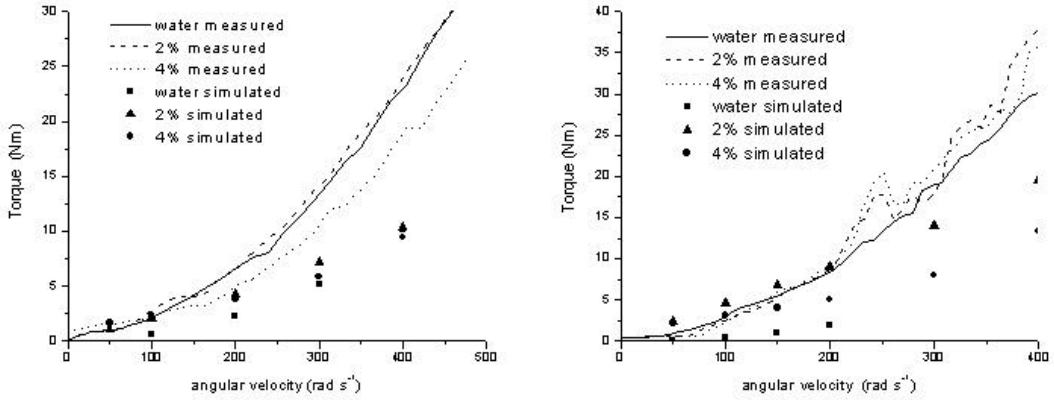

Picture 71-72 The measured and simulated torque

The difference in torque between the measured and simulated values rises the question how the fluid parameters should be defined. Obviously, the point of 'full fluidisation' is not the correct choice for parameter definitions, though the trends are correct. The point of fluidisation was determined visually from a high-velocity film of the measurements by Bennington [68]. This demonstration shows the importance of proper parameter fitting, but also demonstrates that the 'fully fluidised' condition is not a proper way of defining the flow.

What is a cause for alarm in pictures 71-72, is that the measured and simulated values for water are so far off. The simulations were carried out in 2D, but friction from the end plates, or 3D effects should not have such a large influence on the flow, neither does the choice of turbulence model. In cases where measured and simulated values of well-known substances like water disagree, the simulations are an indication on how successful the measurements are, not the opposite.

9.2.2 Smooth Wall Rotating Flow

For the case of a rotary device without baffles, there will be a significant slippage at the walls, especially the rotor wall. The torque is constant, but the shear stress on the two surfaces is not equal, but depends on the radius.

Picture 73 shows the calculated rotational speed for each of the torques measured by Möller [12] according to equation {50}. The angular velocity is thus calculated as the no-slip angular velocity that is the result of the applied shear. The values are presented as torque per meter of pulp column height. The rheology parameters for the calculations in picture 73 are taken from the pipe head loss measurements presented in Hammarström et al [31].

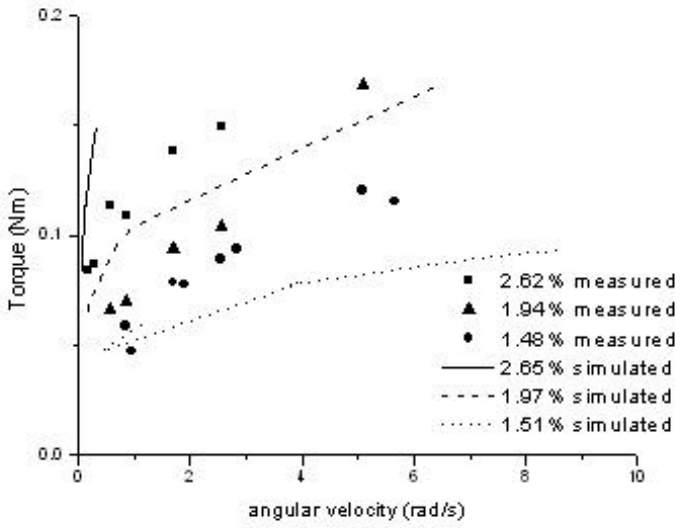

Picture 73 The measured and simulated torque of Möller's [12] shear tester.

The results are a bit confusing, as the calculated torque remains below the measured torque. At low angular velocities the calculated torque is higher than the measured, but at higher angular velocities the measured is higher. This is an analogy to the problematic choice of laminar or turbulent models for pipe flows, except that in this case the turbulence can be neglected. If the line of the calculated torque would higher than the measured values, then this could be corrected by allowing a slip at the rotor surface, but currently this is not possible. The results of picture 73 imply that either the simulation model or the measurements are not accurate enough, or some phenomenon occurring in the measurements is not captured by the simulation model.

Unfortunately the Möller series is the only for which the current approach can be applied, for instance the Durst device would be an excellent application for verification, but it requires 3D simulations. Implementing the slip models for rotating walls with a slip condition in 2D and 3D is very complicated, especially when there is no driving pressure gradient. As shown in section 8.1, with the current implementation the pulp model has a preference for the no-slip case.

9.3 Verification Against Velocity Profile Measurements

In order to either verify or reject the use of continuum based models, the results need to be verified against velocity profile measurements. Velocity measurements in pulp suspensions at higher dry contents are very difficult, and very few sets of measurements have been published.

Brecht and Heller [11] published one series of measurements, but unfortunately the velocity profile measurements have been performed at a different consistency than the head loss measurements in the rest of the paper. For successful model development it is essential that enough head loss data is acquired, at all flow rates, and that the velocity profiles are acquired with the same pulp at the same concentration. The pipe diameter need not necessarily be the same, but preferably. The velocity profiles can be used as verification of the varying consistency pulp modeling that was presented earlier, picture 74 shows both the measured and simulated values.

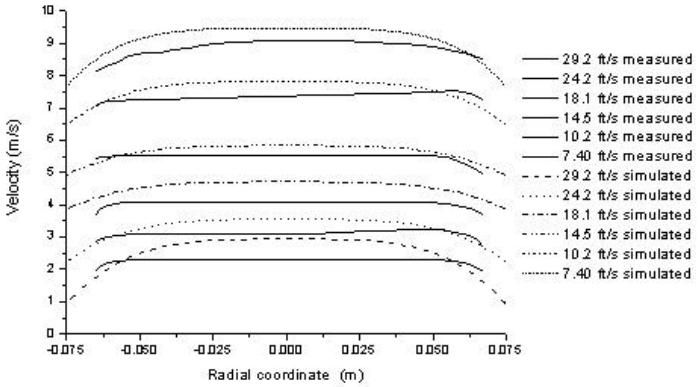

Picture 74 The Brecht and Heller data.

Lee and Duffy [69]-[70] published velocity profiles of pipe flow of very dilute pulp suspensions, two of which are presented in pictures 75-76. Unfortunately, too little or no head loss measurements were supplied with the velocity profiles, otherwise this very data could have been used to evaluate the rheology models. The velocity profiles presented in pictures 75-76 show a very clear velocity profile, there are no "flat" "plugs".

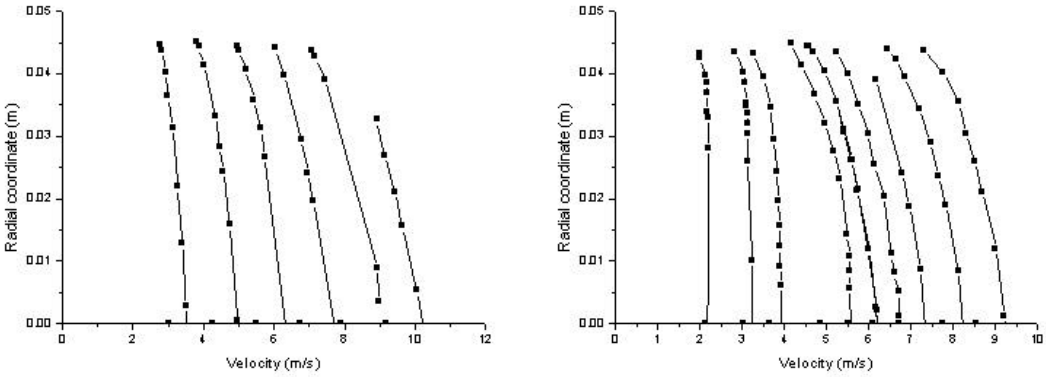

Picture 75-76 2 of 4 velocity profiles presented by Lee and Duffy [69]. As is evident, the velocity profiles are not "flat". 0.21% kraft pine to the left and 1.17% kraft pine to the right.

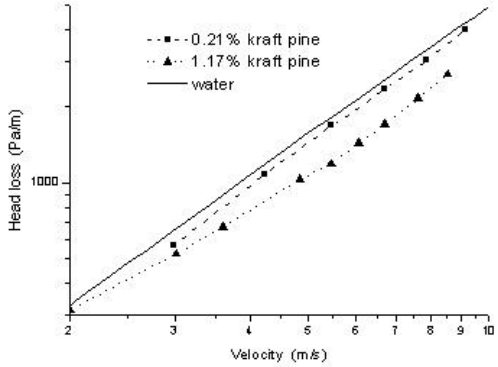

Picture 77 The corresponding head losses to the velocity profile measurements in pictures 69-70, measurements by Lee and Duffy [69-70].

The head losses in picture 77, calculated from the friction factors presented by the authors, show that at infinite dilution the fiber suspensions can be simulated with the properties of water, but already at low concentrations the deviation from water is large. The results by Lee are very useful, though, with the use of them and the measurements by Möller [12], under certain assumptions it can probably be shown that it is possible to build a pulp model that covers the fiber concentration ranging from water (0%) up to almost 4% fiber dry content. This model extension is not presented in this report.

9.3.1 Impact Probe

The measurements of Mih and Parker [17] were performed with an annular purge impact tube, with which the velocity profile was recorded at several locations in pipes of two different diameters. The head loss data was also measured and published, but only for the turbulent part of the flow curve. All measurements were performed at two concentrations, 0.5%-mass and 1%-mass bleached birch pulp.

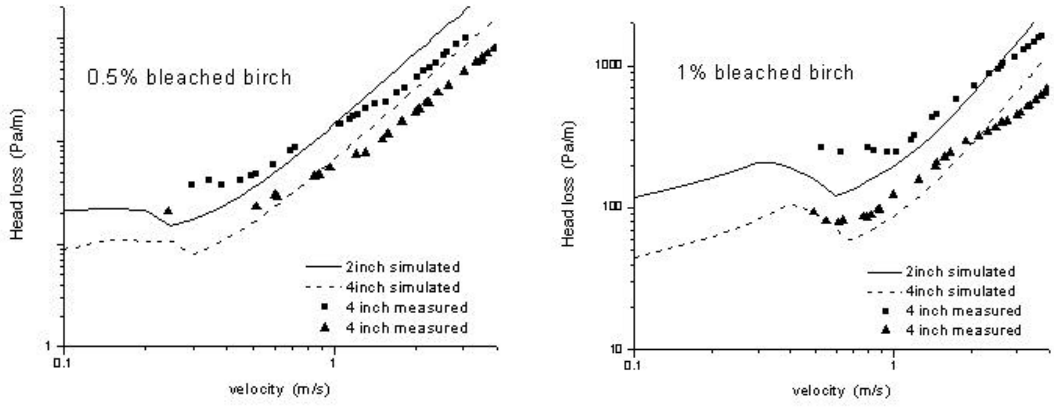

Picture 78-79 Measured and simulated head loss curves of bleached birch in 2 and 4 inch pipes, 0.5%-mass to left and 1%-mass to right.

The simulations were performed with the birch pulp model presented in Hammarström et al [62]. The measurements of Mih and Parker [17] did not contain all the necessary flow rates on the head loss curve, but as the pulp is identical with the pulp as measured in Jyväskylä University by Ari Jäsberg, the same model was used. This leaves open the question of freeness and fiber length, it cannot be guaranteed that they were identical as the suspensions were not taken from the same batch. But by comparing the measured and simulated head losses in the pipes, the suitability of the simulation model can be verified for each consistency.

Pictures 78-79 show that there is a very good agreement between the measured and simulated head losses, hence the model can be used. The pictures also show the validity of rheology modeling.

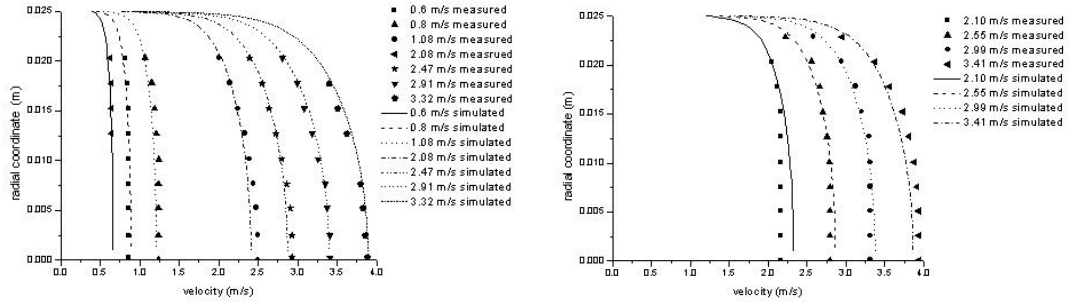

Picture 80-81 Measured and simulated velocity profiles of bleached birch in 2 inch pipe, 0.5%-mass to left and 1%-mass to right.

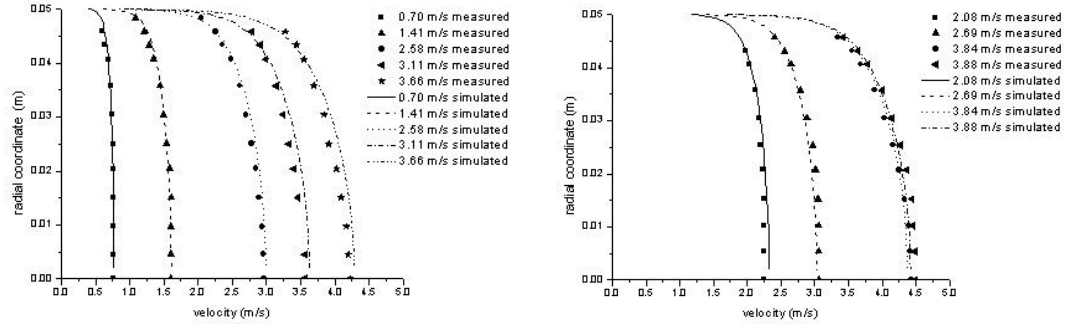

Picture 82-83 Measured and simulated velocity profiles of bleached birch in 4 inch pipe, 0.5%-mass to left and 1%-mass to right.

The resulting velocity profiles are shown for each pipe and each consistency, with several mean flow rates in the pipes. As can be seen from picture 80-83 the agreement between the measured and simulated velocity profiles is excellent. The implications of this will be discussed in section 9.4.

9.3.2 NMR Results

The NMR based velocity measurements performed by Li et al [71] used a hardwood kraft pulp suspension, birch of 0.5% mass. The same simulation model as above was used. In this case the possibility of differences in freeness and fiber length exist, but encouraged by the previous results the models are tested for these flows as well.

The measurements by Li [21], [71] do not give the head losses for any flows, which is a pity. The head loss data would have been very useful for determining the suitability of the models. Further, there is a large uncertainty regarding the flow rate in the experiments. The flow rates has definitely not been what they reported. Evaluating the velocity profiles in the abrupt contraction [72], water flow, revealed differences in flow above 10% of the mean mass flow. Similar errors exist for the other profiles. In any flow channel, the mass flow must be constant at all positions in the flow direction.

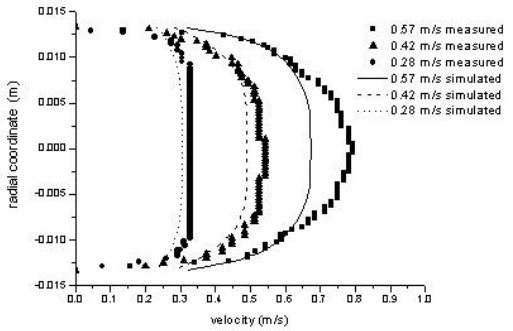

Picture 84 The measured and simulated values of birch pulp in a 26.6 mm pipe.

Regardless of the uncertainty of flow rate, the simulations of birch pulp were compared to the measurements. The flow in a 26.6 mm pipe is shown in picture 84. The flow rates are so low in the measurements, so it is uncertain whether we are in the laminar or turbulent regime. This invokes one of the most important features of the pulp model, in the beginning of the flow curve the contribution by turbulence is negligible compared to the rheology part, hence the turbulence model is always active.

The flow in a 1:1.7 abrupt contraction is simulated in picture 85, which shows the velocity profile at different locations in the channel, the legend gives the distance from the contraction. From the measured profiles it is evident that there is some uncertainty about the flow rate.

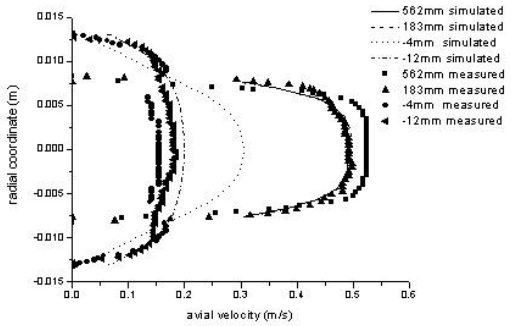

Picture 85 The flow in an abrupt contraction, birch pulp.

Picture 86 shows the corresponding velocity contours in the contraction. The results in pictures 85-87 clearly show that the current pulp model is capable of simulating complex geometries, not only different pipe diameters as shown by pictures 72-73.

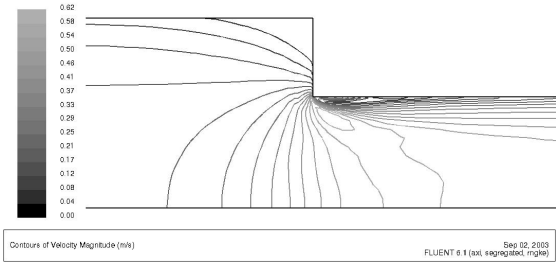

Picture 86 The velocity contours in the abrupt contraction.

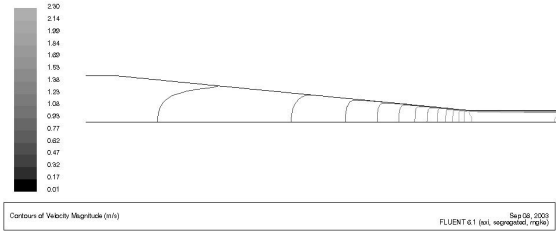

Picture 87 The velocity contours in a conical contraction, birch pulp.

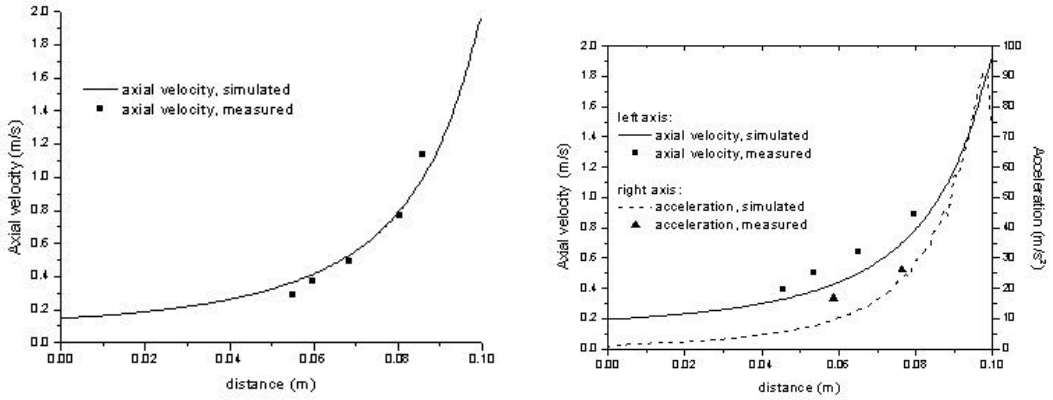

Picture 88-89 The measured and simulated axial velocity and acceleration for birch pulp at 0.5% and 1% consistency.

The simulations of the conical contraction [73] does not contain as much reference points as the pipe and the abrupt contraction, but the validity of the simulations can still be verified from pictures 88-89.

9.3.3 Ultrasound Results

UVP-PD is ultrasound reflection based velocimetry combined with pressure difference measurements, which were done in a 23 mm pipe by Wiklund et al [18]-[19]. The pulp used in their investigation was a commercially available mixture of long and short fibers, for which there exist no suitable head loss measurements for model development.

The measurements done by Wiklund et al still yielded a set of very good velocity profiles, and the head losses at these specific flow rates. This means that a simulation model can be built based on these data. Unfortunately, all data points are well within the turbulent regime and hence no analytical solutions are possible. This means that the developed fluid model is valid in at least the turbulent regime, but it will not be able to predict the local maximum in the head loss curve, such as shown in picture 6 on page 21.

The fluid modeling involves solving the Navier-Stokes equations at all the given flow rates. The parameters that are required for the fluid model must then be determined using an automatic coupling between an optimisation software and the CFD solver.

The cost function for the optimisation is based on the measured head losses and on the measured axial velocity in the pipe. The simplest cost function is a sum of the squared difference between measured and simulated values. In the current case, the velocity profile was compared at 10 equally spaced points between the pipe wall and axis.

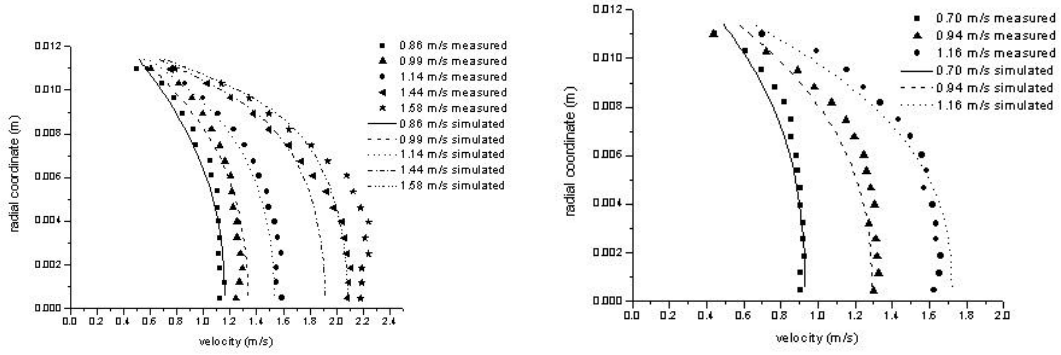

Picture 90-91 The measured and simulated velocity profiles of 0.5% (left) and 1% (right) pulp.

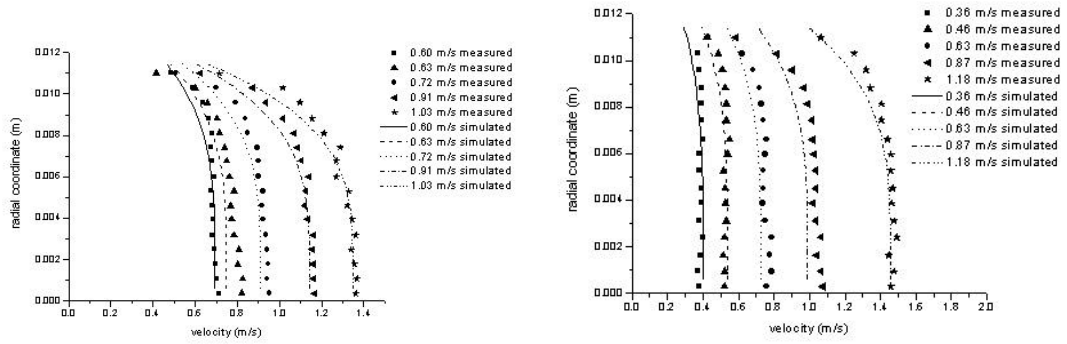

Picture 92-93 The measured and simulated velocity profiles of 2% (left) and 3% (right) pulp.

The resulting velocity profiles are shown in pictures 90-93, plotted with the measured values. The measured values show a large asymmetry, this may be due to the limited range of the measurements or on the too short calming length. The corresponding head losses are plotted in picture 94. Picture 95 again verifies the trend that might be estimated, that the consistency parameter 'k' is increasing as a function of the fiber concentration, and that the fluid behaviour index 'n' decreases.

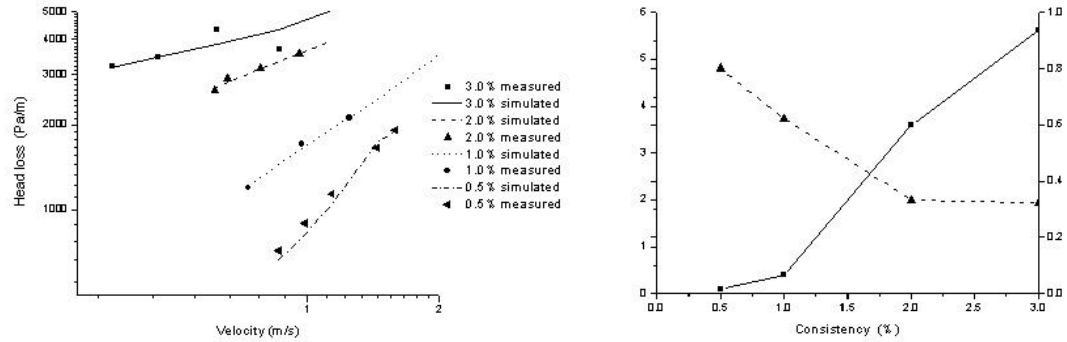

Picture 94-95 The head loss of the pulp flows from pictures 84-87, and the corresponding parameters for the pulp. The k-parameter (left axis) is the shown by the solid curve, the n-parameter by the dotted curve on the right axis.

10 Summary

Combining the measurements that have been published on the flow of pulp suspensions, and simulation of the same, have clearly resulted in a few new observations on the flow of pulp suspensions.

First: The velocity profiles, both measured and simulated, are far from 'flat'. This has been shown to be the case with independently measured suspensions with several different techniques and under several different flow conditions. Most measurements have been combined with head loss measurements, which are further validation of the simulations.

Second: The claim that the rheology models do not apply for the flow of pulp suspensions is shown to be wrong. Independently performed measurements and simulations clearly show that rheology modeling is a valid approach.

Third: Many authors have observed the existency of a slip layer in their measurements, and in simulations the wall function has bee observed to be the missing part, in this report one method for developing this missing link has been presented.

Fourth: The wall slip leads to a 'flat' looking velocity profile, which will look very much like a 'plug', and may lead to conclusions regarding the existence of yield stresses and fluidisation of the suspension.

Fifth: The 'plug' term should perhaps be rejected. As can be seen from all velocity profiles presented in the current paper, no distinct 'plug' exist. The term plug is useful for describing zones of very low shear, but its definition and limitation is unclear and more or less arbitrary.

Six: Study the boundary layer! This is the key for flow modeling of pulp suspensions.

If not earlier, it is now obvious that fiber suspensions are subjected to the same laws of fluid mechanics as any other flowing medium. This has been shown by comparing measured and simulated head losses, and further by comparing measured and simulated velocity profiles.

At least in the first case, section 9.3.1, the agreement between the measured and simulated values leave no room for speculations, the simulation model is valid throughout all flow rates.

In the second case, section 9.3.2, the agreement is not as perfect, due to difficulties in the measurements, but the measurements and simulations are included in order to show the validity of the pulp models for complex geometries, such as conical and abrupt contractions. This, in combination with the independence of geometry shown earlier, shows that the pulp model can be used for simulating any industrial application.

The third case, section 9.3.3, further illustrates the ability of numerical modeling and fluid mechanics to determine the very complex rheology of pulp suspensions, even when the data cannot be evaluated by analytical models. This method can be used to compare the suitability of the different rheology models presented in section 4, and also for verifying flow properties, such as turbulence, in complex geometry.

All the three cases together show the tremendous strength hidden in fluid mechanics and numerical simulations. The usability of the functions for industrial flows is further demonstrated with a few cases that are presented in section 8.

11 Summary of Thesis and the Pulp Model

In this report, a flow model for pulp suspensions has been presented. The flow model has been developed based on macroscopic flow phenomena and previously published measurements. The flow model is mainly intended for use in the research and development work within the pulp and paper industry, and the manufacturer(s) of the process equipment. Thus, no limitations have been imposed on the flow model limiting its general applicability, it can be used for most flow types in most papermaking applications.

The pulp model consists of a rheology model, a turbulence model and a wall function, all of which are required in order to describe the flow phenomena that may occur in the suspension. The type and parameters for all of these three parts must be related to macro scale measurements, preferably pipe flow measurements. With the model, any simulations can be made based on the real flow properties of the pulp in question, rather than making educated guesses regarding its flow properties.

The pulp model presented in this report consists of three parts, of which the first part, the rheology model, is known from before. The second part, the turbulence model, has mainly been included on a phenomenological level, there does not exist any generally valid data regarding the turbulent flow of pulp suspension above very dilute concentrations. The combination of turbulence model and rheology model has been done before, but in a slightly different way than in the present work. The third part, the wall function, is the most important part of the model. This is the first, and so far only, wall function that can predict the flow behaviour of pulp suspensions at arbitrary concentration with a reasonable accuracy.

This wall function is the missing link that corrects and complements all the previous attempts to model the flow of pulp suspensions. The method presented in this work offers a relatively easy way to determine the necessary pulp parameters under standardized conditions, based on which most processes within the pulp and paper industry can be simulated.

12 Acknowledgements

The author wishes to thank the following institutions for contributing to the project:

Process Flow, all of the staff, for any assistance and for allowing ‘space’ to concentrate on this long-term development project.

Metso Paper Inc, especially Jari P Hämäläinen and Erkki Ilmoniemi, for their belief in and support to this project.

Faxén Laboratory, and KTH Mekanik, especially Anders Dahlkild and Fritz Bark, and all the rest of the staff who participated in the scientific work.

TEKES, who participated in the financing of the project.

Ari Jäsberg, at Jyväskylä University, who kindly let us use his measurement data for this project.

Anders Dahlkild and Jari P Hämäläinen have been supervisors of the project, a difficult task, for which the author is grateful.

Tomas Wikström has been opponent at the defence of the thesis, which is also gratefully acknowledged.

13 List of symbols

Viscosity models:

k	Material parameter of dimension time, natural time, viscosity for the Newtonian model
n	Exponent of shear rate in the power models
a	Parameter that controls the range of transition. A low number results in a long transition region, and a high value gives an abrupt transition in the power models
$\dot{g}$	Strain rate = shear rate = $\frac{\partial u}{\partial r}$ in fully developed pipe flow, mathematicians prefer the symbol I_2, the second invariant of the velocity gradient
I_2	Second invariant of the velocity gradient
F	Slip coefficient
F_1	Slip coefficient
e	Slip exponent
F_2	Slip coefficient
c	Model parameter in the wall function of Spalding.
c_{mass}	Concentration by mass, gives the dry fraction of the suspended fibers
c_v	Concentration, gives the volume fraction of the swollen fibers
$?_t$	Eddy viscosity in the ke-turbulence model
?	Model parameter in the wall function of Spalding.
e	Dissipation of turbulence.
µ	Viscosity
μ_0	Zero shear viscosity
μ_8	Infinite shear viscosity
$\mu_{apparent}$	Apparent viscosity, the ratio of shear stress and shear rate calculated from force and velocity measurements as if the liquid were Newtonian.
?	Density
?	Angular velocity
t	Stress, in this report specifically shear stress
t_y	Yield stress
t_{wall}	Shear stress at the wall
? p	Pressure drop, head loss
? l	Length, difference in length
$\dot{g}_{av}$	Mean shear rate, Newtonian
$\dot{g}_{wall}$	Shear rate at the wall, pseudoplastic
C_μ	Model parameter of the ke-turbulence model
y^+	Dimensionless height of the boundary layer
u^+	Dimensionless velocity of the boundary layer
f_s	Shear stress, Navier's law

F_{slip}	Slip coefficient, Navier's law
u_{wall}	Wall slip velocity, apparent or effective wall slip with suspensions and multiphase material, the term apparent slip is used to describe the abnormally high velocity gradients at the boundary wall.
r	Radius, distance from the pipe axis.
R	Pipe radius.

Abbreviations

CFD	Computational fluid dynamics
FFC	Fiber Flocculation Concept
TMP	Thermo-mechanical pulp
SGW	Stone ground wood
SBK	Semi-bleached kraft

14 Household Rheology

In order to further illustrate the rheology issue, a few common fluids are categorized based on their rheological properties.

Mayonnaise	shows a yield stress, or pseudoplastic behaviour with a very long relaxation time
Honey	is usually a Newtonian fluid, even though it has a high viscosity
Flour-water-dough	is definitely viscoelastic. This can be seen as the dough may flow if it is subjected to an outer force, but it also shows elasticity as it tends to regain its shape
Potato starch	in solution is shear-thickening. This is the best example for do-it-yourself rheology experiments. Add a large amount of potato starch in a jar, and add water, only so much water that the starch is dissolved. Mix with a spoon. If you stir slowly, the starch solution offers little resistance, but try stir quickly, and the resistance grows. It may even be possible to lift the starch solution and the jar by pulling out the spoon quickly enough.
Blood	is usually treated as a mildly power-law shear-thinning fluid.
Paint	paint is a suspension, which flows when applied under shear from a brush. When the shear is removed, the paint does not flow due to its rheology.

Fiber suspension :

Fiber suspensions very much resemble porridge. A fiber suspension of 3%-mass resembles porridge of oat, both in appearance and flow properties. The consistency of oat porridge is roughly 10-12%.

15 Literature

[1] Wikström, T; Flow and Rheology of Pulp Suspensions at Medium Consistency, PhD thesis, Chalmer's University of Technology, 2002

[2] Andersson, S; Nordstrand, T; Rasmuson, A: The Influence of Some Fibre and Solution Properties on Pulp Fibre Friction, Journal of Pulp and Paper Science Vol 26 no. 2/2000

[3] Andersson, S; Rasmusson, A; Dry and Wet Friction of Single Pulp and Synthetic Fibres, Journal of Pulp and Paper Science, vol23, 1997

[4] Kerekes, R; Schell, CJ; Characterization of Fibre Flocculation Regimes by a Crowding Factor, Journal of Pulp and Paper Science, vol 18, 1992

[5] Huber, P; Roux, J-C; Mauret, E; Belgacem, N; Pierre, C; Suspension Crowding for a General Fibre-Length Distribution: Application to Flocculation of Mixtures of Short and Long Papermaking Fibres, Journal of Pulp and Paper Science, vol 29, 2003

[6] Ross; Klingenberg; Simulation of Flowing Wood Fibre Suspensions, Journal of Pulp and Paper Science, vol24, 1998

[7] Fan; Phan-Thien; Zheng; A Direct Simulation of Fibre Suspensions, Journal of Non-Newtonian Fluid Mechanics, vol74, 1998

[8] Karema, H; Salmela, J; Tukiainen, M; Lepomäki, H; Prediction of Paper Formation by Fluidization and Reflocculation Experiments, 12th Fundamental Research Symposium, Oxford 2001

[9] Hyensjö, M; Hämäläinen, JP, Dahlkild, A; Turbulent Dilute Fibre Suspension Modeling in a Sudden Circular Pipe Enlargement, PAPTAC 2002

[10] Steen, M; Turbulence and Flocculation in Fibre Suspensions, PhD thesis, University of Trondheim, 1990

[11] Brecht, W; Heller, H; A Study of the Friction Losses of Paper Stock Suspensions, Tappi, vol33 1950

[12] Möller, K; Norman, B; Calming Lengths in Pulp Suspension Flow, Svensk Papperstidning, nr 16, 1975

[13] Durst, R; Jenness, L: The Flow Properties of Paper Pulp Stocks. I. Relationship of Sheer Value to Pipe Friction for Bleached Sulphite Pulp Slurries, Tappi 37 no 10, 1954

[14] Duffy, G; Moller, K; Lee, PFW; Milne, SWA; Design correlations for groundwood pulps and the effects of minor variables on pulp suspension flow, Appita vol 27, 1974

[15] Duffy, G; Abdullah, L; Fibre Suspension Flow in Small Diameter Pipes, Appita 2002

[16] Vielreicher, T; Müller-Steinhagen, H; Allen, M; Duffy, G; Non-Steady-State Flow Behaviour of Wood Pulp Fibre Suspensions, Appita, vol 47, 1994

[17] Mih, W; Parker, J; Velocity Profile Measurements and a Phenomenological Description of Turbulent Fiber Suspension Pipe Flow, Tappi, vol50 1967

[18] Wiklund, J; Johansson, M; In-Line Rheological Measurements of Complex Model Fluids Using an Ultrasound UVP-PD Based Method, M.Sc thesis, Chalmers University of Technology, Sweden, 2001
[19] Wiklund, J; Johansson, M; Shaik; Fischer; Windhab; Stading; Hermansson; In-Line Ultrasound Based Rheometry of Industrial and Model Suspensions Flowing Through Pipes, 3rd International Symposium on Ultrasonic Doppler Methods for Fluid Mechanics and Fluid Engineering, Lausanne 2002
[20] Li; Ödberg; Studies of Flocculation in Cellulose Fibre Suspensions by NMR Imaging, Journal of Pulp and Paper Science, vol28, 1997
[21] Bennington, CPJ; Kerekes, RJ; Grace, JR; The Yield Stress of Fibre Suspensions, Canadian Journal of Chemical engineering, vol68, 1990
[22] Möller, K; The Plug Flow of Paper Pulp Suspensions, PhD Thesis, University of Auckland, New Zealand, 1972
[23] Baines, WD; Laminar Flow of Dilute Fibre Suspension, Svensk Papperstidning, 1959
[24] Head, V; Durst, R; Stock Slurry Hydraulics, Tappi 40, 1957
[25] Soszynski, R; The Plug Flow of Fiber Suspensions in Pipes, Nordic Pulp and Paper Research Journal, no 3, 1991
[26] Myréen, B; Modeling the Flow of Pulp Suspensions in Pipes, Part I, Paperi ja Puu, 5/1989
[27] Myréen, B; Modeling the Flow of Pulp Suspensions in Pipes, Part II, Paperi ja Puu, 7/1989
[28] Hämäläinen, JP; Mathematical Modeling and Simulation of Fluid Flows in the Headbox of Paper Machines, PhD thesis, University of Jyväskylä, 1993
[29] Huhtanen J-P; Non-Newtonian Flows in Paper Making, Licentiate thesis, Tampere University of Technology, 1998
[30] Duffy, G; The Significance of Mechanistic-Based Models in Fibre Suspension Flow, Nordic Pulp and Paper Research Journal, vol 18, 2003
[31] Hammarström, D; Hämäläinen, JP; Dahlkild, A; CFD Simulation of Fiber Suspensions, proceedings "VIII Suomen Mekaniikkapäivät", vol 1, page 71, 2003
[32] Meyer, R; Wahren, D; On the Elastic Properties of Three-Dimensional Fibre Networks, Svensk Papperstidning, 1964
[33] Andersson, S; Ringnér, J; Rasmusson, A; The Network Strength of Non-Flocculated Fibre Suspensions, Nordic Pulp and Paper Research Journal. vol14, 1999
[34] Wikström, T; Rasmusson, A; Transition Modeling of Pulp Suspensions Applied to a Pressure Screen, Journal of Pulp and Paper Science vol28, no 11, 2002
[35] Damani, R; Powel, R; Hagen, N; Viscoelastic Characterization of Medium Consistency Pulp Suspensions, Canadian Journal of Chemical engineering, vol71, 1993

[36] Swerin, A; Powell, R; Ödberg, L: Linear and Nonlinear Dynamic Viscoelasticity of Pulp Fiber Suspensions, Nordic Pulp and Paper Research Journal Vol 3/1992
[37] Bennington, CPJ; Mmbaga, JP; Liquid-Phase Turbulence in Pulp Fibre Suspensions, 12th Fundamental Research Symposium, Oxford, 2001
[38] Lindroos, K; Piirto, M; Huhtanen, JP; The Effect of Fibers on Turbulent Quantities in Backward Facing Step Channel Flow: Measurements and Numerical Simulations, Third International Symposium on Turbulence and Shear Flow Phenomena, Sendai, Japan, 25-27 June, 2003, pp. 233-238
[39] Kuhn, D; Sullivan, P; Analysis and Measurement of the Flocculation Intensity of Flowing Pulp Suspensions, 2001 Papermakers conference, Cincinnati, OH, USA, 11-14 Mar. 2001, session 14, TAPPI Press
[40] Hemström, G; Möller, K; Norman, B: Boundary Layer Studies in Pulp Suspension Flow, Tappi 59 no 8, 1976
[41] Gullichsen, J; Härkönen, E: Medium Consistency Technology I. Fundamental Data, TAPPI Vol 64, no6/1981
[42] Välimäli, A; Mathematical Modeling of Concentrated Colloidal Suspensions, Lic thesis, Åbo Akademi University, 1999
[43] Kokko, A; Evaluation of Viscosity, Elongational Viscosity and Dewatering of Coating Colours at High Shear Rates, Ph.D. thesis, Åbo Akademi University, 2001
[44] Johnson, PC; Jackson, R: Frictional-Collisional Constitutive Relations for Granular Materials, With Application to Plane Shearing, Journal of Fluid Mechanics, Vol 176, pp 67-93, 1987
[45] Phillips; Armstrong; Brown; A Constitutive Equation for Concentrated Suspensions That Accounts for Shear Induced Particle Migration, Phys. Fluids A, vol4, 1992
[46] Nott; Brady; Pressure Driven Flow of Suspensions: Simulation and Theory, Journal of Fluid Mechanics, 1994
[47] Loewenberg, M; Hinch, EJ: Numerical simulation of a concentrated emulsion in shear flow, Journal of Fluid Mechanics, vol 321 pp 395-419, 1996
[48] Turian, RM; Ma, T; Hsu, F; Sung, D; Flow of Concentrated Non-Newtonian Slurries: 1. Friction Losses in Laminar, Turbulent and Transition Flow Through Straight Pipe, International Journal of Multiphase Flow, vol24 no2, pp225-242, 1998
[49] Kim, S; Cho, Y; Jeon, A; Hogenauer, B; Kensey, K; A New Method for Blood Viscosity Measurement, Journal of Non-Newtonian Fluid Mechanics, vol94, 2000
[50] Ramazani; Ait-Kadi, A; Grmela, M: Rheology of Fiber Suspensions in Viscoelastic Media: Experiments and Model Predictions, Journal of Rheology, Vol 45 no 4, 2001
[51] Petrie, CJS; The Rheology of Fibre Suspensions, Journal of Non-Newtonian Fluid Mechanics, vol87, 1999
[52] Morrison, F; Understanding Rheology, Oxford University Press, 2001

[53] Barnes; HA; Walters, K; The Yield Stress Myth, Rheologica Acta, vol 24, 1985
[54] Wilcox, D; Turbulence Modeling for CFD, 2nd edition, 2000, ISB-N 0-9636051-5-1
[55] Malin, MR; Turbulent Pipe Flow of Power-Law Fluids, Int.Comm.Heat Mass Transfer, vol 24, no 7, 1997
[56] Malin, MR; Turbulent Pipe Flow of Herschel-Bulkley Fluids, Int.Comm.Heat Mass Transfer, vol 25, no 3, 1998
[57] Malin, MR; Turbulent Pipe Flow of Bingham Plastic Fluids in Smooth Circular Tubes, Int.Comm.Heat Mass Transfer, vol 24, no 6, 1997
[58] Spalding, DB; A Single Formula for the "Law of the Wall", Journal of Applied Mechanics, 1961
[59] Joshi; Lele; Mashelkar; A Unified Wall Slip Model, Journal of Non-Newtonian Fluid Mechanics, vol 94, 2000
[60] POLYFLOW 3.8 Manual, Fluent Inc, 2000
[61] Hammarström, D; Hämäläinen, JP; Dahlkild, A; Jäsberg, A; Modeling of Laminar Suspension Flows, submitted to 'Computers and Fluids', 2003
[62] Hammarström, D; Hämäläinen, JP; Dahlkild, A; Jäsberg, A; Modeling of Turbulent Suspension Flows, submitted to 'Computers and Fluids', 2003
[63] Schmidt E; Properties of Water and Steam in SI Units, Springer Verlag, Berlin, 1969
[64] Barin I, Knacke O; Thermochemical Properties of Inorganic Substances, Springer Verlag, ISBN 3-540-06053-7, 1963
[65] Fluent Manual
[66] Björkman, Ulf: Flow of flocculated fibres, ISBN 91-7170-178-8, Second printing, 2000
[67] Duffy, G: A review and evaluation of design methods for calculating friction loss in stock piping systems, Tappi 59 no 8, 1976
[68] Bennington, C; Kerekes, R; Grace: Motion of Pulp Fibre Suspension in Rotary devices, The Canadian Journal of Chemical Engineering Vol 69/1991
[69] Lee, P; Duffy, G; Velocity Profiles in the Drag Reducing Regime of Pulp Suspension Flow, APPITA, vol 30, 1976
[70] Lee, P; Duffy, G; Relationships Between Velocity Profiles and Drag Reduction in Turbulent Fiber Suspension Flow, AIChE Journal, vol 22, 1976
[71] Li, T; Powell, R; Ödberg, L; McCarthy, M; McCarthy, K; Velocity measurements of fiber suspensions in pipe flow by the nuclear magnetic resonance imaging method, Tappi, vol77, 1994
[72] Li, Ödberg, Powell, Weldon, McCarthy; Flow of pulp suspensions through an abrupt contraction studied by flow encoded nuclear magnetic resonance imaging, Nordic pulp and paper research journal, no2, 1995
[73] Li, Powell, McCarthy; Flow of pulp suspension through a 4:1 continuous conical contraction studied by NMR imaging technique,

TAPPI Proceedings of 1995 Engineering conference, Loews Anatole, Dallas, Texas, September 11-14. TAPPI Press, pp. 209-219, 1995.

Appendix List of Papers

I **CFD Simulation of Fiber Suspensions**
Presented at the "VIII Suomen Mekaniikkapäivät",
June 12-13 2003, Espoo, Finland
Paper published in the proceedings, vol1, page 71.

II **Modeling of Laminar Suspension Flows**
Paper submitted to "Computers & Fluids"

III **Modeling of Turbulent Suspension Flows**
Paper submitted to "Computers & Fluids",
to be published as a pair to the previous.

CFD Simulation of Fiber Suspensions

David Hammarström, Process Flow Ltd Oy,
fax: +358-2-2759580
email: david.hammarstrom@processflow.fi
Jari P. Hämäläinen, Metso Paper Inc.
Anders Dahlkild, Faxén Laboratory, KTH, Sweden

Abstract
Fiber suspensions are present at many dry contents in the fiber line in the paper making process. Proper fiber handling is of vital importance to maintain the quality of the individual fibers and to optimise each unit process of the fiber line. In order to optimise the process, thorough knowledge of the suspension flow is necessary, both on the level of suspension, fiber networks and individual fibers. Knowledge of the fiber suspension flow behaviour combined with commercial CFD (Computational Fluid Dynamics) provides an efficient design tool for unit processes of the pulp and paper industry.

In this paper the general validity of a pulp flow model presented in a previous paper is demonstrated. The simulation method has been developed in pipe flow, but the method allows the flow of fiber suspensions to be simulated in any industry geometry. The model is presented with one set of measured head loss data for a pipe flow for which the fluid specific parameters are fitted. Numerical solution using the model is compared to experimental head loss data from the literature. The most significant result presented in this paper is that pulp suspension can be modeled using flow models for homogenous fluids, despite what has been argumented in the literature.

1. Introduction

The head losses in pipe flow of pulp suspensions has been measured for many decades. The study of fiber suspension flow must be done in fully controlled environments, such as, pipe flow. Pipe flow of pulp fiber suspensions do not follow the head loss curve of neither the laminar nor the fully turbulent flow curve, but usually show a very characteristic "S"-shaped curve for the head loss plotted against the flow rate. The head loss measurements presented in the literature are based on many different pipe diameters and using many different pulp types. Different pipe diameters can be taken into account when developing flow models for pulp flow, but different pulp types cannot be combined due to the significant differences in behaviour. Several old measurement series have used too short calming lengths for the pulp flow, but a good source is the thesis of Möller [1], from which the reference data presented in this paper is taken.

Earlier only the first, laminar, part of the flow could be properly modeled. Shear thinning viscosity models have been used for slow velocities, but they fail as the velocity increases resulting eventually in decreasing head losses. Myréen [2] demonstrated the use of the power-law viscosity model for pulp flow modeling for the laminar plug-flow region. Duffy [3], on the other hand, arguments that the flow of fiber suspensions cannot be modeled using non-Newtonian laminar flow models. Several important flow features are neglected when using homogenous flow models, for instance, the tendency to form fiber netwoks and agglomerates, flocs.

The region where the head losses decrease with increasing flow rate has been attributed to the formation of a water annulus at the pipe walls. The thickness of this slip layer has been analytically calculated by Soszynski [4] and Hämäläinen [5]. Both authors showed that the water annulus thickness is negligible compared to the other dimensions of the flow. A mathematical model presented by Hammarström et al [6] is capable of describing both flow regimes, that is, increasing and decreasing head losses as a function of increasing velocity. The model is an effective wall slip model, which does not model the slip phenomenon, but only the effects on the flow.

The current results show that the wall slip phenomenon is independent of pipe diameter and that the laminar flow models can be used for simulating complex pulp flows, based on relatively simple head loss measurements in pipe flows.

2. Suspension Rheology

The fiber suspension is modeled as a homogeneous shear-thinning fluid. The power-law viscosity model, equation {1} is used, where t is the shear stress, μ is the viscosity, K is the consistency coefficient and n is the fluid behaviour index and $\dot{g}$ is the strain rate.

$$t = m\dot{g} = K(\dot{g})^{n-1}\dot{g} \qquad \{1\}$$

There are also other generalized Newtonian models, for example, Wikström and Rasmusson [7] used the Bingham model (a yield-stress model) for an industrial screening application. The viscosity model is not a key issue of this paper, the power-law model was chosen in order to demonstrate a new method, with which the same model can be used to describe both the plug-flow regime and the wall-slip regime.

3. Wall slip model

The model derived for the plug-flow regime is assumed valid for the suspension, and that the head loss reduction is due to slip on the wall. This is illustrated in Picture 1. The pulp plug is assumed intact, and the slip velocity is setting the correct flow rate.

By introducing a slip term, the shear stress at the wall is given by {2}

$$m\dot{g} + Fu_{slip} = 0 \qquad \{2\}$$

where the first term is the shear stress near the wall, and the second term is a constant multiplied by the wall slip velocity, u_{slip}. At the pipe wall, the velocity is always zero, but as the current model is not modeling the flow down to the wall, the velocity at the boundary between the pulp core plug and the water layer is used.

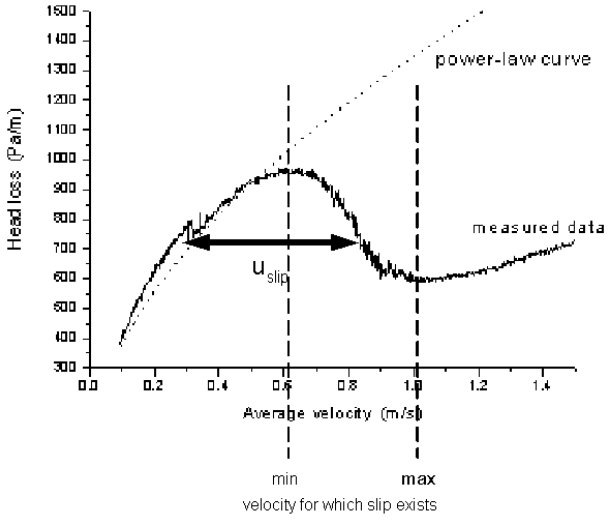

Picture 1. The lower and upper limits of the validity of the wall slip assumption is given by the dashed lines. The region at lower flow rates than the wall slip region is referred to as the plug flow region.

By inserting expression {2} into the axially symmetric two-dimensional Navier-Stokes equation, and solving for the velocity profile in the pipe, the mean flow rate in the pipe is obtained. The first term on the right hand side in equation {3} is the normal solution for the mean velocity in pipe flow of a fluid of which the viscosity is given by power-law model, equation {1}. The second term is the slip velocity required in order to get the correct flow rate, which is illustrated by picture 1.

$$u_{average} = \left(\frac{\Delta p}{\Delta l \, 2k} \right)^{\frac{1}{n}} \frac{n}{3n+1} R^{\frac{n+1}{n}} + u_{slip} \qquad \{3\}$$

The slip term in equation {2} is modified in order to model the head loss curves correctly. The wall shear stress is described by an exponential and a linear term of the wall slip velocity, of which the exponential term is known as the generalized Navier's law [8]. The simplest wall slip model that is able to describe the head loss curve is given by {4}

$$mg + \left(f_1 u_{slip}^{e-1} + f_2 \right) u_{slip} = 0 \qquad \{4\}$$

4. Calculations

The measured data of the flow of Hudson Birch pulp was taken from Möller [1]. The measurement series contained three different pipe diameters, and the measurements had been carried out at many dry contents of the pulp. Four of the consistencies were selected, based on the number of measurement points in the flow rate regions of interest.

Table 1 The model parameters fitted for the measured head loss data of Hudson birch pulp.

	k	n	f_1	e	f_2
1.51%	2.1995	0.2250	5.3701	-0.0019	-1.9576
1.97%	3.8691	0.2530	11.9443	-0.0188	-4.0994
2.65%	7.2163	0.2657	26.5436	-0.0108	-4.4447
3.51%	9.0215	0.2670	35.4059	-0.0306	-2.5706

The viscosity parameters, k and n, of each consistency were determined in the plug flow region, see picture 1. The parameters of each consistency have been determined in the 4 inch pipe, the same parameter have been used for the simulation for all pipes in pictures 2-4. In a similar way, the parameters for the wall friction were determined in the wall slip region according to equation {2}. The parameters of both regions are presented in table 1. The wall slip function was implemented in the commercial CFD code FLUENT, version 6.0.20. As the wall slip function is implemented directly as a wall boundary condition, there is no need to specify in which region the flow is, the solver determines this based on the mass and force balances.

The simulations have been carried out in three pipes with inner diameters 2.09, 3.01 and 3.93 inches. The pipes were modeled in 2D with axial symmetry. The computational grids contained 3600-5500 cells. The cell height was reduced towards the pipe wall. The head loss curve of each pipe and consistency was simulated by incrementing the inlet boundary condition with 0.1m/s for each simulated point. The suitability of the numerical scheme and cell size and convergence criteria has been controlled.

5. Results

The simulation results of the pulps are presented in pictures 2-4. The results are presented in the same way as the measurement results, one picture per pipe diameter. As is clearly visible, the agreement between the simulations and the measurements is quite good. There are a few small differences between the data, this is caused by the difficulty of determining the mean head loss curve for the pipe in which the parameters are fitted. The important thing to notice is that it is not important for which pipe diameter the viscosity and slip paremeters have been fitted, but that the same parameters have been used for all pipes. For a more accurate determination of the pulp parameters more measurement points would be required, the current number is a bare minimum. But still, the results show an excellent agreement for all three pipe diameters.

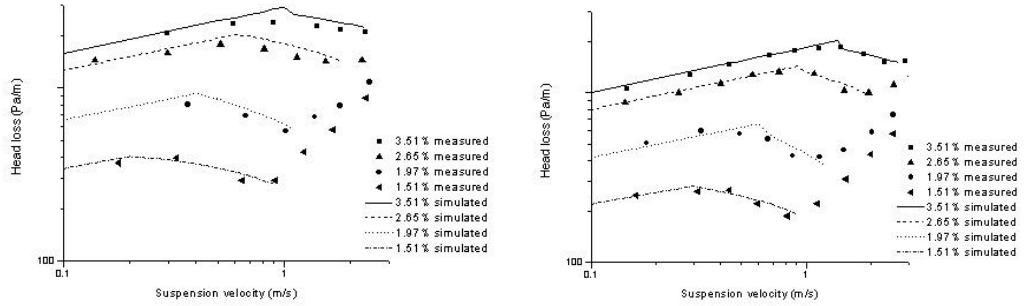

Picture 2-3 Measured and simulated head losses in 2 and 3 inch pipes.

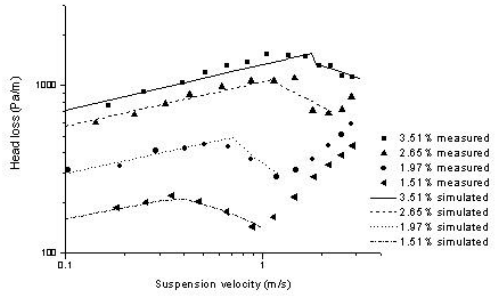

Picture 4 Measured and simulated head losses in 4 inch pipe

The influence of the wall slip model is shown by picture 5. In this picture the resulting velocity profile of four cases are shown. Two velocities, 0.3 and 1.4m/s, from the 3inch pipe at 2.65% consistency were chosen. The velocities were chosen to represent both flow rate region. The lower velocity is in the plug flow region, and the higher is in the wall slip region. For comparison, identical simulation results but without the slip model at the pipe wall have been included in the picture.

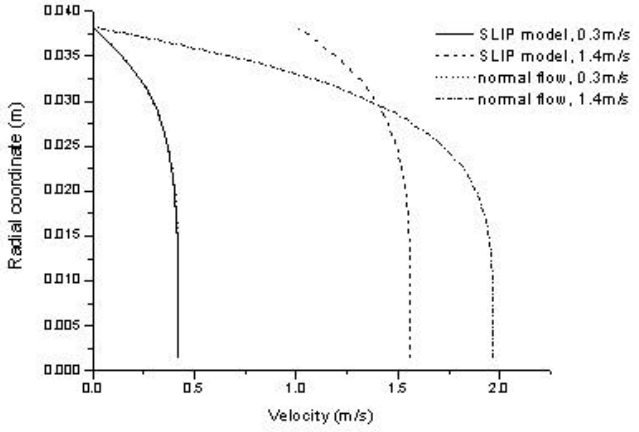

Picture 5 The velocity profile in the pipe. The legends refer to the boundary conditions used at the pipe wall and mean velocity.

In the low velocity cases, both the simulation with the wall slip and the normal no-slip wall boundary condition return identical velocity profiles, which shows that the method can be used for low flow rates as well. In the higher velocity cases, there is a significant slip velocity at the pipe walls. The normal no-slip simulation returns a zero velocity at the pipe wall, the wall slip model returns roughly 1m/s.

This difference is of fundamental importance. If, for instance, the velocity profile in this kind of pipe flow is determined with any kind of instrument, the instrument will need to have a very high resolution near the pipe wall. Otherwise, the instrument will just see one large plug. That the instrument will observe just one large plug has been observed by many authors, for instance, Head and Durst [9] commented that the velocity profile is rectangular. If the viscosity parameters are determined at the higher flow rate case in picture 5 neglecting the wall slip, then the resulting pulp parameters will be incorrect.

5. Discussion

The wall slip has been shown to be a useful and valid method for describing the head loss in laminar pipe flow of fiber suspensions. The method has been shown to be able to correctly describe the flow of several consistencies over a large range of flow rates in three pipe diameters. This quite clearly shows that pulp suspensions can be modeled using laminar flow models for homogenous fluids. The upper limit for the validity of the currently presented wall slip model has been set to the local minimum on the head loss curve. At this point the flow becomes turbulent.

6. Acknowledgements

The financial support from the Finnish National Technology Agency, TEKES, and Faxén Laboratory at the Royal Institute of Technology, Stockholm, Sweden is thankfully acknowledged.

References:

[1] Möller K; **The Plug Flow of Paper Pulp Suspensions**, PhD thesis, University of Auckland, New Zealand, 1972

[2] Myréen B; **Modeling the Flow of Pulp Suspensions in Pipes, Part 1.** Paperi ja Puu, 5/1989.

[3] Duffy G.G; **The Importance of Mechanistic-based Models in Fibre Suspension Flow**, Nordic Pulp and Paper Journal, 2003, in press

[4] Soszynski R; **The Plug Flow of Fiber Suspensions in Pipes. A Case of Clear Water Annulus**, Nordic Pulp and Paper Research Journal, no 3, 1991.

[5] Hämäläinen, J; **Mathematical Modeling and Simulation of Fluid Flows in the Headbox of Paper Machines,** PhD Thesis, University of Jyväskylä, 1993

[6] Hammarström D, Hämäläinen J, Dahlkild A, Jäsberg A; **Modeling of laminar suspension flows**, submitted to JOURNAL OF PULP AND PAPER SCIENCE

[7] Wikström T, Rasmusson A; **Transition Modeling of Pulp Suspensions Applied to a Pressure Screen**, Journal of Pulp and Paper Science, vol 28, 2002
[8] **POLYFLOW 3.8 User Guide**, ch 6, Fluent Inc.
[9] Head V.P, Durst R.E; **Stock Slurry Hydraulics**, TAPPI vol 40 no 12, 1957

Modeling of laminar suspension flows

David Hammarström [a,*], Jari P Hämäläinen [b], Anders Dahlkild [c], Ari Jäsberg [d]

[a] Process Flow Ltd Oy, Puolalanpuisto 1 b A 21, FIN-20100 Turku, Finland
[b] Metso Paper Inc., PO Box 587, FIN-40101 Jyväskylä, Finland
[c] Royal Institute of Technology, Department of Mechanics, SE-10044 Stockholm, Sweden
[d] University of Jyväskylä, Department of Physics, PO Box 35, FIN-40014 Jyväskylä, Finland
* Corresponding author. E-mail address: david.hammarstrom@processflow.fi Fax: +358-2-2759580

Abstract

Mathematical modeling and numerical simulation of a pipe flow of paper pulp suspension is studied in this paper. The flow of wood fiber suspensions do not follow the pressure loss curves for neither laminar, nor fully developed turbulent flow of a Newtonian fluid like pure water, but pulp suspensions often show an "S"-shaped curve for the pressure drop plotted against the average suspension velocity. Shear thinning viscosity models have been used for slow velocities, but the model predictions fail as the velocity increases. A mathematical model derived in this paper is capable of describing two flow regimes, that is, increasing and decreasing head losses as a function of increasing velocity, as long as the flow is laminar. Numerical solution of the model is also compared to new experimental head loss data for pulp suspensions of 1-2% mass fraction.

Keywords: CFD, pulp, rheology, slip

Introduction

Paper pulp suspensions are made from wood fibers, that are released from the wood by either chemical or mechanical treatment. The length and coarseness of the individual fibers varies, the length of a typical birch fiber is 1mm. The influence of the different minor variables, such as bleaching and milling and fiber properties, on the flow of pulp suspensions is not an issue of this paper, and hence any discussion regarding these is left out.

Within the pulp and paper industry, the pulp suspensions have fiber contents varying from 0.5%-mass to above 10%-mass. Wood fiber suspensions within the pulping and paper manufacturing industry are among the technically and financially most important of all industry suspensions.

Head loss measurements of pulp suspension flows of various pulps, dry contents and tube diameters have been made for many decades. The typical S-shaped head loss curves, as those presented here for bleached birch pulp, have been found by many authors, for example, Durst and Jenness [1] and Brecht and Heller [2].

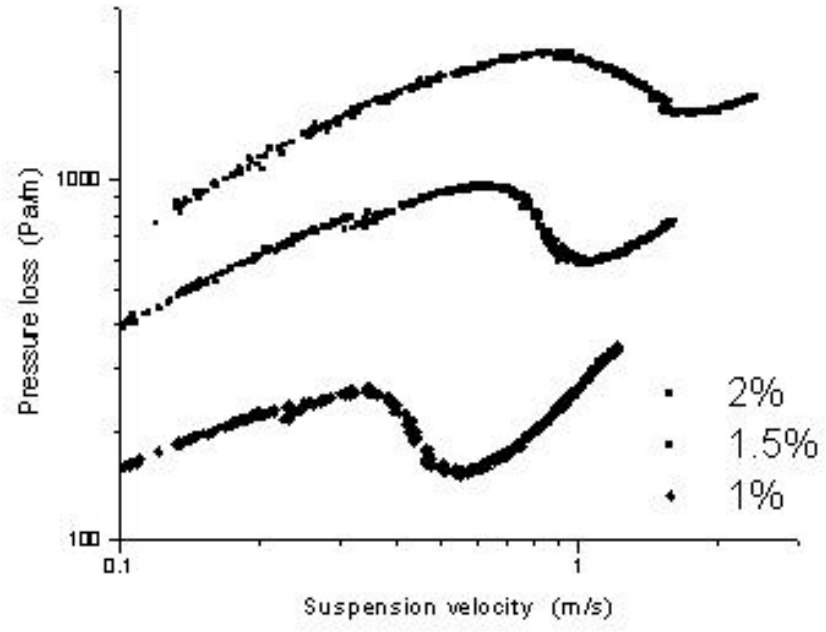

Figure 1. Measured head loss curves of bleached birch pulp.

The peculiar flow regime where the head loss decreases with increasing velocity, as shown by figure 1, is explained by a thin lubricating layer of pure water that is assumed to form on the pipe wall, causing the reduced friction, Head and Durst [3].

The head losses in the "plug-flow" regime, where the head losses increase as a function of velocity, have been modeled using purely empirical equations in many engineering applications, as for example by Duffy, Moller, Lee and Milne [4]. The models are useful in dimensioning of pipes, but are of no help for studying pulp flow in other geometries.

Myréen [5] derived the head loss equation based on basic fluid dynamic equations, assuming the power-law model for the viscosity. This was an important step for understanding pulp flows, because he introduced a model, which is not limited to pipe flow. With computational fluid dynamic (CFD) simulations pulp flows can be simulated for any unit process of the pulp and paper industry.

Myréen [6], Soszynski [7] and Hämäläinen [8] made analytical studies of the "wall-slip" regime to determine the thickness of the water lubrication layer, but they did not derive any general model for the wall-slip regime. The most recent work by Duffy [9] presents an effective slip correlation that describes the reduction in friction loss.

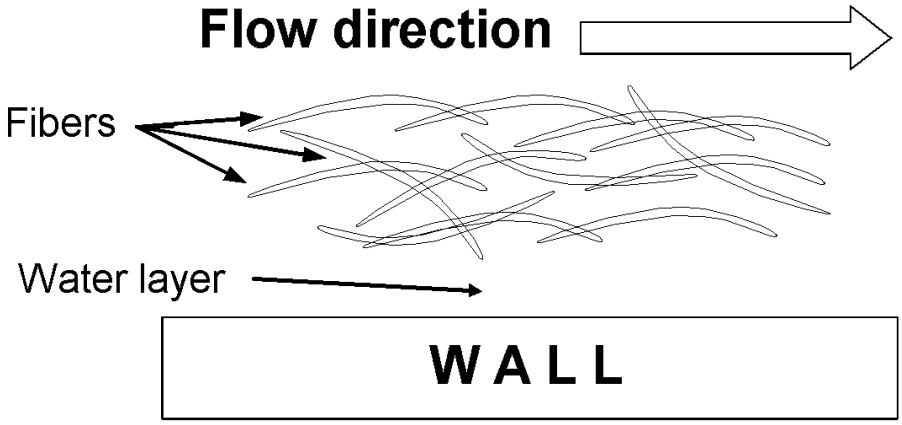

Figure 2. A clear water annulus is formed on the walls. The height of the water layer is negligible compared to other dimensions.

In this paper we are broadening the applicability of the power-law model from the plug-flow regime to the wall-slip regime. The water annulus thickness (schematic Figure 2) was measured using a novel laser-optical technique in a D=40 mm pipe. The thickness was of the order of 100 μm for mass fraction c=1.0% and decreased with increasing consistency to about 10 μm for c=2.0%.

Thus the annulus thickness is negligible compared to the pipe diameter and the shear stress is approximately constant over the water annulus, as also stated by Soszynski [7]. This means that the wall slip regime can be modeled with a slip boundary condition directly on the wall. The magnitude of the slip velocity is assumed to be governed by the flow conditions close to the wall. Here, a non-linear relationship between wall shear stress and slip velocity is determined by adapting analytical solutions of a specific power-law fluid to measurements of head loss in a pipe of a given pulp. The resulting model relationship is of general form, i.e. not restricted to any simple geometry, but can be used for any industry R&D simulation purposes.

Head loss measurements

The head loss was measured in a laboratory scale (D=40mm) flow loop for birch suspension with mass fractions 1.0%, 1.5% and 2.0%. The measurement data are presented in Figure 1. The measurement data presented in figure 1 is not a line graph but points, for each consistency the chart contains 5-800 different mean flow rates. The measurement section was made of two semi-circular channels cut to separate acrylic prisms, which were attached together to form a full circular flow channel. That way the holes for pressure taps could be drilled starting from the interior of the channel to minimize breaking of the channel wall next to the holes, which would produce fluctuations to flow and measured head loss. The distance between the pressure taps was 0.89 m, and the straight free sections upstream and downstream from the taps were 2m and 1m respectively. For each flow rate, 10.000 samples of head loss were measured with a frequency that gave a constant distance of 1 mm in fluid flow between two consecutive samples.

Suspension rheology

The fiber suspension is modeled as a homogeneous shear-thinning fluid. The power-law viscosity model, equation {1} is used, where t is the stress, μ is the viscosity, K is the consistency coefficient and n is the fluid behaviour index and $\dot{g}$ is the strain rate.

$$t = m\dot{g} = K(\dot{g})^{n-1}(\dot{g}) \qquad \{1\}$$

There are also other generalized Newtonian models. For example, Wikström and Rasmusson [10] used a Bingham model (a yield-stress model) for an industrial screening application. The power-law model is used in order to demonstrate a new methodology, with which the same model can be used to describe both the plug-flow regime and the wall-slip regime. Further, with the power-law model some analytical calculations, that are not possible with more complex models, can be made. Other viscosity models can easily be used in the numerical simulations, if it proves necessary.

Table 1 The power-law viscosity coefficients of bleached birch.

	K	n
1%	0.4280	0.4031
1.5%	0.6571	0.5511
2%	1.8418	0.4756

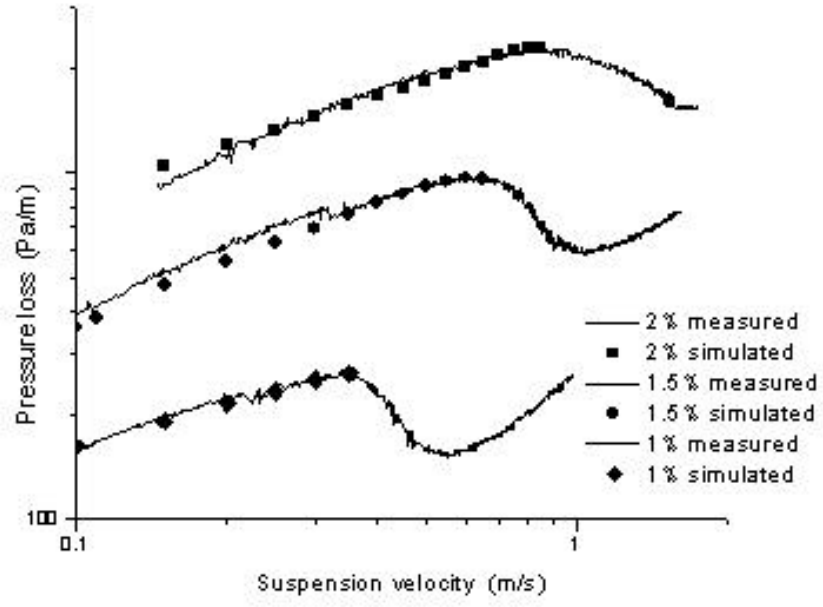

Figure 3 The measured head losses of birch and the head losses from CFD simulations, parameters according to table 1.

Table 1 and Figure 3 show the pulp model parameters in the plug-flow region. The parameters were obtained with least squares fitting to the measured data. The parameters are valid only for this particular pulp; new parameters must be used for other pulps.

Analytical model for the wall-slip regime

The model derived for the plug-flow regime is assumed valid for the suspension, and that the head loss reduction is due to slip on the wall. This is illustrated in Figure 4. The pulp plug is assumed intact, and the slip velocity is setting the correct flow rate.

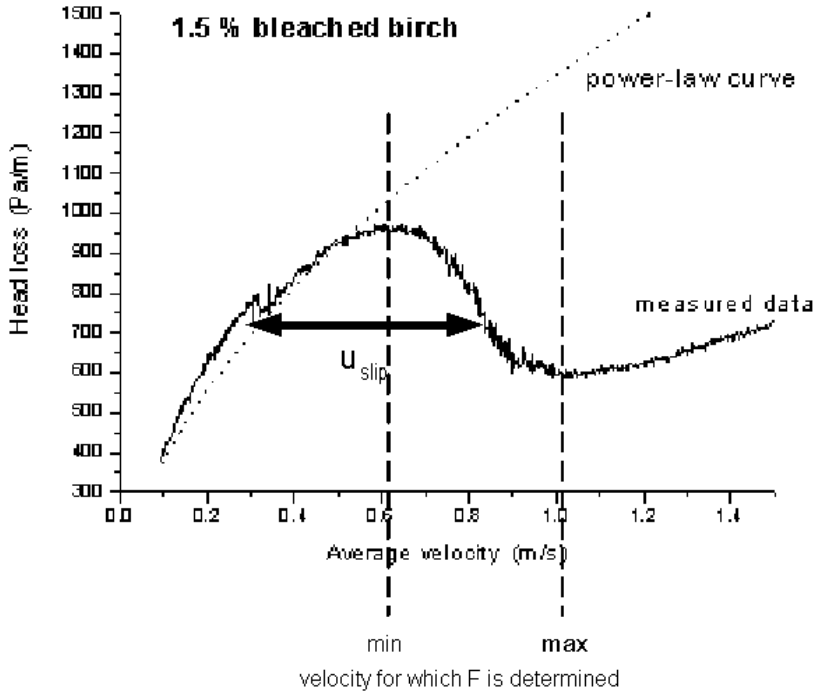

Figure 4. The lower and upper limits of the validity of the wall slip assumption is given by the dashed lines.

The term "wall slip" may seem misleading, but this phenomenon is frequently encountered, for instance, within the polymer processing industry. The term does not mean that there would be zero friction on the walls, but that the velocity at the wall is not equal to zero (Figure 5). In this case a water annulus is present at the wall. On the tube wall, the velocity is zero, but on the boundary between the water boundary layer and the pulp suspension the velocity it is not equal to zero. Therefore, it is reasonable to use a slip-condition on the wall.

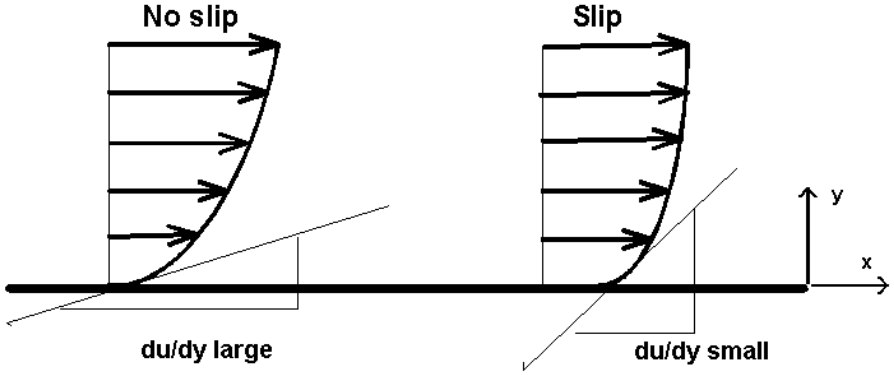

Figure 5. The interpretation of the wall slip.
Slippage reduces the velocity gradient within the bulk fluid, which is equal to a lower friction on the wall.

The rheological significance of this addition to the rheology model is that this reduces the wall friction, and returns a flow profile, which more resembles the "plug" flow observed by many authors. Head and Durst [3] commented that the flow profile is essentially rectangular.

For a full presentation of the wall slip phenomenon and other rheological issues, the reader is referred to Morrison [11]. In this book the fundamentals of rheology and fluid mechanics are covered in an excellent way.

The flow in a tube is modeled with the axi-symmetric Navier-Stokes equations, the flow is assumed fully developed. The momentum equation reduces to

$$-\frac{1}{r}\frac{\partial}{\partial r}\left(r\,s_{rz}\right)+\frac{\Delta p}{\Delta l}=0 \qquad \{2\}$$

For the viscosity the power-law model presented earlier in this paper, is used for each consistency, of which the parameters are presented in table 1.

Next the momentum equation {2} is solved analytically for the following boundary conditions: at the centreline of the tube (r=0), the viscous stress equals zero.

$$m\frac{\partial u}{\partial r}=0\,. \qquad \{3\}$$

At the computational wall (r=R), on the boundary between the water annulus and the pulp plug:

$$u=u_{slip} \qquad \{4\}$$

Then equation {2} can be solved analytically, with the boundary conditions {3} and {4}, which return the velocity profile u(r) in the pipe. Integration over the pipe Cross surface gives the average velocity, which becomes

$$u_{average}=\left(\frac{s_{rz}}{k}\right)^{\frac{1}{n}}\frac{n}{3n+1}R+u_{slip} \qquad \{5\}$$

where the wall shear stress is $s_{rz}=\frac{\Delta p}{\Delta l}\frac{R}{2}$.

The first part of the right side of equation {5} is the solution for the pipe flow of a power-law fluid with no-slip conditions. The second part forms a "correction" term, which adds the slip velocity, u_{slip}, to the mean velocity.

As the slip velocity is not known on beforehand, a slip-friction boundary condition is required to determine u_{slip}. This boundary condition is determined using the experimental data. The slip velocity, u_{slip}, is adapted to each point of the experimental data of $u_{average}$ and ? p using equation {5}. An illustration of this procedure is shown in figure 4, where the analytical relationship {5} with uslip=0 is shown together with the

experimental data. This results in a relation between the slip velocity and wall shear stress of the form

$$m\frac{\partial u_z}{\partial r} + Fu_{slip} = 0, \qquad \{6\}$$

where we term $F(u_{slip})$ as the friction coefficient.

The values of F versus the obtained u_{slip} are given in Figure 6. It shows that for each slip velocity there is a corresponding friction of the power law fluid. It also shows that the relationship between wall shear stress and the slip velocity is strongly non-linear in nature.

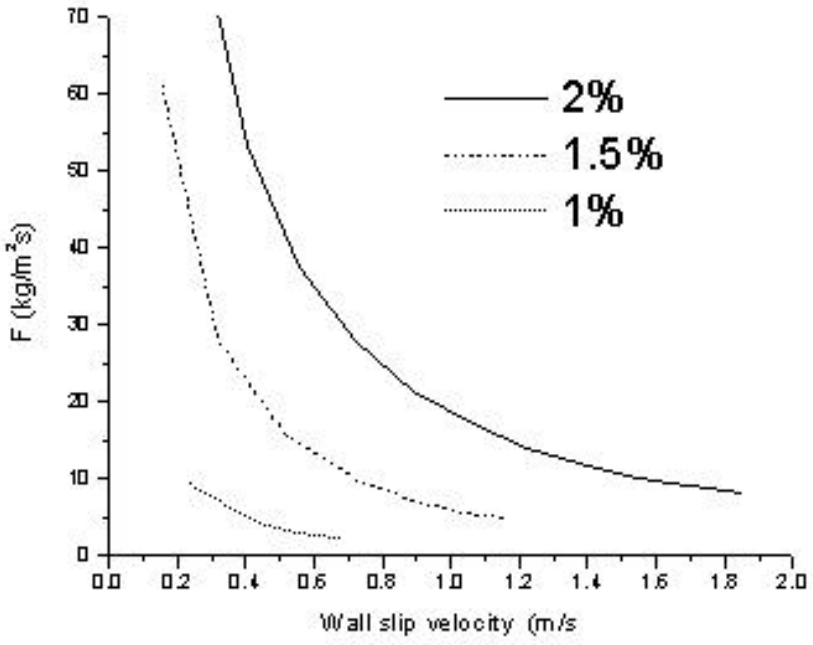

Figure 6 The value of F for bleached birch.

Final explicit mathematical model for the wall-slip regime

In this section we will perform curve fits to the results of figure 6. The aim is to obtain an explicit mathematical model of the friction law that more easily can be incorporated into commercial CFD solvers, such as e.g. FLUENT. The starting point is the ansatz

$$m\frac{\partial u_z}{\partial r} + f(u_{slip})^e = 0 \qquad \{7\}$$

where f is a non-linear function of the slip velocity. The form of equation {7} is known as the generalized Navier's law and is used in rheology problems; see for example the Polyflow manual [12]. Equation {7} is modified slightly to the following form:

$$m\frac{\partial u_z}{\partial r} + \left(f_1 u_{slip}^{e-1} + f_2\right)u_{slip} = 0 \qquad \{8\}$$

Both the linear part and the non-linear forms are included in the same model. This is the simplest form of the function f with which the head loss curve can be described properly. Three additional parameters have been introduced, which need to be fitted to the experimental data in the wall-slip regime. The standard least square method is used, and the parameters are given in table 2 and the simulation results are presented in Figure 7.

Table 2 The friction parameters fitted for the measured head loss data of bleached birch.

	f_1	f_2	e
1%	2.8054	-2.8648	0.0104
1.5%	11.7693	-7.7092	0.0535
2%	23.8603	-6.3557	0.0098

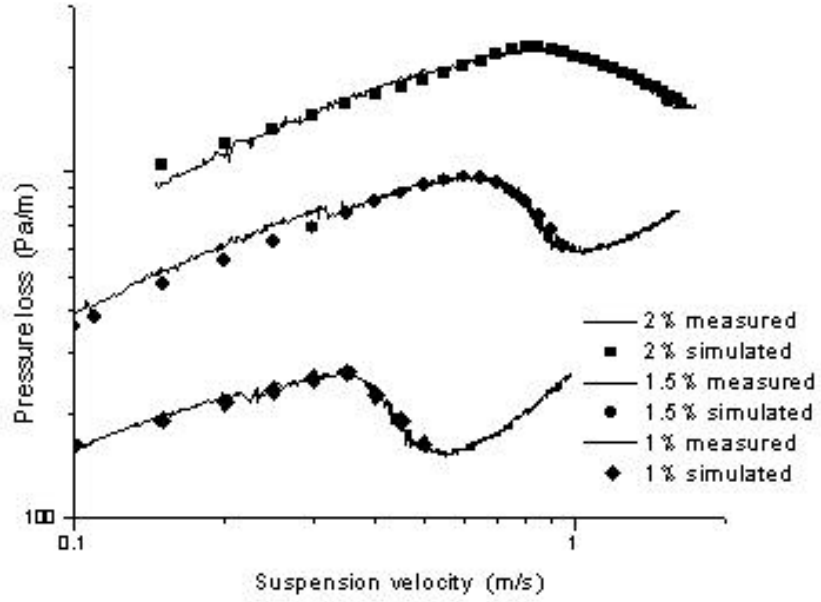

Figure 7 The measured and simulated data for bleached birch, both the plug-flow (Figure 3) and wall-slip regions are included.

For the moment, the model validity is restricted to the plug-flow and wall-slip regions. At higher flow rates the water annulus and pulp plug behave more like a turbulent flow.

Simulations

By implementing equation {8} as a wall boundary function in FLUENT, the two first regions of fiber suspension flow can be described. The largest benefit of method is that no global input parameters are required; the function is evaluated in each wall face by the CFD solver.

The simulations were performed with FLUENT version 6.0.20 in 2 dimensions with axial symmetry. The mesh was fully structured with 5400 cells. The cell height was reduced towards the wall. The suitability of the numerical scheme and convergence criteria was verified.

Results

The velocity profile in the pipe is also obtained for each flow rate. In Figure 8 the velocity profile of the fully developed "slipping" flow is compared to the fully developed no-slip flow for two flow rates.

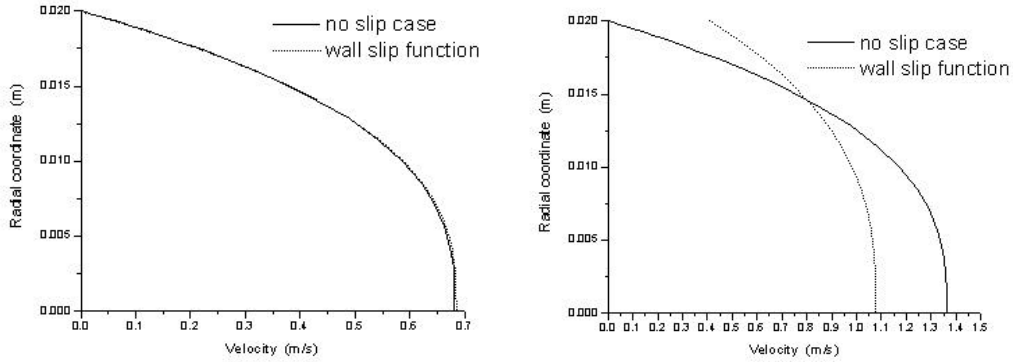

Figure 8 The velocity profile in the pipe, with 0.4 m/s (left) and 0.8 m/s (right) average velocity. Simulation of 1.5% birch pulp. The legends refer to the boundary conditions used at the pipe wall.

Table 3 Head loss of the cases in Figure 8. The headings refer to the boundary condition used on the pipe wall in the simulations.

	no slip (Pa/m)	wall slip (Pa/m)
0.4 m/s	812	812
0.8m/s	1190	806

There is a quite significant difference in the velocity profile between the two cases, and the head losses for both cases can be compared in table 3.

In the no-slip case of Figure 8 the velocity profile is identical for the slip and the no-slip cases, as is the head loss, which is presented in table 3. The regions can also be identified in Figure 4. This shows that the wall slip function is valid in the plug-flow region as well. The friction coefficient becomes large enough to ensure zero or infinitesimal slip velocity.

The difference in head loss per pipe length is quite significant (50%) in the case from the wall-slip regime. The velocity profile is also quite distinctive. The importance of this difference is that when a complex flow is simulated, some parts of the flow domain have large velocity gradients, either due to large flow rates in small dimensions or added momentum via mixing, while other parts of the flow domain have very small wall stresses, as for instance in large settling tanks.

This type of wall boundary function can predict a correct shear stress at the walls in all the domains mentioned above, for the time being provided that the flow remains laminar. A correct boundary treatment is vital for the simulation results, as also stated

by Wikström and Rasmusson [10]. The presented type of wall function forms a large part of the solution to the challenging problem of pulp flow simulations.

Discussion

The wall slip has been shown to be a useful and valid method for describing the head loss in laminar pipe flow of fiber suspensions. The slip-stress relation has been given a very simple function in this paper, a more complex function may be developed as well.

The wall slip functions developed in this way can be used for any fiber flows in the development of any unit process in the paper and pulp industry. This paper shows that it is possible to determine parameters for all flow rates of pulp suspension flow.

The validity of this approach has been tested for a few different pulps and pipe diameters, but it has not been verified for other geometries. This is a part of future investigations.

Acknowledgements:
The financial support from the Finnish National Technology Agency, TEKES, and Faxén Laboratory at the Royal Institute of Technology, Stockholm, Sweden is thankfully acknowledged.

The measurement work of Esa Rehn at Jyväskylä University, and the valuable discussions with Hannu Karema are also acknowledged.

References:

[1] Durst R.E, Jenness L.C; **The Flow Properties of Paper Pulp Stock. I. Relationship of Sheer Value to Pipe Friction for Bleached Sulphite Pulp Slurries**, TAPPI 37 no. 10, 1954.

[2] Brecht W, Heller H; **A Study of the Pipe Friction Losses of Paper Stock Suspensions**, TAPPI 33 no. 9, 1950.

[3] Head V.P, Durst R.E; **Stock Slurry Hydraulics**, TAPPI vol 40 no 12, 1957

[4] Duffy G.G, Moller K, Lee P.F.W, Milne S.W.A; **Design Correlations for Groundwood Pulps and the Effects of Minor Variables on Pulp Suspension Flow**, APPITA vol 27 no 5, 1974.

[5] Myréen B; **Modeling the Flow of Pulp Suspensions in Pipes, Part 1.** Paperi ja Puu, 5/1989.

[6] Myréen B; **Modeling the Flow of Pulp Suspensions in Pipes, Part 2**, Paperi ja Puu, no 7 1989

[7] Soszynski R; **The Plug Flow of Fiber Suspensions in Pipes. A Case of Clear Water Annulus**, Nordic Pulp and Paper Research Journal, no 3, 1991.

[8] Hämäläinen, J; **Mathematical Modeling and Simulation of Fluid Flows in the Headbox of Paper Machines,** PhD Thesis, University of Jyväskylä, 1993

[9] Duffy G.G; **The Importance of Mechanistic-based Models in Fibre Suspension Flow**, Nordic Pulp and Paper Journal, 2003, in press

[10] Wikström T, Rasmusson A; **Transition Modeling of Pulp Suspensions Applied to a Pressure Screen**, Journal of Pulp and Paper Science, vol 28, 2002
[11] Morrison F; **Understanding Rheology**, Oxford University Press 2001, ISBN 0-19-514166-0
[12] **POLYFLOW 3.8 User Guide**, ch 6, Fluent Inc

Modeling of Turbulent Suspension Flows

David Hammarström [a,*], Jari P Hämäläinen [b], Anders Dahlkild [c], Ari Jäsberg [d]

[a] Process Flow Ltd Oy, Puolalanpuisto 1 b A 21, FIN-20100 Turku, Finland
[b] Metso Paper Inc., PO Box 587, FIN-40101 Jyväskylä, Finland
[c] Royal Institute of Technology, Department of Mechanics, SE-10044 Stockholm, Sweden
[d] University of Jyväskylä, Department of Physics, PO Box 35, FIN-40014 Jyväskylä, Finland
* Corresponding author. E-mail address: david.hammarstrom@processflow.fi Fax: +358-2-2759580

Abstract

Mathematical modeling and numerical simulation of a pipe flow of pulp suspension is studied in this paper. The flow of fiber suspensions does not follow the pressure loss curves for neither laminar, nor fully developed turbulent flow of a Newtonian fluid like pure water, but pulp suspensions often show an "S"-shaped curve for the pressure drop plotted against the average suspension velocity. Turbulent flow of pulp suspensions has been modeled with water, but this tends to result in incorrect results. A new method incorporating a laminar wall slip method presented in an accompanying paper is introduced for turbulent flow. Numerical solution of the model is also compared to new experimental head loss data for pulp suspensions of 0.5-2% mass fraction.

Keywords: CFD, pulp, rheology, turbulence, slip

Introduction

The flow of paper pulp stock is mainly laminar, but in all the most important processes the conditions are best described as turbulent. Turbulence increases the mixing of chemicals and plays an important role in the formation and dispersion of fiber agglomerates known as flocs. Flocculation is one of the most important features of a fiber suspension, but any discussion regarding the nature of the fiber suspension and its phenomena are not the issue of the paper, and are left out.

Head loss measurements of pulp suspension flows of varying pulps, dry contents and tube diameters have been made for many decades. The typical S-shaped head loss curves, as those presented here for pine pulp, have been found by many authors, for example, Möller [1].

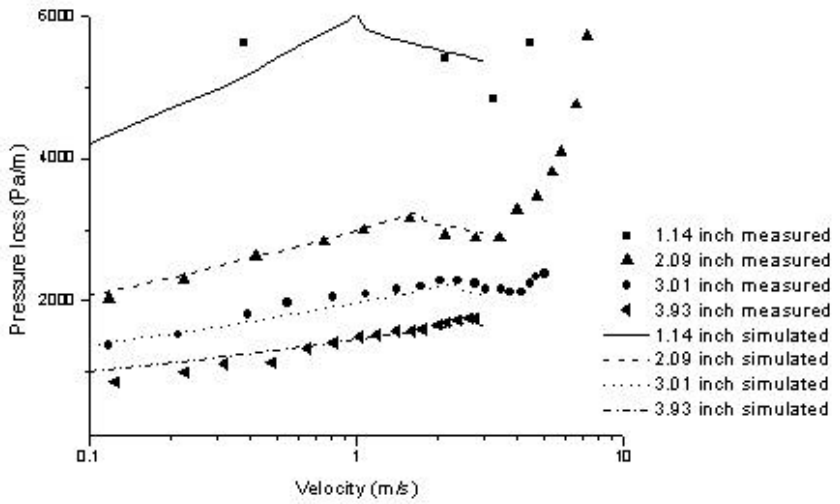

Picture 1. Measured and simulated head losses of a 3.11% suspension of pine in four different pipes. Measurements by Möller [1].

Myréen [2] derived the head loss equation based on basic fluid dynamic equations, assuming the power-law model for the viscosity. This was an important step for understanding pulp flows, because he introduced a model, which is not limited to pipe flow. With computational fluid dynamic (CFD) simulations pulp flows can be simulated for any unit process of the pulp and paper industry.

Water has been used to simulate the flow of very dilute fiber suspensions. Hämäläinen [3] modeled the turbulent flow of dilute fiber suspensions in complex industry geometries using a finite element based flow simulation software.

Yield stress based rheology models, such as the Bingham and Herschel-Bulkley models, have been used by Wikström and Rasmusson [4] for simulations of a pressure screen operating at higher consistency. They applied rheology modeling combined with turbulence modeling, with which all the trends observed in measurements could also be observed in the simulations. Wikström [5] also simulated the flow in a high-consistency shear tester, here the consistency was 10%-mass.

The peculiar flow regime where the head loss decreases with increasing velocity, as shown by picture 1 and picture 3, is explained by a thin lubricating layer of pure water that is assumed to form on the pipe wall, as shown by picture 2.

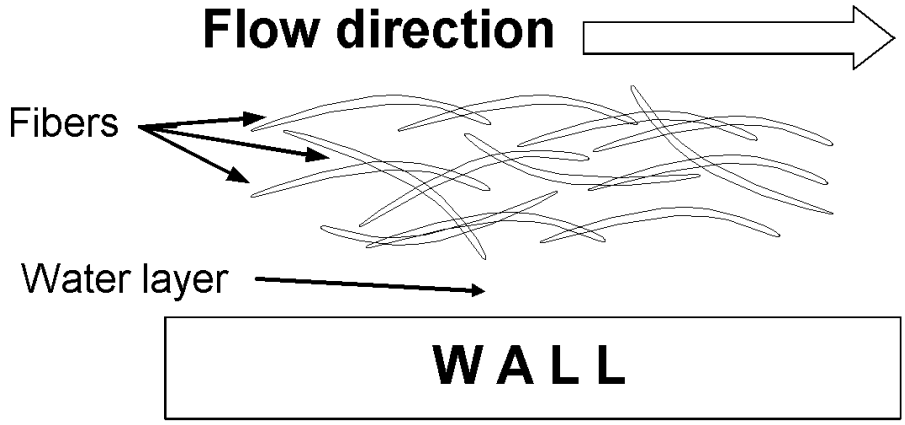

Picture 2. A clear water annulus is formed on the walls. The height of the water layer is negligible compared to other dimensions.

The annular water layer causes the reduced friction, which has been observed by many, but first modeled by Myréen [6]. Hammarström et al [7] used a different modeling approach for the wall slip region in an accompanying paper. In the paper the applicability of the rheology model is extended from the plug-flow regime to the wall-slip regime. The simulations showed good agreement with measured head loss data for both regimes.

The validity of the laminar modeling, as presented by Hammarström et al [7], is shown by picture 1. In the picture are the measurements by Möller [1], for a 3.11%-mass pine pulp suspension. The head loss measurements have been performed in four different pipe diameters. The method described by Hammarström is applied, where the model parameters are attached in one pipe. As is clearly visible, the agreement between the simulations and the measurements is quite good. The important thing to notice is that it is not important for which pipe diameter the rheology and slip parameters have been set, but that the same parameters have been used for all pipes. For a more accurate determination of the pulp parameters more measurement points would be required, the current number is a bare minimum. But still, the results show an excellent agreement for all four pipe diameters.

In this paper, the wall slip approach is further extended into the turbulent flow region, with flow rates higher than the local minimum on the head loss curve.

Head loss measurements

The head loss measurements presented in picture 1 contain too few measurement point, hence the model development in this paper is based on new measurements for a pine suspension of lower concentration. The measurements are identical to those presented in Hammarström et al [7], except for a different wood species for the pulp. A birch fiber is typically 1mm long, whereas a pine fiber is almost 3mm long.

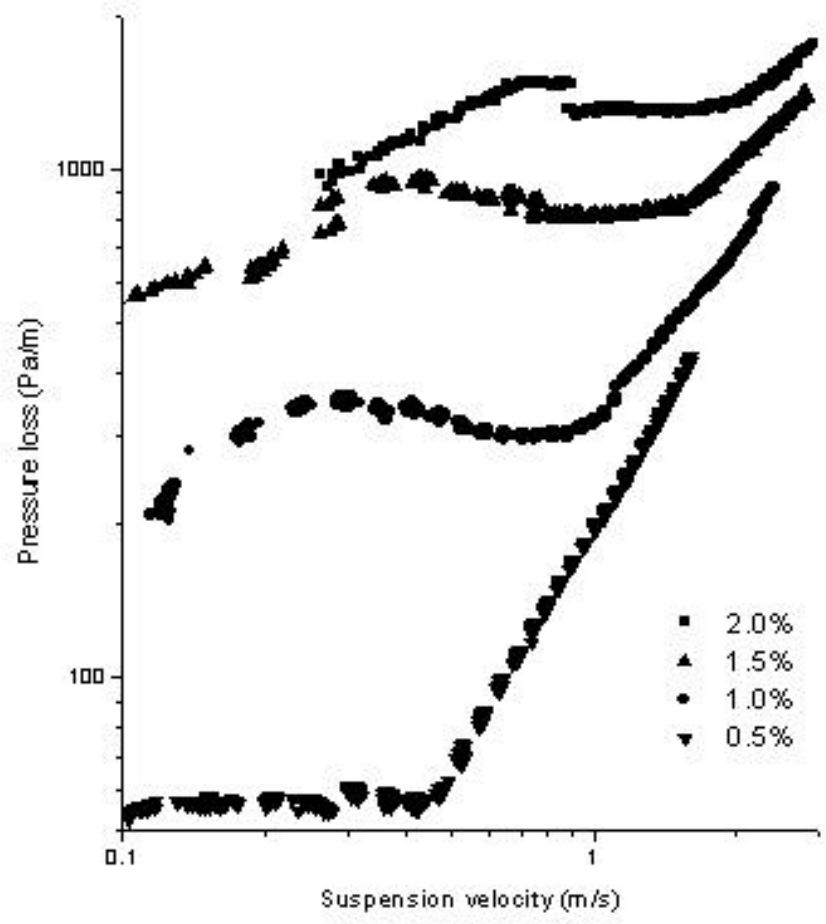

Picture 3. Measured head loss curves of pine pulp.

The head loss was measured in a laboratory scale (D=40mm) flow loop for pine suspension with mass fractions 0.5%, 1.0%, 1.5% and 2.0%. The measurement data are presented in Picture 3. The presented measurement data is not a line graph but points, for each consistency the chart contains 5-800 different mean flow rates. The measurement section was made of two semi-circular channels cut to separate acrylic prisms, which were attached together to form a full circular flow channel. That way the holes for pressure taps could be drilled starting from the interior of the channel to minimize breaking of the channel wall next to the holes, which would produce fluctuations to flow and measured head loss. The distance between the pressure taps was 0.89 m, and the straight free sections upstream and downstream from the taps were 2m and 1m respectively. For each flow rate, 10.000 samples of head loss were measured with a frequency that gave a constant distance of 1 mm in fluid flow between two consecutive samples.

Suspension rheology

The fiber suspension is modeled as a homogeneous shear-thinning fluid. The power-law viscosity model, equation {1} is used, where t is the stress, μ is the viscosity, K is the consistency coefficient and n is the fluid behaviour index and $\dot{g}$ is the strain rate.

$$t = m\dot{g} = K(\dot{g})^{n-1}(\dot{g}) \qquad \{1\}$$

Table 1 The power-law viscosity coefficients of bleached pine.

	K	n
0.5%	0.3260	0.1187
1%	0.2705	0.6386
1.5%	1.2923	0.4247
2%	1.9707	0.3738

Table 1 show the pulp model parameters in the plug-flow region. The parameters were obtained with least squares fitting to the measured data.

$$m\frac{\partial u_z}{\partial r} + \left(f_1 u_{slip}^{e-1} + f_2\right)u_{slip} = 0 \qquad \{2\}$$

The parameters for the wall slip region, calculated according to the equation {2}, presented by Hammarström et al [7] are presented in table 2.

Table 2 The wall slip parameters of bleached pine.

	f_1	e	f_2
0.5%	0.6016	-0.0006	-0.1634
1%	3.5206	-0.0043	-1.1767
1.5%	8.7243	-0.0290	-1.0730
2%	13.1778	-0.0324	-0.3559

For the 0.5% suspension the parameters presented in tables 1 and 2 seem a bit odd. This is probably due to the very small number of measured points in the region and due to small differences in head losses making it difficult to determine the parameters for the flow rate regions.

The lowest consistency is also on the limit where the fibers do not necessarily form a continuous network structure, but may exist as free fibers suspended in water.

Turbulence modeling

Turbulent flow of fluids which are known to possess non-Newtonian properties have been investigated by many authors, but the only a few of them have CFD based approach. Dodge and Metzner [8] discussed the turbulent flow of non-Newtonian systems, mainly based on polymer solutions. They presented the generalized Reynolds number, which can be applied to generalized Newtonian fluids, both shear thinning and thickening. Turian et al [9] investigated the flow of non-Newtonian slurries with fine particulates, such as gypsum. They noted that the Sisko viscosity model is good for describing the rheology of concentrated slurries. The Sisko model is identical to the power-law model, equation {1}, but has one constant value added to the right hand side. This constant value is the viscosity at infinite shear rate. For a power-law fluid this infinite shear rate viscosity is zero.

Among the very few CFD based papers, those of Malin [10-11] and Wikström and Rasmusson [4] have included turbulence and non-Newtonian rheology. Malin used a low Reynolds number approach for his modeling, and introduced an addition to the Lam-Bremhorst k-e turbulence model in order to correct the equation for the turbulent dissipation e due to the viscous damping near the wall.

Wikström and Rasmusson [4] used a similar approach for a pulp suspension, which he modeled with a yield-stress model for the shear-rate dependence of the viscosity. Two different turbulence models were tried, one high Reynolds number k-e and one low Reynolds number k-? model were tried. Both models returned approximately the same predictions for an industrial screening application. The trends were correctly predicted, but the absolute values differed due to the incorrect wall boundary condition.

In this work the standard k-e turbulence model is used. The k-e model is an eddy viscosity model, in which the effective viscosity is the sum of the laminar and turbulent viscosity, according to {3}.

$$\mu_{effective} = \mu_{laminar} + \mu_{turbulent} \qquad \{3\}$$

The reasons for the choice of models are the following: By combining a continuous rheology model and a turbulence model which is always activated, there is no need for deciding whether the flow is laminar or turbulent, the models themselves take care of that. It is also unnecessary to use complicated models, such as the low Reynolds number models, for simulating the flow down to the wall as the most significant wall phenomenon is the slip, which cannot be described by the turbulence models anyway.

The validity of the assumption can be debated, for fiber suspensions the concepts of "laminar" and "turbulent" are not trivial. The Reynolds number is not either a relevant number as it can be based on many different length scales, i.e. pipe diameter, fiber length, floc size or preferably water annulus height. One other feature is the strong damping the fibers exert on any turbulence. Within any flocs or fiber networks the degree of turbulence can be assumed zero.

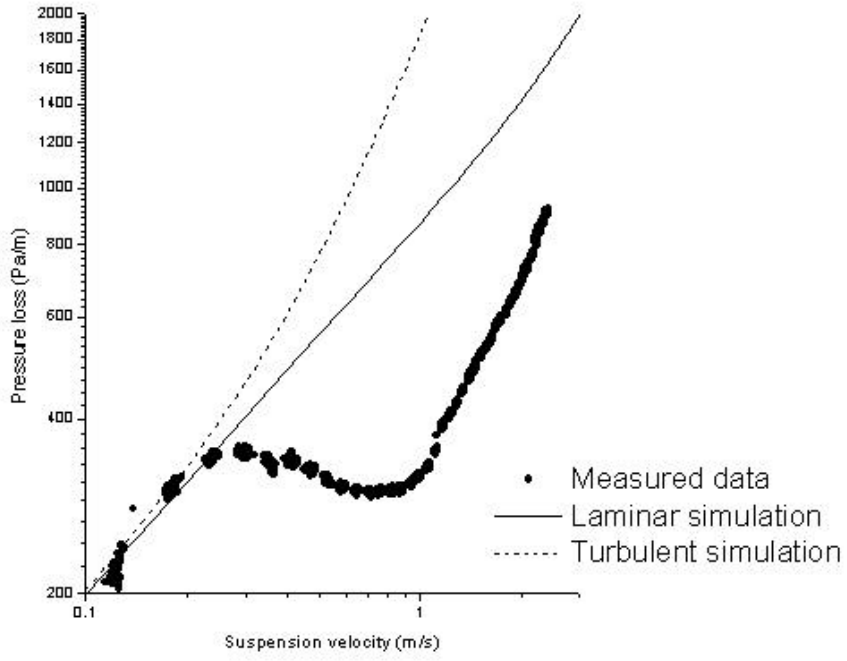

Picture 4 Illustration on the simulation alternatives, pulp 1.0% bleached pine.

Picture 4 illustrates the principle for the combined use of a non-Newtonian rheology model and a turbulence models. Both simulation curves have been simulated with identical meshes and parameters, the only difference is the activation of the turbulence model. The picture can be explained as follows:

In the beginning of the curve, at low flow rates, the influence of the power-law model is larger than the influence of turbulence. With increasing flow rates, the laminar viscosity is decreasing, whereas the turbulent viscosity is increasing. At some instant the increase of the turbulent viscosity will be larger than the decrease of the laminar viscosity, which leads to a change of curve type from logarithmic growth to exponential growth.

Comparing the two curves with the measured data, the laminar model will Cross the curve of the measured values, whereas the turbulent curve will not Cross it. The deviation between the measured data and the curve predicted by the turbulent simulation is explained by the wall treatment. This is not possible for the laminar curve as it eventually Crosses the curve of the measured data.

Wall functions

In the normal turbulence models the boundary layer friction is modeled either by simulating all the way to the wall or by using wall functions. The wall functions are using dimensionless wall similarity values, the friction velocity u^+ and cell wall distance y^+, for calculating the wall shear stress. For calculating the height of the water annulus, the formula of Spalding [12] is used {3}. This formula is valid throughout the boundary layer.

$$y^+ = u^+ + e^{-k\,c}\left[e^{k\,u^+} - 1 - k\,u^+ - \frac{(k\,u^+)^2}{2} - \frac{(k\,u^+)^3}{6}\right] \qquad \{3\}$$

?=0.41, c=5.0

The purpose of using this formula instead of the usual, is that this formula does not require different versions for different parts of the boundary layer, i.e. viscous sublayer and logarithmic layer.

Modeling the 'slip' in the turbulent region

The model derived for the plug-flow regime and the wall slip regime are assumed valid for the suspension, and that the increasing head loss is resulted from turbulence, as illustrated by picture 4.

The slip velocity required to satisfy the mass balance is calculated in a similar way using the simulated turbulent head loss curve instead of the simulated laminar head loss curve. The curves are presented in picture 4 for a 1.0% suspension of bleached pine.

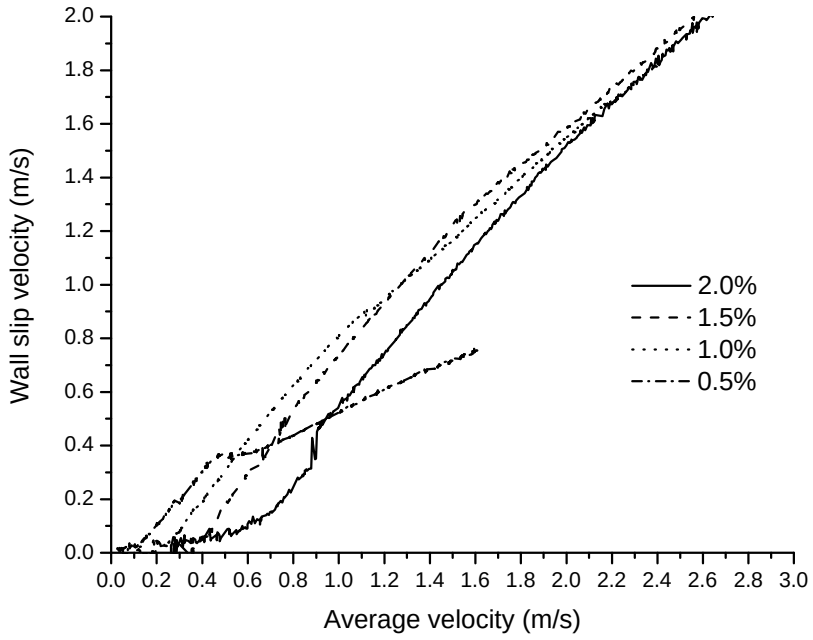

Picture 5 The slip velocity plotted against the average flow velocity for bleached pine

Picture 5 shows that this slip velocity is not constant, nor is it growing at the same rate as the mean flow rate. As the slip layer is assumed negligibly thin, and that the stress aCross it is uniform, the height of the water annulus can be calculated for all flow rates.

The height of the water annulus becomes even more interesting if the height is plotted as the wall similarity variable y+, for instance using the formula {3}.

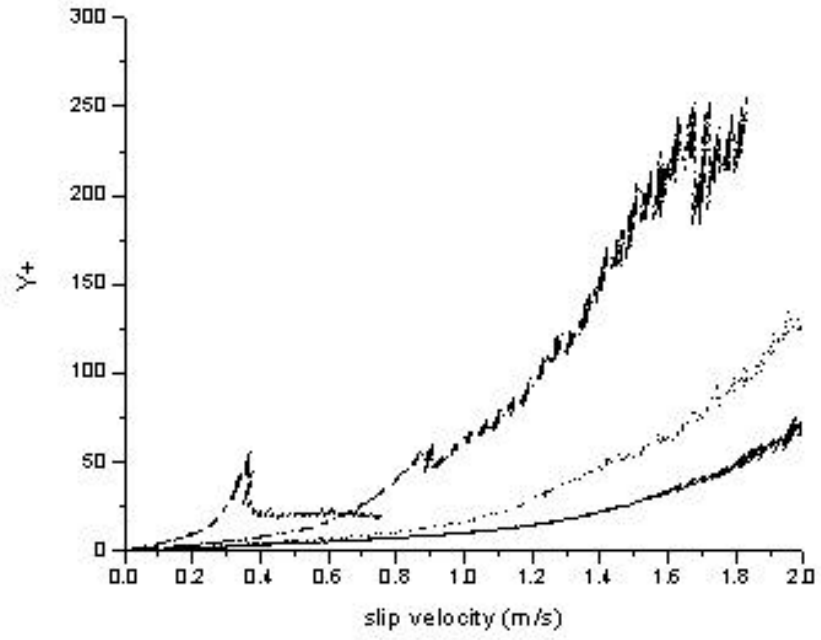

Picture 6 The height of the water annulus in dimensionless units for pine pulp.

At very low flow rates the slip velocity is zero or very small, indicating a very thin slip layer. At higher flow rates, the head loss decreases with increasing flow rate, for which the only possible explanation is a water layer that is increasing in height.

For the lowest consistency the layer height seems to have stabilized within what would be the logarithmic layer, whereas for the higher consistencies the layer height does not appear to have stabilized, though the flow rate exceeds the flow rate of the local minimum on the head loss curves in picture 1. This may partly depend on the fitting of the rheology parameters.

Simulations

By implementing equation {8} as a wall boundary function in FLUENT, all regions of fiber suspension flow can be described. The largest benefit of method is that no global input parameters are required; the function is evaluated in each wall face by the CFD solver.

The simulations were performed with FLUENT version 6.1.18 in 2 dimensions with axial symmetry. The mesh was fully structured with 7425 cells. The cell height was reduced towards the wall. The suitability of the numerical scheme and convergence criteria was verified.

Results

In picture 7 the head loss of bleached pine, and in picture 8 the head loss of bleached birch, are presented for four dry contents. The birch pulp data is the data that was presented in Hammarström et al [7], the picture is included in order to show the similarity in behaviour, even though the wood fibers have totally different properties.

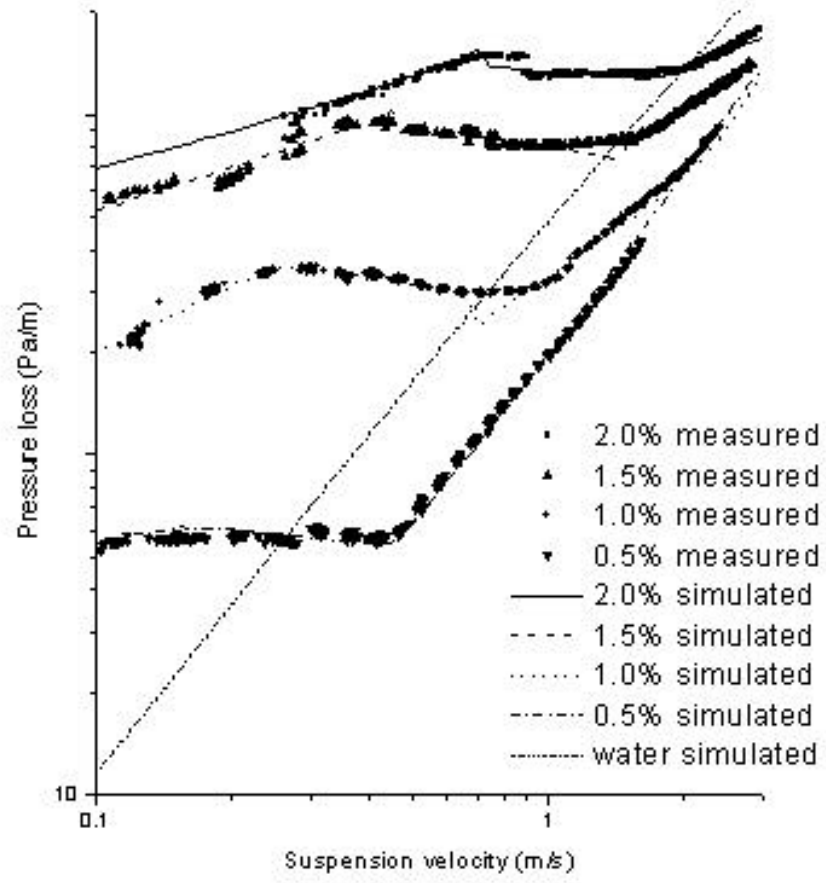

Picture 7 Measured and simulated head losses for bleached pine pulp.

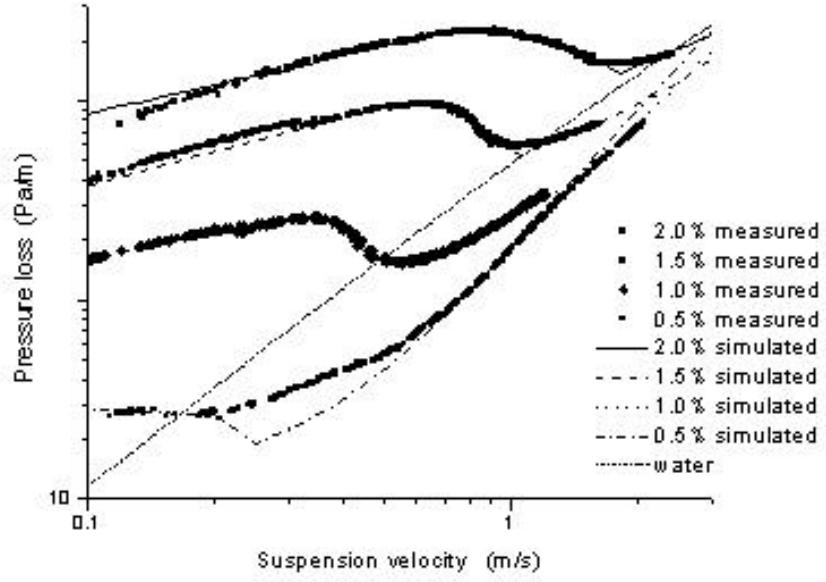

Picture 8 Measured and simulated head losses for bleached birch pulp.

In order to illustrate the different simulation options, the velocity profiles of four flow rates are presented in pictures 9-12. The pulp used in the simulations is 1.5% pine. The flow rates are 0.25m/s, 1.25m/s, 2.5m/s and 8m/s.

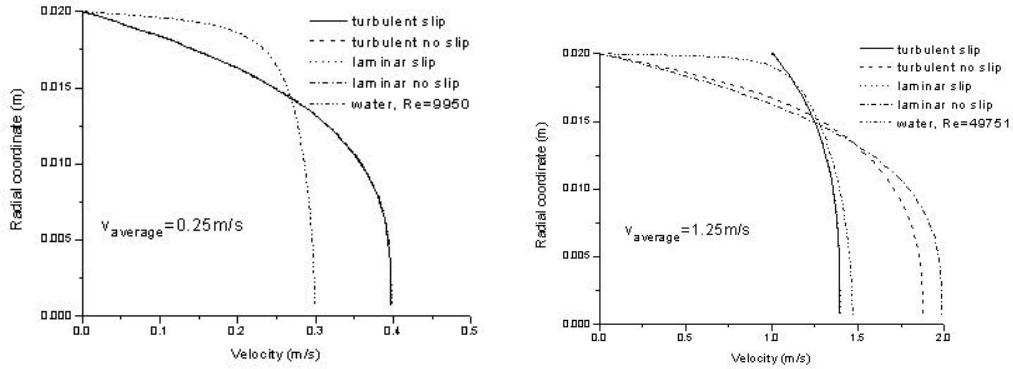

Picture 9-10 Velocity profile of 1.5% bleached pine. Flow rate 0.25m/s (left) and 1.25m/s (right).

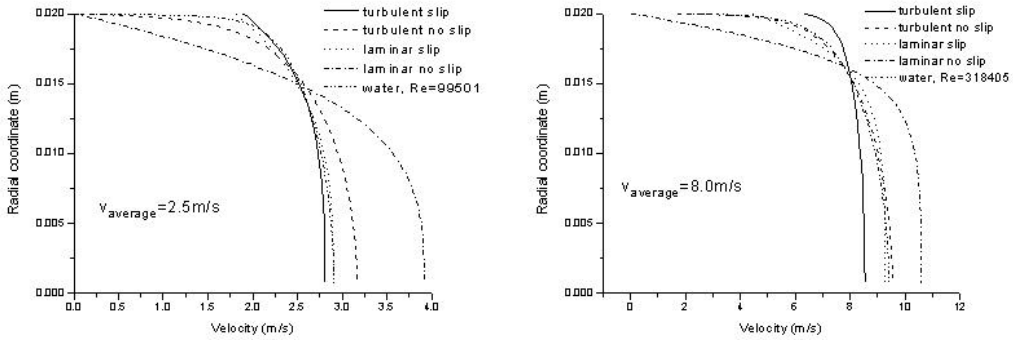

Picture 11-12 Velocity profile of 1.5% bleached pine. Flow rate 2.5m/s (left) and 8.0m/s (right).

The different curves have been simulated as turbulent flow with the wall slip function activated, turbulent flow with the standard wall functions, laminar flow with the wall slip function and laminar flow with no slip on the wall. The velocity profile of water is included for comparison, the Reynolds number of the water flow is given in each picture.

In picture 9, all curves except the velocity profile of water collapse onto each other, as they should. This flow rate is in the 'plug-flow' region, where the flow is laminar and no slip should occur. From the head loss results presented in picture 13, it is evident that all modeling approaches return approximately the same head loss.

In picture 10, there is a significant degree of slip on the pipe walls. The velocity profiles of the turbulent and laminar cases, both with wall slip, are quite similar. The curves without wall slip are also quite similar. This is due to the very large laminar viscosity. The water velocity profile is almost identical to the profiles of the wall slip cases.

At the higher flow rates of pictures 11-12, the velocity profiles are more "flat", and the slip on the wall is more pronounced. There is a significant difference in head loss between the cases, the turbulent simulation without wall slip is many times larger than the measured values, and at 10m/s the laminar flow curve seems to Cross a line that can be extrapolated from the measured values.

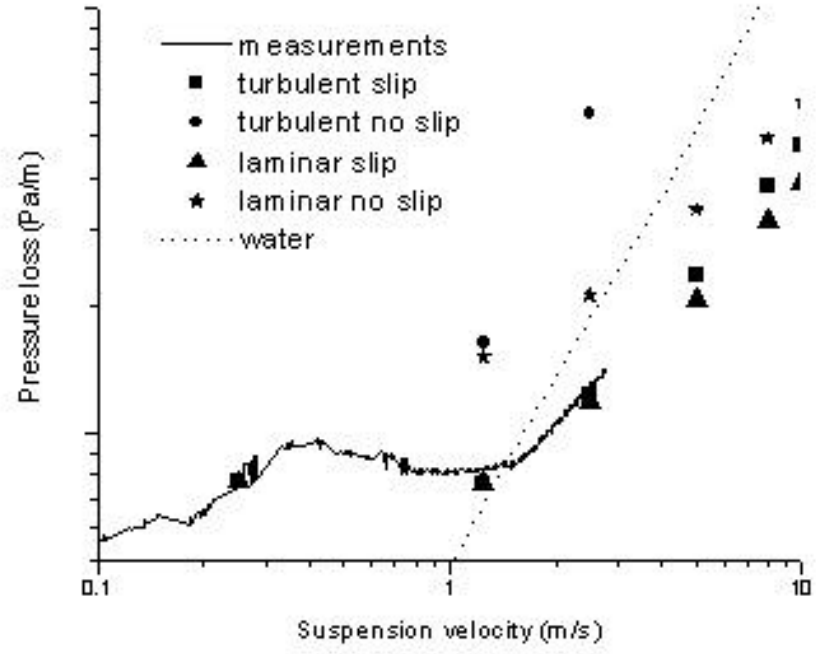

Picture 13 Head losses of the cases in pictures 9-12, compared to the measured values.

The values returned by be laminar and turbulent simulation with the slip function return approximately similar values, because the same slip function has been used for both cases.

Regarding the velocity profiles, in case any kind of velocimetry is used to determine the velocity profile for pipe flow of pulp suspensions, it will be very difficult to distinguish between any of these models. If the instrument does not have a very high resolution near the wall it will only see one large plug, as observed by e.g. Duffy [13].

Discussion

The wall slip has been shown to be a useful and valid method for describing the head loss in both laminar and turbulent pipe flow of fiber suspensions. The slip-stress relation has been given a very simple function in this paper, a more complex function may be developed as well.

The validity of this approach has been tested for a few different pulps and pipe diameters, but it has not been verified for other geometries. This is a part of future investigations.

The term "wall slip function" will be dropped in favour of "pulp wall function", because the wall slip too much refers to the region of decreasing head loss. The pulp wall function has a much broader applicability, in fact, it can be suited for all flow rates, which has been show in this paper.

Acknowledgements:
The financial support from the Finnish National Technology Agency, TEKES, and Faxén Laboratory at the Royal Institute of Technology, Stockholm, Sweden is thankfully acknowledged.

The excellent measurement work by Esa Rehn at Jyväskylä University is also acknowledged.

References:

[1] Möller K; **The Plug Flow of Paper Pulp Suspensions**, PhD thesis, University of Auckland, 1972

[2] Myréen B; **Modeling the Flow of Pulp Suspensions in Pipes, Part 1.** Paperi ja Puu, 5/1989.

[3] Hämäläinen, J; **Mathematical Modeling and Simulation of Fluid Flows in the Headbox of Paper Machines,** PhD Thesis, University of Jyväskylä, 1993

[4] Wikström T, Rasmusson A; **Transition Modeling of Pulp Suspensions Applied to a Pressure Screen**, Journal of Pulp and Paper Science, vol 28, 2002

[5] Wikström T, Rasmusson A; **Flow and Rheology of medium-consistency pulp** , PhD thesis, Chalmers University od Technology, Sweden, 2002

[6] Myréen B; **Modeling the Flow of Pulp Suspensions in Pipes, Part 2**, Paperi ja Puu, no 7 1989

[7] Hammarström D, Hämäläinen J, Dahlkild A, Jäsberg A; **Modeling of Laminar Suspension Flows**, submitted to Computers & Fluids, toghether with this paper

[8] Dodge DW, Metzner AB; **Turbulent Flow of Non-Newtonian Systems**, AIChE Journal, vol 5, 1959

[9] Turian RM, Ma T-W, Hsu F-LG, Sung D-J; **Flow of Concentrated Non-Newtonian Slurries: 1. Friction Losses in Laminar, Turbulent and Transition Flow Through Straight Pipe**, Int. J. Multiphase Flow, vol 24, 1998

[10] Malin MR; **Turbulent Pipe flow of Power-Law Fluids**, Int. Comm. Heat Mass Transfer, vol24, 1997

[11] Malin MR; **Turbulent Pipe flow of Herschel-Bulkley Fluids**, Int. Comm. Heat Mass Transfer, vol 25, 1998

[12] Spalding; **A single formula for the law of the wall**, Journal of Applied Mechanics, vol 28, 1961

[13] Duffy G.G; **The Importance of Mechanistic-based Models in Fibre Suspension Flow**, Nordic Pulp and Paper Journal, 2003, in press